

Identification and Characterization of ABCA1-Interactive Proteins and Their Relevance to Atherosclerosis

Dissertation zur Erlangung des Doktorgrades der Naturwissenschaften

(Dr. rer. nat.)

an der Fakultät für Chemie und Pharmazie

der Universität Regensburg



vorgelegt von

Salim Maa Bared

Regensburg im April 2005

This work was performed at the institute of Clinical Chemistry and Laboratory Medicine at the University of Regensburg between August 2000 and December 2004 under the supervision of Prof. Dr. Gerd Schmitz.

Date of colloquium: 17. 10. 2005

Board of examiners: Chairman: Prof.Dr. Sigurd Elz
First Examiner: Prof. Dr. Armin Buschauer
Second Examiner: Prof. Dr. Gerd Schmitz
Third Examiner: Prof. Dr. Jörg Heilmann

„When you make the finding yourself, . . . even if you're the last person on earth to see the light, you'll never forget it. “

Carl Sagan

American astronomer and science writer (1934-1996)

Acknowledgement

I would like to express my gratitude to Prof. Dr. Gerd Schmitz for supporting me in performing my PhD at his fine institute and who was such a great help in correcting my thesis always pushing it with new ideas and interesting views.

Further, my thanks go to PD. Dr. Christa Buechler, my group leader, for sharing her knowledge with me. Special thanks go to Prof. Dr. Armin Buschauer, my supervisor at the Faculty of Pharmacy at Regensburg University as well as to my colleagues and friends: Prof. Dr. Charalampos Aslanidis, Dr. Alfred Boettcher and Dr. Wolfgang Kaminski, all specialists in their fields.

My friends: Margot Grandl, Alex Siguener, Mirko Ritter and many others.

Last, but definitely not least, for their technical assistance: Nadine, Connie, Andrea and Sylvia.

I thank my Parents who spared no efforts and always care so much for me.

On top of them all, I thank the crown of my life, Rania. Without her, many things would have come in another unexpected way.

Table of contents

I. INTRODUCTION.....	1
1. PATHOGENESIS OF ATHEROSCLEROSIS	2
1.1. RESPONSE TO INJURY HYPOTHESIS	2
1.2. RESPONSE TO RETENTION HYPOTHESIS.....	4
2. METABOLISM OF APOB CONTAINING LIPOPROTEINS.....	5
2.1. CHYLOMICRONS	5
2.2. VERY LOW DENSITY LIPOPROTEIN (VLDL)	6
2.3. LOW DENSITY LIPOPROTEIN (LDL).....	6
2.4. LDL-RECEPTOR.....	6
2.5. NIEMANN-PICK DISEASE TYPE C, A CHOLESTEROL TRAFFIC DISORDER.....	7
3. MODIFIED LOW DENSITY LIPOPROTEINS.....	8
3.1. ENZYMATICALLY MODIFIED LOW DENSITY LIPOPROTEIN (E-LDL).....	9
3.2. OXIDIZED LOW DENSITY LIPOPROTEIN (Ox-LDL).....	9
4. CHOLESTEROL INFLUX PATHWAYS	10
4.1. CLATHRIN-DEPENDENT ENDOCYTOSIS	10
4.2. CLATHRIN-INDEPENDENT ENDOCYTOSIS.....	12
4.2.1. <i>Phagocytosis</i>	13
4.2.2. <i>Pinocytosis and Macropinocytosis</i>	13
4.2.3. <i>Caveolin-Dependent Endocytosis</i>	14
4.2.4. <i>Novel Uptake Mechanisms</i>	15
4.2.4.1 Surface Connected Compartments (SSC)	15
4.2.4.2 Endocytosis Through Compartments Involving CD14.....	15
4.2.4.3. Deep Tubular Invaginations	16
4.2.4.4. Continuous Cellular Membrane System.....	17
5. METABOLISM OF APO-AI CONTAINING HIGH DENSITY LIPOPROTEIN (HDL)	18
5.1. CHOLESTEROL EFFLUX FROM MACROPHAGES	19
5.2. MULTIPLE PATHWAYS FOR CELLULAR CHOLESTEROL EFFLUX.....	20
5.2.1. <i>Passive Diffusion</i>	20
5.2.2. <i>SR-BI-Facilitated Diffusion of Cholesterol to HDL</i>	21
5.2.3. <i>ABCA1-Mediated Active Efflux</i>	22
5.3. ATP-BINDING CASSETTE TRANSPORTER.....	23
5.3.1. <i>ABCA Subfamily</i>	24
5.3.2. <i>ABCA1 and Familial HDL-Deficiency</i>	24

5.4. TANGIER DISEASE	25
5.5. ATP-SYNTASE, A NEW CONCEPT IN THE DUAL REGULATION OF ENDOCYTOSIS AND APOAI-MEDIATED CHOLESTEROL EFFLUX	25
6. VESICLE FORMATION IN THE GOLGI-DEPENDENT ABCA1 SECRETORY PATHWAY.....	27
6.1. COATED VESICLE ASSEMBLY	32
6.2. SYNTAXINS AS CONSTITUENTS OF THE SNARE FAMILY	35
6.3. THE RAB PATHWAY AND ITS INVOLVEMENT IN VESICULAR TRANSPORT.....	36
7. GENE ARRAYS.....	37
8. THE YEAST TWO-HYBRID SYSTEM.....	39
II. AIM OF THE THESIS.....	41
III. MATERIALS	43
1. CHEMICALS	44
2. STANDARDS AND KITS	44
3. RADIOACTIVE MATERIALS	45
4. ENZYMES	45
5. HUMAN PRIMARY CELLS AND CELL LINES	46
5.1. <i>Monocytes</i>	46
5.2. <i>Fibroblasts</i>	46
5.3. <i>Human cell lines</i>	46
6. BACTERIA (E.COLI)	46
7. PLASMIDS	46
8. MEDIA AND BUFFERS	47
9. MICROARRAYS	47
10. TECHNICAL EQUIPMENTS	47
11. SILENCING RNA.....	49
12. GENE BANKS	49
13. FILMS AND MEMBRANES	49
14. ANTIBODIES	49
15. PREPARATION OF SOLUTIONS	50
IV. METHODS	53
1. PRIMARY CELLS AND CELL LINES.....	54
1.1. <i>Elutriation of human monocytes</i>	54
1.2. <i>Cultivation and differentiation of human monocytes</i>	55
1.3. <i>Cultivation of human tumor cell lines</i>	55
1.4. <i>Transfection of cell lines</i>	55
2. LIPOPROTEINS.....	56

2.1. Isolation of Lipoproteins.....	56
2.2. Enzymatic and Oxidative Modification of LDL.....	56
3. PROTEIN METHODS	56
3.1. Isolation of proteins	56
3.2. Protein concentration Determination.....	56
3.3. SDS-PAGE and western blotting.....	57
3.4. Isolation of phagosomes with phagobeads.....	57
3.5. Sucrose gradient centrifugation and isolation of rafts.....	58
3.6. Co-Immunoprecipitation	59
3.7. Immunofluorescent staining and microscopy.....	59
3.8. Flow cytometry	59
4. RADIOACTIVE LIPID EFFLUX	60
5. CULTIVATION OF ESCHERICHIA COLI.....	60
6. NUCLEIC ACID METHODS	60
6.1. Restriction enzyme digestion of DNA.....	60
6.2. DNA gel electrophoresis and DNA extraction from agarose gels.....	61
6.3. Cloning of DNA fragments.....	61
6.4. Small interference RNA (siRNA).....	62
6.5. RNA isolation.....	62
6.6. Quality assessment and quantification of RNA (Agilent).....	63
6.7. RNA gel electrophoresis.....	63
6.8. Reverse Transcription PCR (RT-PCR).....	64
6.9. Real-Time PCR	64
6.9.1. Gene Expression Monitoring With SYBR-Green-I Dye (LightCycler).....	64
6.9.2. Gene Expression Monitoring With Hydrolysis Probes (Taqman).....	65
7. AFFYMETRIX® MICROARRAYS	66
8. YEAST-TWO-HYBRID SYSTEM	68
9. MASS SPECTROMETRY.....	68
V. RESULTS	69
1. IDENTIFICATION OF ABCA1 INTERACTIVE PROTEINS BY YEAST-TWO-HYBRID SYSTEM	70
2. CHARACTERIZATION OF THE ABCA1-FADD COMPLEX	71
3. CHARACTERIZATION OF THE ABCA1 - □2-SYNTROPHIN COMPLEX.....	76
4. PROTEIN-PROTEIN INTERACTIONS OF SYNTAXIN 13, ABCA1 AND FLOTILLIN-1	79
5. LIPOPROTEIN ANALYSIS OF THE PALLIDIN KO MICE.....	87
6. IDENTIFICATION OF MACROPHAGE-SPECIFIC GENES INVOLVED IN LIPID TRAFFICKING USING GENE-CHIPS.....	89
6.1. E-LDL mediated cholesterol flux	93
6.2. Ox-LDL mediated cholesterol flux	96

6.3. <i>Biochemical Pathways and Candidate Genes With Relevance to Lipid Traffic in Macrophages</i>	97
6.3.1. Regulation of Genes in the Endocytic and Phagocytic Pathway in Macrophages.....	98
6.3.2. Regulation of Genes in the Coated Vesicle Pathway in Macrophages.....	99
6.3.3. Regulation of Genes in the Vesicular Transport Pathway in Macrophages.....	100
6.3.4. Regulation of Genes in the COP Machinery in Macrophages	101
6.3.5. Regulation of Genes in the Calcium Signalling Pathway in Macrophages	102
6.3.6. Regulation of ABCA1-Related Genes in the Exocytosis Pathway in Macrophages	104
VI. DISCUSSION	106
VII. REFERENCES	121
VIII. SUMMARY	142
PUBLICATION LIST	145

I. INTRODUCTION

1. PATHOGENESIS OF ATHEROSCLEROSIS

Atherosclerosis is the most common cause of coronary heart disease and stroke in industrialized countries. It is characterized by the progressive accumulation of lipids (atheroma) and connective tissue (sclerosis) in the inner layer of the arterial wall leading to plaque formation and plaque rupture in combination with the formation of a blood clot which leads to a major blockage of blood flow. Atherosclerotic lesions occur principally in large and medium-sized arteries and can lead to vascular ischemic diseases in heart or brain, resulting in infarction. Atherosclerotic lesions can not only be found in adults but are already present in infants and young children as fatty streaks ¹³⁶.

Arteries are built up by several layers of specialized cells, the **endothelium**, that lines the blood vessel wall immediately adjacent to the lumen through which the blood flows. Beneath the endothelium are several concentric layers of extracellular matrix and cells that make up the artery wall: the **intima** is composed largely of amorphous collagens, proteoglycans, and elastic fibers. The **media**, a well-organized layer of smooth muscle cells whose contraction controls the diameter of the vessel lumen and thus influences blood pressure; and the **adventitia**, a layer of connective tissue and cells that form the interface between the vessel and the adjacent tissue (Figure 1-A).

1.1. RESPONSE TO INJURY HYPOTHESIS

This hypothesis, first introduced by Russell Ross in the early 90^{ies} explains the molecular processes which lead to atherosclerotic lesions ¹⁵⁵.

The impaired function of the vesicular epithelium, caused by several factors such as diabetes, smoking, increased blood pressure, hypercholesterolaemia and low HDL-levels, lead to increased deposition of LDL in the intima. Macrophages in the artery wall endocytose and degrade LDL. The cells become filled with cholesteryl esters in lipid droplets and turn to foam cells. Macrophage foam cells accumulate in the arterial wall and initially form early fatty streaks (Figure 1-B).

The next stage in atherosclerosis is marked by the continued accumulation of macrophage foam cells, T-cells, proliferation of smooth muscle cells, and migration of these cells from the media into the intima. Smooth muscle cells secrete additional extracellular matrix and the early fatty streak grows as the disease progresses, forming an early atherosclerotic plaque (Figure 1-C). As the atherosclerotic plaque grows into the lumen of the artery, it may disrupt and block the blood flow by spontaneous clot formation. In some cases, the plaque alone can fully occlude the artery ¹⁵⁶ (Figure 1-D).

Macrophages not only produce reactive oxygen species, proteases and cytokines they also provide scavenging functions mediated through pattern recognition receptors (PRRs) such as scavenger receptor CD36, SR-BI and SR-A. Those PRRs are rate-limiting in atherosclerosis because they internalize oxidized LDL (OxLDL) which activates macrophages, affects gene expression of e.g. PPAR- γ , CD36 and ABCA1 and leads to the formation of foam cells ¹⁸⁴.

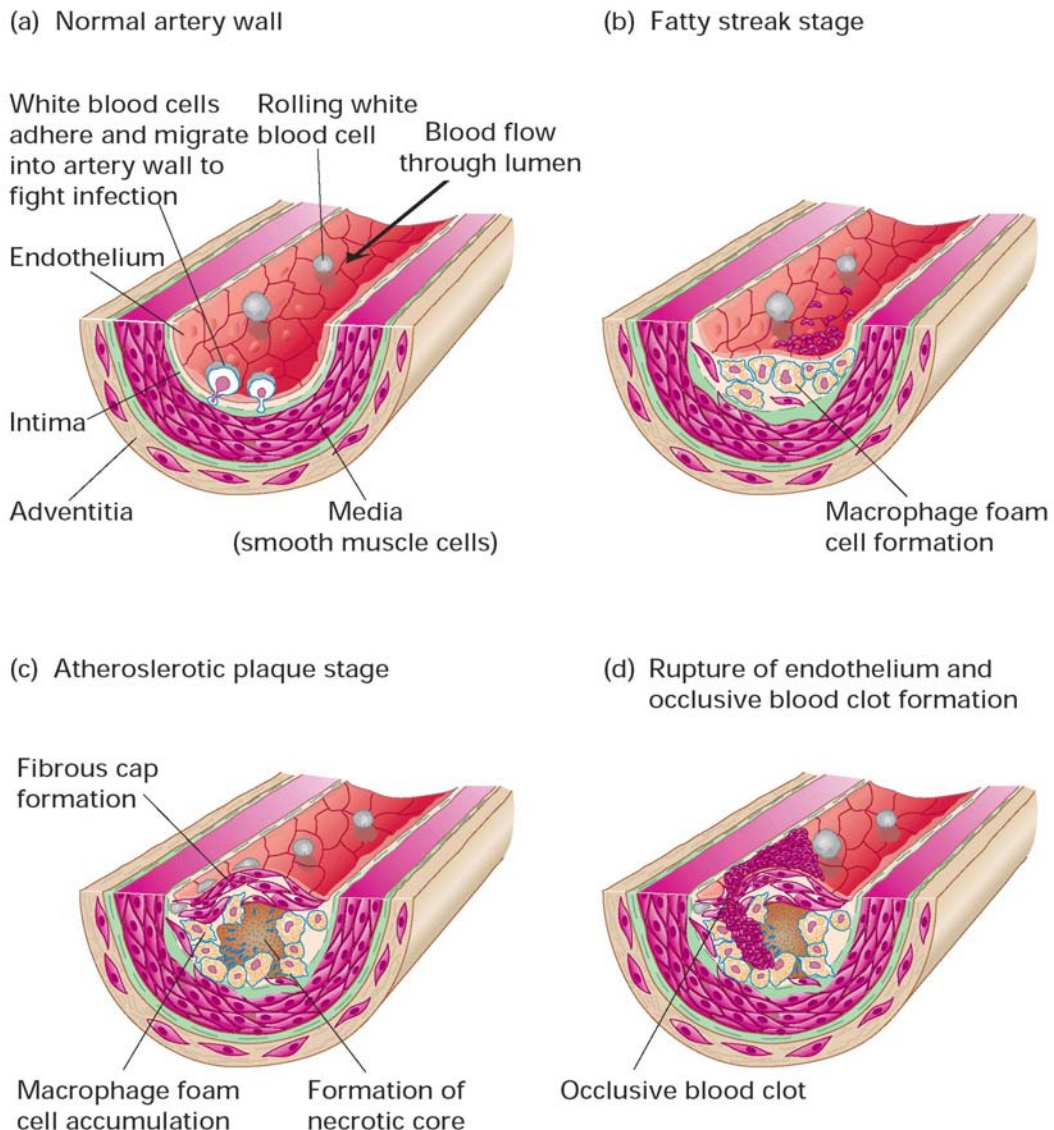


Figure 1: Major stages in the onset and progression of atherosclerosis in the artery wall. (a) The anatomy of a normal artery wall. (b) Accumulation of foam cells produces a fatty streak in the vessel wall that is only visible microscopically. (c) Continued generation of foam cells and migration of smooth muscle cells from the media into the intima is followed by cell death, producing an advanced atherosclerotic plaque. (d) As an atherosclerotic plaque grows into the lumen of the artery, it disrupts and reduces the flow of blood or can fully occlude the artery. [Adapted from Ross ²]

Toll like receptors (TLRs) are expressed in atherosclerotic lesions and may also participate in inflammatory signaling⁵⁶ and a TLR4 polymorphism is associated with reduced atherosclerosis in humans¹⁰¹. CD14, a non-transmembrane receptor for lipopolysaccharide, initiates inflammatory response through interaction with TLRs¹⁶⁹.

The immune response between macrophages and T-lymphocytes leads to proliferation of each of these cell types through IL-2 and colony stimulating factors (CSF's). Cells within the center of the plaque die, producing a necrotic core containing large amounts of cholesteryl esters and unesterified cholesterol.

1.2. RESPONSE TO RETENTION HYPOTHESIS

Schwenke and Carew^{171,172} showed in vivo that accumulation of atherogenic lipoproteins within the arterial wall is concentrated to sites where atheromas develop later on. This indicates that retention and not enhanced lipoprotein influx due to endothelial permeability, is the pathological key event in atherosclerosis. Subsequent studies in several animal models have demonstrated either increased¹⁴⁰ or decreased¹⁷³ rates of lipoprotein entry into atherosclerosis-susceptible sites, suggesting a nonessential role for alterations in endothelial permeability. All studies agree, however, that prelesional susceptible arterial sites show enhanced retention of apoB-rich, atherogenic lipoproteins⁵⁸. Furthermore, at sufficiently high plasma lipoprotein concentrations, lesions develop even at sites of low shear stress, such as non-branch points, or within the pulmonary arteries⁹³. Although stress-induced endothelial changes contribute to atherogenesis, the most directly relevant functional changes at prelesional sites that are susceptible to atherogenesis are turbulent blood flow, altered proteoglycan structure²⁸ and increased lipoprotein retention²⁰³.

The second process that has been proposed to be central to atherogenesis is lipoprotein oxidation^{180,201}. Current evidence indicates that pathophysiologically important oxidation can occur only after the retention of LDL. Following its retention by proteoglycans, LDL undergoes several modifications with important biological consequences. Proteoglycan-bound LDL in vitro forms aggregates⁹⁰ and vesicular structures¹⁸⁶ that resemble material seen in vivo. LDL-proteoglycan complexes show increased susceptibility to oxidation under typical serum-free, albumin-free pro-oxidative experimental conditions⁸⁹. Minimally oxidized LDL induces endothelial and smooth muscle cells to express monocyte chemotactic activity⁴⁵.

The response to retention hypothesis predicts that these vessel wall factors include molecules involved in lipoprotein retention, like proteoglycans, lipoprotein lipase, SMase, apoE, apoB, and apo(a).

2. METABOLISM OF APOB CONTAINING LIPOPROTEINS

In order to make use of dietary lipids, they must first be absorbed from the small intestine in the body. Since these molecules are oils, they are essentially insoluble in the aqueous environment of the intestine. The solubilization (or emulsification) of dietary lipids is therefore accomplished by means of bile salts, which are synthesized from cholesterol in the liver and then stored in the gall bladder; they are secreted following the ingestion of fat.

Dietary triacylglycerols and cholesterol are solubilized in lipid-protein complexes called lipoproteins. These complexes contain triacylglycerol lipid droplets and cholesteryl esters surrounded by the polar phospholipids and proteins identified as apolipoproteins. Lipoproteins differ in their content of proteins and lipids and are classified based on their density:

- Chylomicron: the largest in size and lowest in density due to high lipid/protein ratio.
- VLDL: very low density lipoprotein; 2nd highest in triacylglycerols as % of weight.
- IDL: intermediate density lipoprotein
- LDL: low density lipoprotein, highest in cholesteryl esters as % of weight and leads to lipid deposit in the peripheral tissue.

2.1. CHYLOMICRONS

In the intestine, cholesterol is present in the free, unesterified form. After its absorption, cholesterol - along with TG, PL, and apoproteins - is reassembled into a large micelle called chylomicron which undergoes the exogenous pathway to be transported from the intestine to the liver. There, cholesterol is esterified to fatty acid by an enzyme called Acyl coenzyme A:cholesterol acyltransferase (ACAT), in the plasma this is done by lecithin-cholesterol acyltransferase (LCAT).

Afterwards, cholesterol is either transported via the endogenous pathway from the liver to be stored in peripheral tissues, or it undergoes the reverse cholesterol pathway which transports it from peripheral tissues towards the liver, where it is excreted via the bile.

Chylomicrons are synthesized in the intestinal tract and transport dietary fats, cholesterol and fat-soluble nutrients (vitamins etc.) Triglycerides are hydrolyzed by lipoprotein lipase (LPL) which is activated by ApoC-II. This hydrolysis reduces the surface area of chylomicrons and fatty acids are released. The remnant particles, rich in cholesteryl esters and ApoE, are taken up by receptors on hepatocytes and removed from the circulation. Chylomicrons are normally not detectable in the postprandial state.

2.2. VERY LOW DENSITY LIPOPROTEIN (VLDL)

VLDL contains ApoB100 and phospholipids and is involved in the transport of triglycerides from the liver to peripheral tissues. The cholesterol in VLDL is either synthesized in the liver or is derived via chylomicron remnants. After secretion VLDL acquires ApoCII and ApoE from HDL. The size of VLDL is determined by the availability of triglycerides, large VLDL particles result from excess triglycerides such as in insulin resistance. Small VLDL particles result from limited triglyceride availability, those particles, rich in cholesterol, are secreted during weight loss.

The triglycerides and fatty acids in the VLDL are hydrolyzed by LPL in the peripheral tissues and VLDL shrinks in size, becoming IDL which is taken up by a receptor mediated pathway in the liver.

2.3. LOW DENSITY LIPOPROTEIN (LDL)

LDL mainly contains cholesteryl esters and ApoB100 and is formed from the catabolism of VLDL and IDL. The main factor controlling the clearance of LDL from the plasma is the availability and activity of the LDL-receptor (LDLR)^{6,67}. After internalization, LDL is either degraded by the lysosome (Figure 2) or directly re-secreted by the liver via retroendocytosis⁷¹. Macrophages take up LDL by scavenger receptors, which is not feedback-regulated thus leading to extensive LDL-uptake and diverting macrophages to foam cells. This occurs at normal LDL concentrations and is enhanced when LDL is elevated or modified by enzymes or oxidants. Another internalization pathway is via the LDL-receptor which is feedback-regulated.

2.4. LDL-RECEPTOR

The level of plasma LDL is regulated by the LDL receptor, a cell surface glycoprotein that removes VLDL, IDL and LDL from plasma by receptor-mediated endocytosis. These LDL receptors are found on all cells with predominance on hepatocytes and steroid hormone-producing cells. Defects in the gene encoding the LDL receptor lead to familial hypercholesterolemia (FH) a disease associated with elevated plasma LDL levels and coronary atherosclerosis. In the liver, the number of LDL-receptors is regulated by the cholesterol content of the hepatocyte. When the cholesterol content of hepatocytes is raised by ingestion of diets high in saturated fat and cholesterol, LDL receptors are reduced and plasma LDL levels rise. Conversely, lowering the cholesterol content of hepatocytes stimulates LDL receptor production and lowers plasma LDL levels^{25,82}.

The LDL receptor gene is located on the short arm of chromosome 19¹¹⁹. It consists of 18 exons and 17 introns that span 45 kilobases (kb)¹⁸². The amino-terminus of the protein contains the LDL-binding elements that recognize ApoB:100, the major apolipoprotein in LDL. LDL-receptor mediated cholesterol uptake downregulates intracellular cholesterol synthesis by inhibition of 3-hydroxy-3-methylglutaryl-coenzyme A (HMGCoA) reductase and also the LDL-receptor expression to limit cholesterol uptake. Concomitantly, cholesterol released from the LDL degradation pathway is esterified by acyl coenzyme A:cholesterol acyltransferase (ACAT) and stored in lipid droplets.

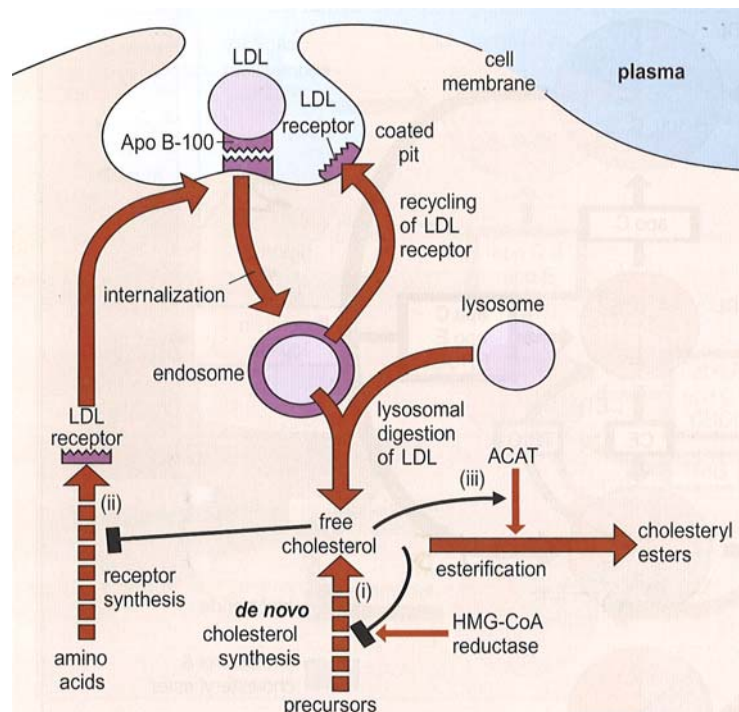


Figure 2: LDL uptake and metabolism. After uptake of LDL by the feedback-regulated LDL-receptor it is degraded in the lysosome [Adapted from Alberts 2003]

2.5. NIEMANN-PICK DISEASE TYPE C, A CHOLESTEROL TRAFFIC DISORDER

After leaving the endosome, cholesterol trafficking critically depends on lipid trafficking effector proteins. Two genes are involved in this post-endosomal traffic, namely: NPC1 and NPC2, mutations in these genes cause the autosomal recessive neurovascular lipid storage disorder Niemann-Pick type C disease (NPC)^{23,122,149}. One of the most striking abnormalities in affected cells is the accumulation of LDL-derived free cholesterol in late endosomes, lysosomes and the Golgi apparatus^{18,148}. In contrast to TD, plasma

lipoprotein levels are only slightly affected with a 20-30% reduction in HDL-cholesterol³⁷ and the patients do not develop vascular disease. In fibroblasts from individuals with NPC, LDL-derived cholesterol accumulates in lysosomes and the transport to the ER and the plasma membrane is delayed compared with normal cells. Normal feedback regulation of cholesterol homeostasis by oxysterols and de novo synthesized cholesterol suggests that the regulatory machinery in NPC cells is intact but that the transport of LDL-cholesterol to regulatory sites is compromised¹²¹.

The first gene mutated in NPC, NPC1, was identified by Carstea et al.²⁹ and it was shown that transport of the NPC1 protein to the cholesterol-laden lysosomal compartment is essential for expression of its biologic activity¹⁹⁸. NPC1 is an eukaryotic member of the resistance-nodulation-division (RND) permease family. Its detailed biologic role is still unclear, however, a recent study demonstrated that it functions as a transmembrane efflux pump which exports accumulated acriflavine from the endosomal / lysosomal system⁴⁶, Figure 3 shows the NPC gene mutation and it's effect.

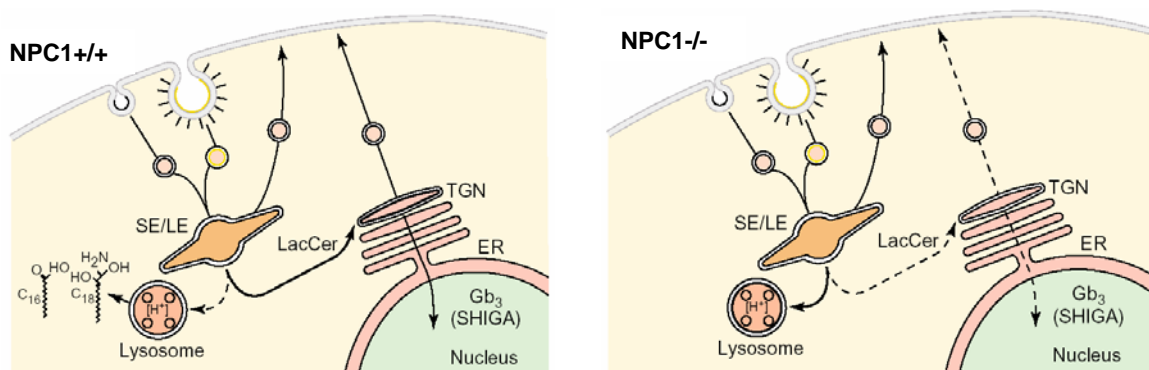


Figure 3: Disturbed vesicular trafficking leads to lipid accumulation in endosomal compartments. 1. In the normal state, lipids are endocytosed and then trafficked through the TGN towards the cell surface where it is exocytosed. 2. in the case of NPC^{-/-} the lipids are shunted towards the lysosome and degraded there. Thus, leaving NPC patients without a cholesterol pool [Figure adapted from Alberts, 2003].

Recently, the cholesterol binding molecule HE1¹⁴⁴, originally identified as a major secretory protein of the human epididymis¹⁰³ was reported as the second gene (NPC2) causing Niemann-Pick disease¹³⁷.

3. MODIFIED LOW DENSITY LIPOPROTEINS

LDL has a density ranging from 1,019 -1,063 g/ml and an average diameter of 22 nm. It is composed mainly from cholesterol esters, free cholesterol, phospholipids and triglycerides. The main protein component is ApoB-100⁶⁹.

Native LDL has been shown not to induce foam cell formation⁸¹ but depends on atherogenic modification of LDL¹³². Native LDL is taken up by endocytosis via the LDLR which is feedback regulated whereas modified LDLs are assimilated by scavenger receptors not underlying this feedback mechanism, leading to an uncontrolled accumulation of cholesterol in the cells and subsequent foam cell formation⁴⁷.

While oxidation of lipoproteins²⁰⁸ is the most studied modification, recently other types of modifications like enzymatic modification¹⁵ and acetylation⁶⁸ attracted increasing interest as potentially important in atherosclerosis.

3.1. ENZYMATICALLY MODIFIED LOW DENSITY LIPOPROTEIN (E-LDL)

Bhakdi et al. postulated that extracellular, enzymatic modification of LDL in atherosclerotic lesions contributes mainly to the initiation of atherosclerosis. Combined treatment with trypsin, cholesterol esterase, and neuraminidase transforms LDL, but not HDL or VLDL, to particles with properties similar to those of lipid extracted from atherosclerotic lesions. The mechanism proposed is that the proteolytic nicking of Apo-B by trypsin renders cholesterol esters accessible to the action of cholesterol esterase. E-LDL is rapidly taken up by human macrophages to an extent exceeding the uptake of acetylated LDL (Ac-LDL) or oxidatively modified LDL (Ox-LDL)¹⁶. *In-vitro* E-LDL, similar to aggregated LDL found in lesions, fuse to a particle size of 200 nm in diameter. Moreover, E-LDL is much more potent in transforming macrophages into foam cells than Ox-LDL¹⁰⁰. Upon the enzymes that can modify E-LDL and are detected in the intima of arteries are: trypsin, plasmin, metalloproteases, lysosomal acid lipase (LAL), phospholipase A2 and cholinesterase⁷⁷.

3.2. OXIDIZED LOW DENSITY LIPOPROTEIN (OX-LDL)

LDL oxidation involves oxidative modification of apolipoprotein B-100 (ApoB-100) in addition to lipid peroxidation. Many reactive radical species can initiate lipid peroxidation. These reactions involve lipoxygenases, superoxide anions, hydroxyl radicals, peroxynitrite, heme proteins, ceruloplasmin and myeloperoxidase²⁰².

Oxidation of LDL is believed to occur mainly in the extracellular matrix of the arterial intima. Ox-LDL accumulates in macrophages and in foam cells in atherosclerotic lesions. Ox-LDL exerts both proliferation and apoptosis in vascular cells, depending on its concentration and the exposure time. Low Ox-LDL concentrations (<10 µg/mL) induced proliferation, while higher concentrations (50-300 µg/mL) induced apoptotic cell death⁶². It is specifically taken up by macrophages via scavenger receptors (SR) and induces the production of M-CSF which markedly and selectively increases the synthesis of type I and type II class-A macrophage scavenger receptors, again leading to an increase in Ox-LDL

uptake. Figure 6 shows the internalization steps of minimally oxidized LDL through clathrin dependent endocytosis.

4. CHOLESTEROL INFLUX PATHWAYS

Accumulation of cholesterol in artery walls characterizes the onset of atherosclerosis. This accumulation is subject to a tight homeostasis and follows several intake models. This homeostasis depends on the cellular uptake of LDL and the ongoing retention of LDL in the vessel wall. This retention underlies the physical and chemical characteristics of the involved lipoproteins. LDL is a 22 nm particle covered mainly with the hydrophobic apolipoprotein apoB100 whereas HDL is only 5-12 nm in size and is partially covered with the amphiphilic apolipoproteins: apoA1, apoAII, apoE and apoA. The smaller size and the relative lack of affinity to the vessel wall allow HDL to transit through the vessel wall without retention, leading to depletion of the atherogenic LDL. Several pathways have been suggested for cholesterol entry into the cell. Studies indicate that the endothelium actively takes up lipoproteins and transports them into the subendothelial space. The type of entry differs according to the type of LDL.

While Ox-LDL enters mainly via the scavenger receptors, aggregated LDL is taken up by phagocytosis and is rapidly degraded in lysosomes. Several receptors have been shown to be implicated in the cholesterol accumulation in macrophages (Table 1).

4.1. CLATHRIN-DEPENDENT ENDOCYTOSIS

Uptake of LDL via clathrin-coated vesicles is typically a pathway for receptor mediated

Receptor	Lipoprotein ligands
apoB48	chylomicrons, hypertriglyceridemic-VLDL
CD36	VLDL, LDL, HDL, AcLDL, OxLDL
CD68/macrosialin	AcLDL, OxLDL
CLA-1/SR-BI (CD36 and LIMPII analogous-1/scavenger receptor BI)	VLDL, LDL, HDL, AcLDL, OxLDL
Fc gamma RII-B2	OxLDL
LDL (low density lipoprotein)	LDL, β -VLDL
LOX-1 (lectin-like oxidized LDL receptor-1)	OxLDL
LRP (lipoprotein receptor-related protein)	β -VLDL
LSR (lipolysis stimulated receptor)	chylomicron remnants, VLDL
SR-AI (scavenger receptor-AI)	AcLDL, OxLDL
SR-PSOX (scavenger receptor that binds phosphatidylserine and oxidized lipoprotein)	OxLDL
VLDL (very low density lipoprotein)	chylomicron remnants, VLDL, lipoprotein(a)

Table 1: Receptors implicated in cholesterol accumulation. The table shows the receptors expressed in macrophages and their lipoprotein ligands.

uptake of lipoproteins. Cells have receptors for LDL, β -VLDL and modified forms of LDL such as Ox-LDL. Apo-B containing lipoproteins taken up into coated vesicles are delivered to lysosomes¹⁰⁹, where they are degraded to amino acids, unesterified cholesterol and fatty acids, this pathway is actin-independent and leads to LDL uptake via peripheral surface-connected tubules.

Three major steps are involved in this type of endocytosis:

- *Clathrin-pit formation*: clathrin coat assembly is initiated by the binding of coat components to a docking site at the plasma membrane. First, transmembrane receptors bind to the heterotetrameric adaptor protein complex (AP-2), this complex binds to clathrin which polymerizes into a grid, pulling the plasma membrane inside¹⁵² (Figure 4).

This action requires local changes in phospholipids composition leading to changes in the membrane curvature. Once the inward bending of the membrane is complete, the vesicle is separated from the membrane. To date, four ubiquitously expressed AP complexes have been identified in human and mouse: AP-1, AP-2, AP-3 and AP-4. In 1986, Goldstein et al. demonstrated that the LDL-R from a hypercholesterolemia patient revealed a mutation which led to an impaired internalization of the receptor. This led to

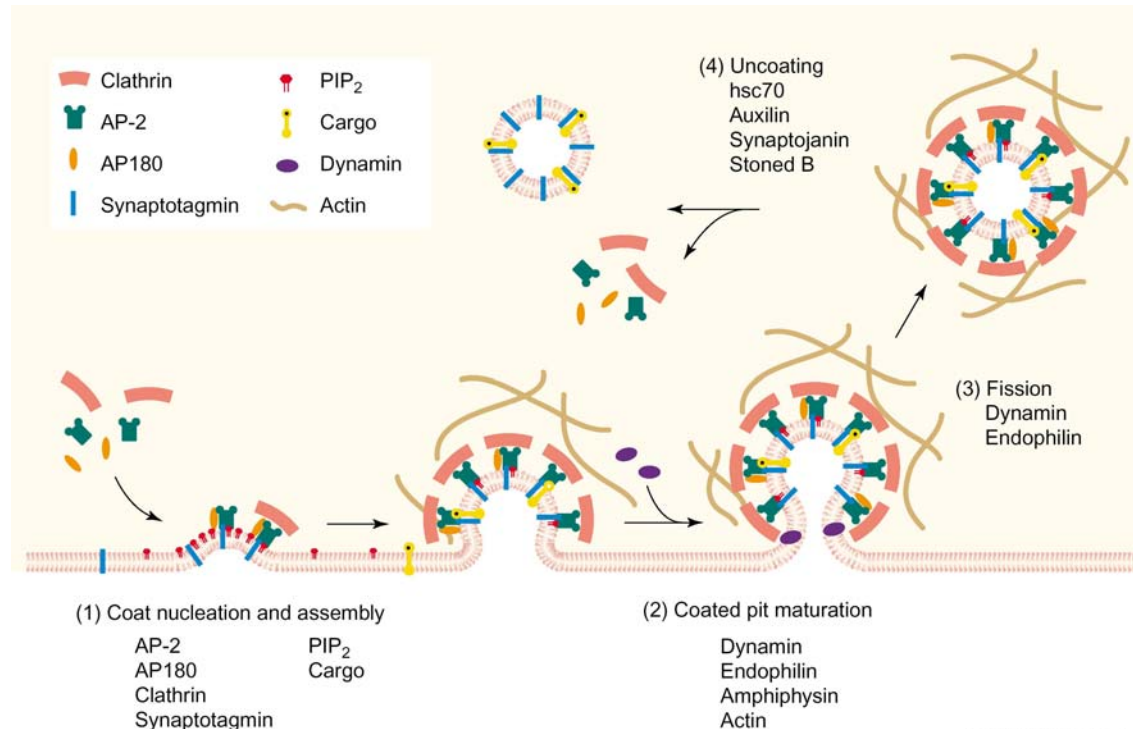


Figure 4: Clathrin coated-pit endocytosis. The assembly of clathrin molecules on the pit leads to invagination of the pit. Clathrin coated pits move in the plane of the membrane, but are also tethered to cytoskeletal elements, like actin. After the pit has fissioned from the membrane by the influence of dynamin, clathrin is recycled [Adapted from Takei¹⁸⁷

the discovery of an endocytosis signal which involves tyrosine- and leucine-based motifs¹³⁵. The leucine motif further provides a signal for lysosomal sorting.

- *Early endosome fusion:* After the pit is internalized and converted into a clathrin coated vesicle, the clathrin coat is removed. Two proteins involved in this step are: Rab5 and early endosomal antigen-1 (EEA-1). In addition to endosome fusion, Rab5 mediates the movement of the endosome along the cytoskeleton.

At this stage, Phosphatidylinositol-3-phosphate (PI3P), a product of PI3-Kinase, is enriched in early endosomes and contributes to endosome fusion. Furthermore, soluble *N*-ethylmaleimide-sensitive factor attachment protein receptors (SNAREs) are required for endosome fusion (e.g. syntaxins, synaptotagmin).

- *Late endosome formation:* Until now it is unclear whether transport vehicles move cargo between early endosomes (EE) and late endosomes (LE), or whether EE mature into LE. However, LE tend to be more acidic (pH 5,5 in comparison to 6,5 in EE) and spherical in shape.

It seems that ubiquitination is an essential step for many proteins to move from the EE to LE. As example, the clathrin-dependent internalization of Ox-LDL is shown in figure 5.

4.2. CLATHRIN-INDEPENDENT ENDOCYTOSIS

A variety of pathways do not utilize clathrin but are responsible for uptake of large particles, these include:

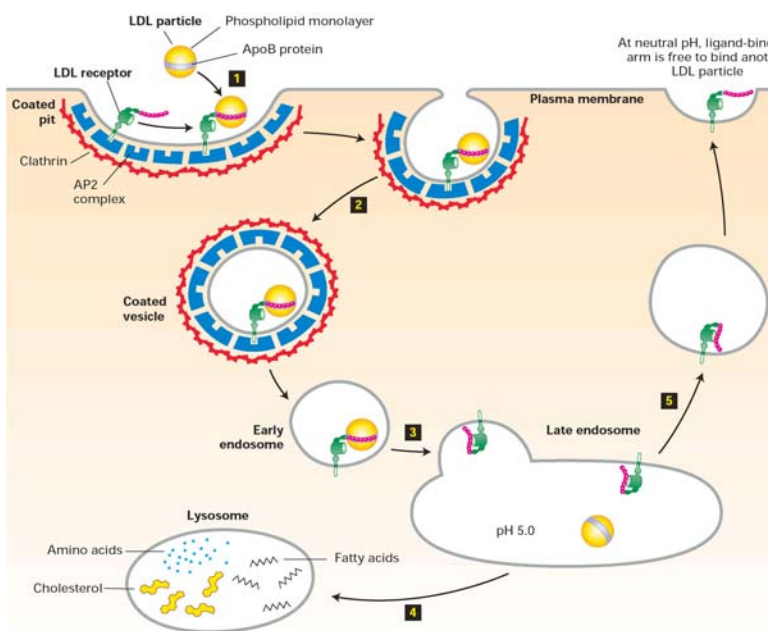


Figure 5: Clathrin-dependent internalization of mildly oxidized LDL.

(1) The LDL receptors bind to apoB embedded in the phospholipid layer of LDL particles. Interaction between the LDL receptor and the AP2 complex incorporates the receptor-ligand complex forming endocytic vesicles. (2) Clathrin-coated pits are pinched off by the same mechanism used to form clathrin/AP1 vesicles on the TGN. (3) After the vesicle coat is shed, the uncoated endocytic vesicle (early endosome) fuses with the late endosome. (4) The acidic pH causes a conformational change in the LDL receptor leading to release of the bound LDL particle. The late endosome fuses with the lysosome, and the proteins and lipids of the free LDL particle are broken down by enzymes in the lysosome. (5) The LDL receptor recycles to the cell surface where it can bind another LDL particle. Brown and Goldstein²² [Adapted from Alberts 2003].

- Phagocytosis
- Caveolin-dependent endocytosis
- Pinocytosis
- Novel pathways

4.2.1. PHAGOCYTOSIS

Phagocytosis is an actin-dependent process by which large particles are taken up by macrophages. This type of endocytosis is triggered by binding of the particle to the cell-surface receptors capable of transducing a phagocytic stimulus. This results in localized exocytosis at the site of particle attachment and subsequent pseudopodia extension that wraps around and engulfs the bound particle into a cytoplasmic phagosome. Phagocytosis is usually restricted to macrophages and other phagocytes specialized in uptake and digestion of large particles. Macrophages take up aggregated LDL by phagocytosis which leads to rapid lysosomal degradation of the aggregated LDL, since this pathway is not feedback regulated by cholesterol. According of the kind of membrane folding, two types of phagocytosis can be observed (Figure 6).

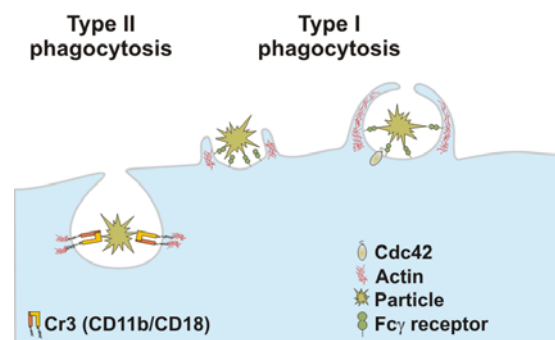


Figure 6. The two types of phagocytosis. To the left: type-II phagocytosis, to the right: type-I phagocytosis. Adapted from Castellano et.al.³¹.

Type-I phagocytosis: This type of phagocytosis is mediated by Fc γ -receptors (CD64, CD32, and CD16); it occurs via the 'zipper' mechanism and uses the GTP-ases Cdc42 and Rac.

Type-II phagocytosis: This phagocytosis is complement receptor-mediated (CR3: CD11b; CD18) and particles 'sink' into the cell. This mechanism uses the GTPase Rho.

4.2.2. PINOCYTOSIS AND MACROPINOCYTOSIS

Pinocytosis is one of the pathways for cellular uptake and transport of lipoproteins, in this mechanism dissolved substances and particles of about 70 nm are being taken up non-selectively, thus, all lipoproteins small enough to enter the pinocytic vesicles can be

transported in this manner. Chylomicrons for instance are too big (>75 nm) to enter the pinocytotic vesicles, explaining why they don't enter the vessel wall and therefore are not associated with atherosclerosis. Pinocytotic vesicles accumulate bulk plasma fluid at the luminal side of the endothelium and then transport the fluid and its constituents to the abluminal side of the endothelium where the vesicle contents are released¹²³.

Macropinocytosis refers to the formation of large and irregular actin-driven invaginations of the plasma membrane leading to primary endocytic vesicles (typically 0,5-2,5 μ M in diameter) by the closure of lamellipodia. They frequently move inwards towards the centre of the cell, and persist for approximately 5–20 min¹⁸⁵.

The membrane components of macropinosomes are likely to be recycled back to the plasma membrane over a similar time-scale, potentially passing via other organelles within the cell, and macropinosomes must recruit specific machinery in order to do this. Membrane recycling between the plasma membrane and endosomal compartments during macropinocytosis is most likely regulated by the small GTPase ARF6 and its related protein ADP-ribosylation factor-like 7 (ARL7).

This pathway is distinguished from other pinocytic pathways by its susceptibility to agents, which depolymerize actin and tubulin. Macropinocytosis might account for some of the pinocytosis observed when clathrin dependent endocytosis is inhibited. Formation of the macropinosome generally involves the protein dynamin.

4.2.3. CAVEOLIN-DEPENDENT ENDOCYTOSIS

Caveolae are flask-shaped, non-coated plasma membrane invaginations present in many cell types, especially in endothelial cells. Biochemically, caveolae can be isolated as detergent-resistant membranes (DRMs) enriched in cholesterol and glycosphingolipids, a characteristic shared with lipid rafts and other membrane microdomains¹¹⁴. Several membrane receptors, signaling molecules and membrane transporters localize to caveolae as well as molecules found within lipid rafts. The finding that caveolae contain one key element of the machinery involved in vesicle budding, the GTPase dynamin 15 and dynamin 16, suggests that they also participate in membrane internalization. The fact that elements of the docking and fusion machinery, such as SNARE proteins, are enriched in caveolae strengthens this theory¹⁶⁸.

Insight into the mechanism of caveolar internalization of cell-surface molecules has been obtained by visualizing the cargo that internalizes through caveolae. It is important to point out that, in contrast to classic clathrin-dependent endocytosis, the caveolar internalization pathway seems to bypass lysosomes. Internalized caveolae fuse with caveosomes, and the caveosomes deliver their contents into other subcellular (non-lysosomal)

compartments. The bypass of the acidic and harmful milieu might be a major advantage for the SV40 virus which uses caveolae to gain entry into the cell, where ultimately it is delivered to the ER ¹⁴².

Owing to their cholesterol binding ability, caveolae are undoubtedly involved in cholesterol transport and homeostasis ⁵⁹.

Whether the presence of caveolin, which distinguishes caveolae from other lipid rafts, could play the role of a classical coat by providing the driving force necessary for membrane deformation remains a matter of debate.

4.2.4. NOVEL UPTAKE MECHANISMS

In addition to this established uptake pathways, newly defined mechanisms have been elucidated. They are summarized in the following sections:

4.2.4.1 SURFACE CONNECTED COMPARTMENTS (SSC)

The existence of alternative cellular lipid transport routes along continuous tubular membrane complexes is also supported by the observations that macrophages can endocytose LDL via "surface connected compartments", plasma membrane invaginations that are directly connected to the cell surface ¹¹⁰. LDL liposomes enter the surface connected compartments in macrophages through a unique endocytic pathway which involves ApoE, this uptake did not occur through LDL-receptors, LDL-receptor-related proteins, or scavenger receptors. Aggregated LDL enters surface-connected membrane bound compartments (SSC) and is mostly stored rather than degraded ¹¹².

4.2.4.2 ENDOCYTOSIS THROUGH COMPARTMENTS INVOLVING CD14

Another alternative tubular transport route for lipophilic substrates has been reported by Thieblemont involving the cellular uptake of bacterial lipopolysaccharides LPS-micelles via CD14 a GPI-anchored receptor. It could be demonstrated that LPS is imported into the Golgi of polymorphonuclear leukocytes and HeLa cells independently from the endosomal and lysosomal endocytotic pathway ¹⁸⁹. Soluble CD14, the shedded form of the LPS-receptor glycoprotein is found in plasma and acts as a shuttle for LPS and lysophospholipids and can mediate efflux from THP-1 cells ¹⁸³. It has been shown that treatment of cells with LPS leads to an increase of ABCA1 expression through an LXR-independent pathway. Nevertheless, induction of LPS led to reduced HDL levels. This is possibly due to reduction of ApoAI, ApoE, LCAT and CETP.

In light of these independent observations, it can be postulated that (i) the cell surface and cell organelles, in addition to established lipid trafficking routes, are capable of interacting

with each other via continuous membrane systems and (ii) that these membrane structures provide a morphologic basis for alternative cellular lipid transport mechanisms. This implies that translocation processes of lipid substrates along tubular membrane compartments may be involved in important physiologic functions in cellular lipid transport. For example, it is conceivable that the known translocation of metabolites of the cholesterol biosynthesis pathway between the ER and peroxisomes occurs via continuous tubular membrane systems.

4.2.4.3. DEEP TUBULAR INVAGINATIONS

Deep tubular invaginations are hardly detectable in normal electron microscopy, but their existence is revealed by exposure of mucosal tissue to the non permeable surface marker Ruthenium Red. They appear as a part of the apical surface of the enterocyte. In some cases, they can be seen penetrating up to 0,5-1 μm into the cytoplasm, a distance sufficient to reach across the terminal web and obtain a close proximity to the subapical compartment (SAC).

Caveolin-1, a frequently used marker for lipid rafts and caveolae, as well as the glycolipid GM1, distinctly localize to deep apical tubules.

Annexin A2, another protein known to be associated with lipid rafts and proposed to be involved in membrane trafficking events, is also present in deep apical tubules. Annexin A2 is capable of interacting with actin and actin-binding proteins such as α -actinin, ezrin, and moesin, and thus to function as an interface between lipid raft membranes and the actin cytoskeleton⁷⁸. It is also a known substrate for protein kinases, including protein kinase C.

CD13 is also present in deep tubular invaginations and is the target for ezetrol, a specific inhibitor of intestinal cholesterol absorption, which blocks endocytosis of cholesterol-rich membrane microdomains, thereby limiting intestinal cholesterol absorption¹⁰⁶. Deep tubular invaginations connect to the NPC1 and NPC1L pathway that direct exogenous cholesterol towards late endosomes. NPC1 and its homologue NPC1L may belong to a family of related proteins that have similar functions at different subcellular locations, perhaps at sequential steps of the same cholesterol transport pathway⁹².

This particular transcytotic trafficking route has been studied intensively for many years revealing details in the intracellular transport events leading from internalization into basolateral early endosomes, via a common endosome, to an apical recycling endosome before secretion from the apical surface. The apical recycling endosome, also referred to as the SAC, is crucial in sorting of both proteins and lipids in dynamic transit between the basolateral and apical plasma membrane domains. The SAC is the last known stage in

the basolateral-to-apical transcytotic pathway, and in the enterocyte, it is typically found in the apical cytoplasm just beneath the terminal web region. Deep apical tubules are the only part of the brush border surface directly accessible to membrane traffic from the SAC and are often seen in very close proximity to this endosomal compartment, lending support to the notion that elements of the SAC may fuse directly with the cell surface. Alternatively, the final stage of transport could be vesicle-mediated, but regardless of the mechanism, the function of deep apical tubules is that of a hub in the final exocytotic stage of transcytosis, a process that has previously been shown to occur through lipid raft containing compartments in enterocytes.

Aggregated LDL enters the macrophage vacuolar labyrinth which remains connected to the macrophage surface by the surface invagination, where it remains before it is degraded by fusion with primary lysosomes. Plasmin-mediated LDL-degradation, reverts LDL aggregation allowing disaggregated LDL to efflux from the open surface-connected compartments back to the extracellular space.

4.2.4.4. CONTINUOUS CELLULAR MEMBRANE SYSTEM

Scow and Blanchette-Mackie 174 demonstrated the existence of continuous cellular membrane systems in brown and white fat cells, along which lipids such as fatty acids and monoacylglycerols are translocated via lateral movement as shown in figure 7.

The external leaflet of the plasma membrane of the endothelial cell and that of the adipocyte form a continuum at the site of contact between the cells. The interfacial continuum would include the chylomicron surface film when the surface film is fused temporarily with the external leaflet of the endothelial plasma membrane. FA formed by lipoprotein lipase are expected to enter the continuum from the capillary lumen, move in the continuum to the ER of the adipocyte, leave the continuum after reesterification to triacylglycerol and then accumulate as lipid droplets between leaflets of the reticulum. FA formed by action of tissue lipase on intracellular triacylglycerol would reenter the continuum at the site of lipolysis in the ER, move along the continuum to mitochondria, and leave the continuum after activation of FA in the outer mitochondrial membrane for transfer to the inner mitochondrial membrane.

In neuroendocrine PC12 cells, a tubular subplasmalemmal membrane system was identified that is continuously connected with the plasma membrane and from which synaptic-like microvesicles (SLMV) originate¹⁶⁰.

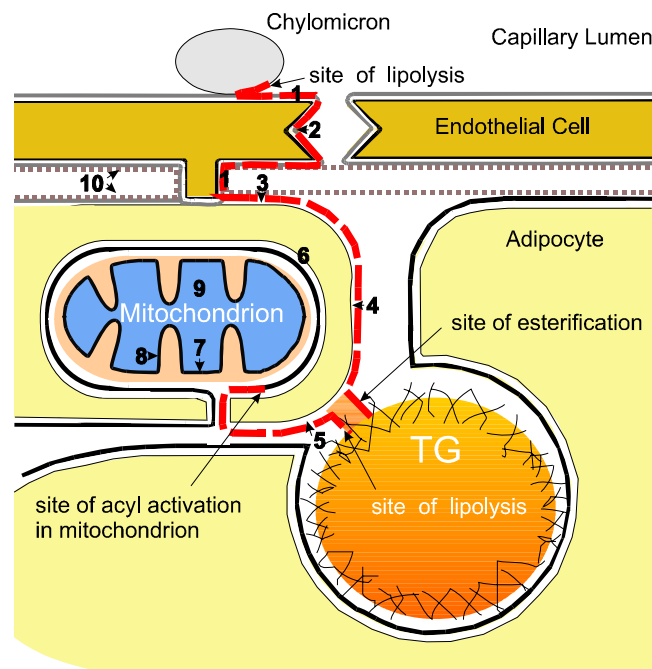


Figure 7: Alternative lipid transport routes for transport of fatty acids (FA) from capillary lumen to adipocytes. 1. plasma membrane of endothelium, 2. membrane of transcellular channels in endothelium, 3. plasma membrane of adipocytes, 4. Membrane of surface-connected channels, 5. ER-membrane, 6. Outer mitochondrial membrane in adipocytes. [According to Blanchette-Mackie and Scow¹⁹].

Recent experiments show that endophilin I, in conjunction with the GTPase dynamin, plays a critical role in the segregation of SLMV from the plasma membrane¹⁶¹. Moreover, we were able to detect SLMV in steroidogenic cells (Orsó and Schmitz, unpublished data).

5. METABOLISM OF APO-AI CONTAINING HIGH DENSITY LIPOPROTEIN (HDL)

High-density lipoprotein (HDL) is an acceptor of free cholesterol and in concert with cholesteryl ester transfer protein (CETP), lipoprotein lipase (LPL), hepatic lipase (HL) and lecithin:cholesterol acyltransferase (LCAT) it mediates the transport of cholesterol from peripheral tissues to the liver for elimination from the body, a mechanism called “reverse cholesterol transport”.

Lipid-poor apoA-I (pre β -HDL) is mainly synthesized in the liver, intestinal mucosa cells and nascent HDL acquires phospholipids, free cholesterol and apoE during maturation. Pre β -HDL is produced by interaction of apoA-I, the major apolipoprotein in HDL, with ABCA1. Free cholesterol transferred from the cell to HDL, is esterified by LCAT, which is activated by apoA-I. This increases the density of HDL particles which are thus converted from HDL₃ to the denser HDL₂. HDL₂ exchanges cholesterol for triglycerides, a process mediated by CETP and PLTP. Cholesteryl esters are taken up by the liver for further

excretion into the bile. HDLs are believed to be antiatherogenic by several mechanisms including reverse cholesterol transport (RCT), inhibition of cytokine induced expression of adhesion molecules by endothelial cells and protection of LDL from oxidation. In particular, participation of HDL in the RCT pathway is considered to be most important in preventing atherosclerosis development by delivering cholesterol synthesized or stored in peripheral tissues to the liver for ultimate excretion.

5.1. CHOLESTEROL EFFLUX FROM MACROPHAGES

Macrophages can excrete the cholesterol they accumulate through many processes. Most of these processes involve the use of lipid particles rich in phospholipids which remove cholesterol from the macrophage. HDLs are specialized lipoprotein cholesterol acceptors containing amphipathic apolipoproteins like apoA1 that circulate in the blood and are present in atherosclerotic plaques¹⁷⁸. When incubated with macrophages they induce cholesterol efflux¹⁶⁷, by stimulating translocation of cholesterol from intracellular membranes to the plasma membrane⁸. Then, HDL acquires excess plasma membrane cholesterol¹⁴⁵.

ATP-binding cassette transporter A1 (ABCA1), a protein mutated in Tangier Disease, functions in the lipidation of the amphipathic apolipoproteins apoA1 and apoAIV, a required step for these apolipoproteins to stimulate cholesterol efflux¹⁶⁶.

Macrophages also can produce their own HDL particles that mediate macrophage cholesterol efflux through an autocrine/paracrine mechanism. This occurs when macrophages secrete apolipoprotein E (apoE) and PLTP which associate with macrophage phospholipids (possibly similar to exogenous amphipathic apolipoproteins) to form apoE-phospholipid discoidal complexes¹¹¹. Macrophage specific expression of human apoE reduces atherosclerosis in hypercholesterolemic apoE-null mice, supporting a possible function of macrophage-produced apoE within atherosclerotic plaques in promoting cholesterol efflux. In the presence of HDL the resecretion of apoE and cholesterol leads to the formation of apoE/cholesterol-enriched HDL particles. Furthermore, apoE recycling involves the internalization of HDL₃-derived apoA1 and its targeting to apoE/cholesterol-containing endosomes. Subsequently, HDL could interact with ATP-binding cassette transporter A1 (ABCA1)¹⁶⁵ and scavenger receptor class B type I (SR-BI) at the cell surface²⁰⁵, leading to cholesterol efflux.

Alternatively, macrophages can secrete CETP/apoC1 containing lipoprotein particles upon stimulation with apoA1.

After cholesterol is incorporated into HDL, it is esterified by lecithin:cholesterol acyl transferase (LCAT), an enzyme present in the plasma. Large HDL particles can transfer

their cholesteryl esters to other apoB-containing lipoproteins through cholesteryl ester-transfer protein (CETP) or to cells (e.g. liver and steroidogenic cells) through SR-BI receptors. Selective uptake of cholesteryl esters from HDL can also be mediated by the SR-BI receptors. After HDL binds to SR-BI, cholesteryl esters in the core are selectively transferred to the cell membrane and then translocated into the cytosol. The remaining lipid-depleted HDL particle rapidly dissociates from the receptor and returns to the circulation¹⁰⁷.

Studies conducted by Peng et. al,¹⁴⁷ showed that SR-BI is not strongly associated with detergent resistant membranes (DRM's) also called "rafts". This observation raises an important issue of lipids in these DRMs where SR-BI mediates HDL uptake of cholesterol thus mediating a bidirectional flux of free cholesterol between the membrane and HDL. It has been shown that liposomes rich in unesterified cholesterol (UC) are able to carry cholesterol during cholesterol excretion from macrophages. Similar liposome accumulation of cholesterol can be seen in patients with defective NPC1 protein.

5.2. MULTIPLE PATHWAYS FOR CELLULAR CHOLESTEROL EFFLUX

Three pathways are currently known by which cellular cholesterol is transported out of the cell and HDL is the acceptor of cellular lipids.

5.2.1. PASSIVE DIFFUSION

In this mechanism, also called diffusion-mediated cell cholesterol efflux, cholesterol diffuses to the HDL particle in a passive way. This pathway predominates in erythrocytes in the absence of vesicular transport in these cells⁵¹. Free cholesterol molecules spontaneously desorb from the plasma membrane, diffuse through the aqueous phase and subsequently incorporate into HDL particles¹²⁸. A variety of acceptors can mediate this diffusion, namely: LDL, globulins, phospholipid vesicles and cyclodextrins, (nicely reviewed in¹⁵⁷). During this reaction, cholesterol is mainly mobilized from the plasma membrane compartment rather than from intracellular compartments⁷⁹.

Net cholesterol efflux is regulated by the gradient of free cholesterol contents between the acceptor and donor cell membrane compartments and by the acceptor's ability for cholesterol adsorption and desorption. Consequently, the reaction is mostly bidirectional and is driven by the phospholipid content of lipoprotein acceptors, but does not involve any specific factor such as HDL binding to the cell or intracellular signaling pathways. However, HDL particles are excellent physiological acceptors involved in passive diffusion because of the ability of the HDL particle to esterify free cholesterol through the action of its associated enzyme lecithin:cholesterol acyltransferase (LCAT)¹². In conclusion, active

esterification of cholesterol within the HDL particle by LCAT plays a physiological role in passive diffusion of cell cholesterol from peripheral cells and cholesteryl ester transfer protein (CETP) and phospholipid transfer protein (PLTP) are key proteins involved in this intravascular lipoprotein metabolism. CETP enables the transfer of cholesteryl esters, generated by the LCAT reaction, from HDL to very low density lipoproteins (VLDL) and LDL. PLTP catalyzes the transfer of phospholipids between lipoproteins.

5.2.2. SR-BI-FACILITATED DIFFUSION OF CHOLESTEROL TO HDL

SR-BI is an ubiquitous multi-ligand receptor that interacts with a broad range of acceptors, including HDL₂, LDL, oxidized LDL and acetylated LDL¹, it yields a high level of expression in steroidogenic tissues and the liver, where it is implicated in the selective uptake of cholesteryl esters⁶⁶.

Expression levels of SR-BI correlate with the efflux of free cholesterol (FC) from cultured cells as well as efflux to LDL and other nonlipoprotein acceptors such as phospholipid vesicles¹⁵⁷. Therefore, SR-BI mediates a bidirectional exchange of FC via a concentration gradient between the plasma membrane of the cell and a wide variety of phospholipid-containing acceptors, in a process defined as 'facilitated aqueous diffusion'.

The detailed mechanism by which SR-BI facilitates cellular cholesterol efflux remains unclear but it seems that distinct extracellular receptor domains besides the lipids and apolipoproteins in HDL may be involved in SR-BI binding to HDL. The interaction between SR-BI and the class A amphipathic α -helices was earlier reported by Williams and colleagues²⁰⁰. These studies strongly suggest that SR-BI interacts with HDL via the amphipathic α -helical repeat units of apoA-I, which may therefore explain the interaction of SR-BI with a wide variety of apolipoproteins via a specific secondary structure, the class A amphipathic α -helix, which is a common structural motif in the apolipoproteins of HDL. Nevertheless, HDL binding to SR-BI is not enough to ensure efficient FC efflux¹²⁸.

SR-BI seems to function in a two-step process where HDL binding to SR-BI (step 1) is coupled to the flux of FC (step 2). Therefore, HDL binding to cell surface SR-BI may enhance FC efflux via SR-BI at low ligand concentrations¹⁹⁰, but is independent of SR-BI in a more physiological situation, i.e. when the receptor is saturated.

Peng and colleagues showed that SR-BI-facilitated cholesterol trafficking between cells and HDL occurs primarily in clusters of SR-BI on microvillar extensions of the plasma membrane, but independently of caveolae or raft domains¹⁴⁷.

In conclusion, it is likely that the ability of SR-BI to stimulate cholesterol efflux may reflect the reorganization of membrane cholesterol domains that are distinct from rafts or caveolae. HDL-apolipoprotein composition, conformation and binding to SR-BI may

enhance this process. This would explain why HDL is the most physiological particle involved in SR-BI facilitated cholesterol efflux. In the liver, SR-BI rather mediates HDL₂-mediated selective uptake of cholesteryl esters than cholesterol efflux¹⁹⁴.

In addition, SR-BI mediates the selective uptake of cholesteryl esters from HDL₂. This pathway is defined as a high-capacity system in which cells internalize cholesteryl esters rather than apolipoprotein components of the HDL-particle. This is in contrast to the LDL-receptor pathway in which particles are internalized through clathrin coated vesicles for degradation and lipid recycling.

SR-BI mediates a bidirectional exchange of lipids, mainly promoting transfer of cholesteryl esters and free cholesterol from HDL and LDL to the cell¹⁷⁹, and a cholesterol efflux from cell plasma membranes to lipoproteins and non-lipoprotein receptors⁹⁵.

This function underlies a tight equilibrium between apolipoproteins and lipids and any modification of the lipoprotein particles that modulate this steady state will modify selective CE uptake, thus, an increasing TG/CE ratio will decrease CE uptake, in contrast to LPL- or HL-mediated HDL-TG hydrolysis which increases CE uptake⁷⁰.

In addition, HDL can be endocytosed by two different pathways: one dependent on internalization via SR-BI, representing the selective transfer of lipoprotein cholesterol which could explain selective sorting of cholesterol to the bile canaliculus. The other endocytic route is independent of SR-BI, representing the HDL protein catabolic pathway, mediated by an as yet unknown receptor¹⁷⁷.

HDL-mediated cholesterol efflux may involve a passive diffusion-mediated process in which HDL interacts with SR-BI.

5.2.3. ABCA1-MEDIATED ACTIVE EFFLUX

Lipid-free apoA-I is a physiological acceptor involved in phospholipid and cholesterol efflux from cells. A breakthrough in this area has been the discovery that apoA-I-mediated specific phospholipids and cholesterol efflux from the cell is critically dependent on the function of ABCA1, a member of the ABC transporter family of proteins. It was also shown in cross-linking experiments that the ABCA1 transporter may act as an apoA-I receptor⁶¹. Chimini and colleagues however, assessed that binding of apoA-I may not involve a direct molecular interaction between ABCA1 and apoA-I³³. ABCA1 expression was directly correlated both with lipid efflux and with an increase in lipid-free apoA-I binding, but not with any increase in HDL binding¹⁹⁵. Helical lipid-free apolipoproteins of HDL, such as apoA-I, A-II and E are able to induce phospholipid and cholesterol release from cells to generate nascent HDL particles with physical and biochemical characteristics of pre- β -HDL.

5.3. ATP-BINDING CASSETTE TRANSPORTER

The ATP-binding cassette (ABC) superfamily is composed of about 50 functionally diverse transmembrane proteins⁵³. These proteins are fundamental to intracellular compartmental transport as well as transport through the plasma membrane. These proteins utilize energy derived from the hydrolysis of ATP to transport the substrate across the membrane against a concentration gradient. The typical ABC transporter consists of two transmembrane domains and two nucleotide-binding domains (NBDs) or ATP-binding cassettes (ABC) encoded by a single polypeptide. Each nucleotide-binding domain contains two sequence motifs, the Walker A and Walker B motifs, common motifs of nucleotide binding proteins. The distinctive feature of all ABC transporters is the C motif that has the consensus sequence "LeuSerGlyGlyGln". ABC transporters are termed either „full-size“, standing for full functionality, like ABCA1 or „half-size“ like ABCG family which means they have to form homodimers or heterodimers in order to gain functionality.

ABC transporters are gaining attention because mutations in these proteins cause various human inherited diseases. Among these are: familial HDL deficiency (ABCA1)²¹, fatal surfactant deficiency in newborns (ABCA3)¹⁷⁶, different chorioretinal diseases (ABCR or ABCA4)⁵, Progressive Familial Intrahepatic Cholestasis (PFIC) type II (ABCB11) and type III (MDR3 or ABCB4)⁴⁸, lamellar ichthyosis type 2 (ABCA12)¹¹⁷, Dubin-Johnson syndrome (ABCC2)¹⁰⁵, Pseudoxanthoma Elasticum (MRP6 or ABCC6)¹⁹³, Adrenoleukodystrophy (ALDR or ABCD2)¹³³ and β -Sitosterolemia (ABCG5, ABCG8)¹¹⁶.

Recently, a novel missense mutation in ABCA1 was described in a patient with Scott syndrome, a mild bleeding disorder that also affects platelet aggregation, leading to altered protein trafficking and reduced phosphatidylserine translocation⁴. A number of human ABC transporters is involved in bile acid, phospholipid and sterol transport^{22,164}, and the expression of these ABC proteins is controlled by lipids¹¹⁵.

The full-size transporters are mainly localized at the plasma membrane but can also be found intracellularly as a result of vesicular trafficking. On the other hand, most half size molecules are routed to intracellular membrane systems such as mitochondria, peroxisomes, the endoplasmic reticulum and the Golgi compartment.

ABC transporters can be divided into two categories according to their mode of action: active transporters or pumps, such as members of the ABCB (MDR/TAP) subfamily which show a high movement of molecules across membranes against a chemical concentration gradient and transport facilitators, which show nucleotide binding and a subsequent conformational change but very low ATP hydrolysis such as ABCC7 (CFTR), ABCC8 (SUR1), ABCC9 (SUR2) and ABCA1.

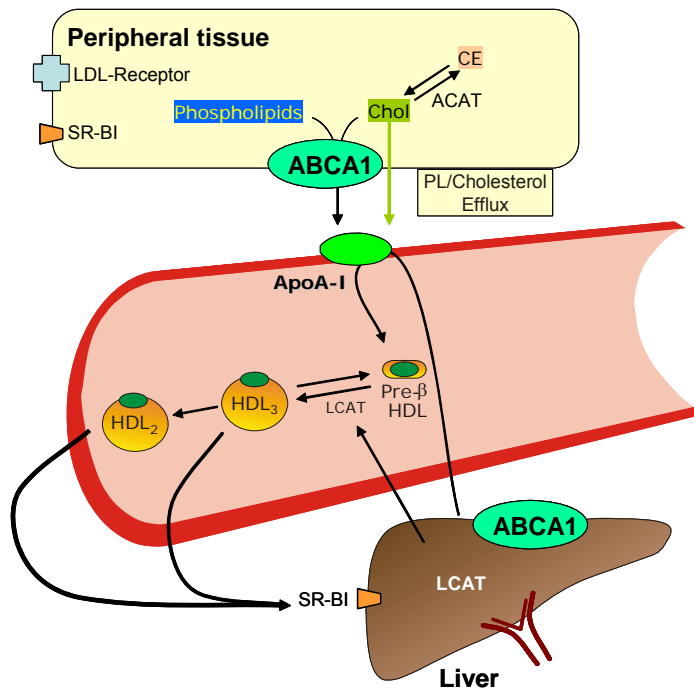


Figure 8: Reverse cholesterol transport and role of ABCA1.

Cholesterol esters are hydrolyzed into free cholesterol in peripheral tissues and are transported by ABCA1 to ApoA-I. In the circulation, a pre-β HDL particle is formed and through further modification by LCAT, this particle matures to HDL₃ and HDL₂. Cholesterol from these HDLs is internalized by the liver via the scavenger receptor SR-BI and then cholesterol is excreted via the bile.

5.3.1. ABCA SUBFAMILY

This subfamily is composed only of full-size transporters. The ABCA1-family contains 12 proteins: (ABCA5, ABCA6, ABCA8, ABCA9, and ABCA10) which cluster on chromosome 17q24 and (ABCA1, ABCA2, ABCA3, ABCA4, ABCA7, ABCA12, ABCA13) which are distributed over six different chromosomes. Interestingly, the transcription of at least seven ABCA members is regulated by and sensitive to lipids^{96-99,104} indicating an important role of the whole ABCA subfamily in cellular lipid transport processes.

ABCA1 mediates cellular phospholipid and cholesterol release via an indirect mechanism, possibly by ATP-sensitive regulation of a not yet characterized molecule and mutations of ABCA1 lead to HDL-Deficiency Syndromes such as Tangier Disease²¹.

5.3.2. ABCA1 AND FAMILIAL HDL-DEFICIENCY

The cellular expression of ABCA1 is highly regulated both on transcriptional and posttranscriptional levels¹⁹⁶. The turnover of ABCA1 protein is rapid, with a half-life of less than one hour in murine macrophage-like cells and differentiated THP-1 cells¹⁴⁶. It was shown that calpain-mediated ABCA1 protein degradation is regulated by a PEST sequence in the cytoplasmic region of ABCA1. Interestingly, the interaction of ABCA1 with extracellular apoA-I inhibits calpain degradation of ABCA1 in a PEST-sequence dependent fashion and thereby increases ABCA1 protein level at the cell surface. It was observed that apoA-I promotes PEST sequence dephosphorylation. Furthermore, calpain-

mediated degradation of ABCA1 can be induced by the phosphorylation of a target protein ¹²⁶.

Mutations in the human ABCA1 gene lead to familial HDL-deficiency syndromes such as classical Tangier disease (TD) ^{24,165}. These patients almost completely lack plasma HDL, due to an enhanced catabolism of HDL precursors; they reveal low serum cholesterol levels and a reduced efflux of cholesterol and phospholipids from cells.

Not only HDL-plasma levels are affected in TD, also the composition is impaired, thus plasma HDL from TD patients is composed of small pre- β 1-migrating HDL particles containing only apoAI and phospholipids but lack free cholesterol and apoAII ⁷. In TD patients, concentration of LDL-cholesterol is only 40% of healthy controls and the particles are often rich in triglycerides. This is caused by disturbance of the cholesteryl ester transfer pathways and phospholipid transfer, resulting in changes of LDL composition and size. TD patients suffer from accumulation of cholesteryl esters either in the cells of the reticulo-endothelial system (RES) leading to splenomegaly and enlargement of tonsils or lymph nodes, or in the vascular wall, leading to premature atherosclerosis (Figure 8 shows the function of ABCA1 in RCT).

5.4. TANGIER DISEASE

Tangier disease, a rare and severe form of HDL deficiency characterized by a biochemical defect in cellular cholesterol efflux, is caused by mutations in the ATP-binding-cassette (ABC1) gene. This gene codes for the cholesterol-efflux regulatory protein (CERP). Complete loss of ABCA1 function leads to severely decreased cellular cholesterol efflux and cholesteryl ester accumulation in macrophages and other cells of the reticuloendothelial system. Clinically, TD patients often present with hepatosplenomegaly, peripheral neuropathy, enlarged yellow tonsils and fatty deposits in the rectal mucosa. Earlier studies suggested that certain carriers of ABCA1 defects bear a moderately increased risk for CAD ²¹.

Because of its ability to reduce macrophage cholesterol content and to raise plasma HDL levels, ABCA1 has become a promising therapeutic target for preventing cardiovascular disease.

5.5. ATP-SYNTASE, A NEW CONCEPT IN THE DUAL REGULATION OF ENDOCYTOSIS AND APOAI-MEDIATED CHOLESTEROL EFFLUX

Plasma HDL is involved in a complex interplay with several cellular partners in order to establish the reverse cholesterol transport. Among those partners are: ABCA1 and ApoAI

as contributors of HDL formation and others which are mostly involved in HDL catabolism like SR-BI and ATP synthase ¹²⁸.

Several binding sites for HDL or ApoAI have been identified in the liver plasma membrane and the internalization of HDL in the liver is accomplished via clathrin-coated vesicles, following engagement of the low-affinity binding sites ⁶³.

Moreover, recent data showed that remodeling of HDL induces different binding and internalization characteristics of the HDL particles and that the high-affinity HDL binding sites might trigger the internalization of apo HDL through the low-affinity binding sites ⁷².

A newly purified and characterized ApoAI-high-affinity binding site in the plasma membrane was the β -chain of human ATP-synthase, a major protein complex of the mitochondrial inner membrane also present in the plasma membrane, involved in ATP synthesis ¹²⁷. It has two major domains: F_0 and F_1 , the latter containing five different subunits among which the β -chain interacts with ApoAI.

Beisiegel and Mahley already reported in 1988 that both, the α - and β -chain of ATP synthase, are receptors for ApoE-enriched HDL in the plasma membrane ¹³. Furthermore, apoE recycling involves the internalization of HDL₃-derived apoAI and its targeting to apoE/cholesterol-containing endosomes, indicating that apoAI regulates the resecretion of apoE ⁸⁰.

Recently, Martinez et. al demonstrated that by adding free ApoAI, ADP generation through hydrolysis activity of ATP synthase at the cell surface was strongly stimulated in HepG2 cells, a proof that the binding of ApoAI regulates the hydrolysis activity of ATP synthase ¹²⁸. The synthesis of ATP requires an electrochemical proton gradient across the inner mitochondrial membrane. The collapse or absence (for instance when the F_1 complex is present alone) of the electrochemical proton gradient induces a switch in enzymatic activity from ATP synthesis to ATP hydrolysis.

The same group showed that the F_1 -domain of ATPase contributes to HDL internalization. Thus, ApoAI binds to high-affinity binding sites i.e. the β -chain of ATP synthase, which is an upstream event in the HDL endocytosis pathway.

A possible concept for this action is shown in figure 9, since the ATP synthase catalyzes the conversion of ADP to ATP and vice versa. ATP synthase is regulated by ApoAI leading to enhanced conversion of ATP to ADP. The absence of apoAI would lead to enhanced synthesis of ATP resulting in enhanced sinking in phagocytosis since actin can bind ATP, polymerize and form F-actin which is essential for type I phagocytosis. Hence ApoAI could lead to increased influx. On the other hand, ApoAI binds to ABCA1 leading to enhanced efflux.

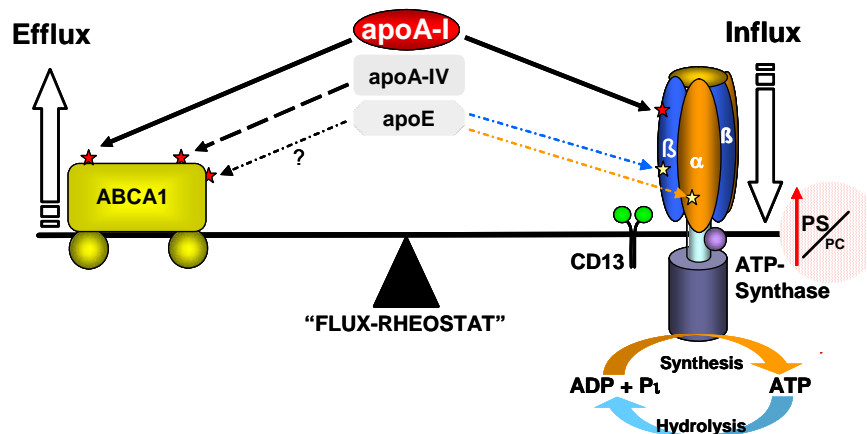


Figure 9: Proposed model of a flux compensation of cholesterol/phospholipid traffic in macrophages. ApoA-I either binds to ABCA1 leading to increased efflux, or to ATP synthase where it activates the β -chain, leading to increased influx.

This influx / efflux rheostat model controls cellular lipid homeostasis in a balance; dysfunction of this equilibrium may lead to severe disturbances of cellular lipid traffic. This is obvious in TD patients where ABCA1 is inoperative and apoA-I-dependent cholesterol is absent. Cholesterol influx however, is enhanced due to apoA-I-dependent stimulation of ATP synthase B leading to cholesteryl ester formation and enhanced foam cell formation.

6. VESICLE FORMATION IN THE GOLGI-DEPENDENT ABCA1 SECRETORY PATHWAY

The group of Alan Tall³⁵ reported earlier that ABCA1 promotes the formation of phospholipid-apoA-I-complexes which initially stimulate cholesterol efflux from certain regions in the plasma membrane that preferably utilize cholesteryl esters deposited by modified LDL in late endosomes and lysosomes rather than cholesterol deposited in other intracellular sites. This would explain the fact that de novo synthesized cholesterol and cholesterol entering via the HDL/SR-BI pathway can be metabolized normally, whereas LDL-derived cholesterol becomes sequestered in the late endosome compartment and can not be metabolized in Niemann-Pick C (NPC)-defective cells. However, other studies with ACAT inhibition such as Sandoz (S)-58035 also indicated that release of unesterified cholesterol from lipid droplets also stimulates apoA-I/ABCA1 dependent cholesterol efflux¹⁰⁸.

NPC1 and 2, a protein whose defect leads to selective impairment in cholesterol trafficking to the endoplasmic reticulum (ER) and excessive lysosomal storage of LDL cholesterol, controls this equilibrium of intracellular sterol trafficking and regulates cholesterol exit from late endosomes. Nevertheless, trafficking of ABCA1 to late

endosomes/lysosomes is not required for the formation of phospholipid-apoAI-complexes. ABCA1 is present in late endosomes and Trans-Golgi network and traffics between these compartments and the cell surface ¹³⁸. These data suggested that ABCA1 trafficking between late endosomes and the cell surface is involved in cholesterol efflux, a thesis supported by the recent finding of Chen et al ³⁶ that ABCA1 colocalizes with LAMP2 in late endosomes. This transport requires transport vesicle formation which carries the lipoproteins from the Golgi to the cell surface.

A multi-protein complex, called exocyst, is required for this internal exocytosis. The yeast exocyst complex consists of eight components: Sec3, Sec5, Sec6, Sec8, Sec10, Sec15, Exo70 and Exo84, yeast genes which are homologous to the human COP, ARF, Rab, NSF and SNAREs as shown in table 2.

Table 2: The Sec family in yeast and their homologs in human

Human	Yeast
Sec3-like	Sec3p
Sec6-like1	Sec6
RAS-like protein	Sec15
COP $\beta, \beta', \gamma, \alpha, \delta, \epsilon, \zeta$	Sec26/27/21 (COP1)
ARF1 (ADP-ribosylation factor)	Sar1 (Parts from COPII)
RAB5A	Sec4
Syntaxin 1A binding protein	Sec1
NSF	Sec18
SNAP- α	Sec17
SNAREs	Sec22

All of them localized to sites of active exocytosis, where they mediate the targeting and tethering of post-Golgi secretory vesicles for subsequent membrane fusion ⁸⁵. Polarized exocytosis has three stages: first, post-Golgi secretory vesicles are transported along cytoskeletal elements, involving actin, towards specific regions of the plasma membrane. Second, the vesicles, mediated by the exocyst complex, are tethered and docked at specific domains of the plasma membrane. Finally, the lipid bilayers of the vesicle membrane and plasma membrane fuse in a reaction catalyzed by the interaction of integral membrane proteins called v-SNAREs and t-SNAREs. This action is regulated by small GTP-binding proteins, the Rab family. The exocyst proteins interact with the Rab GTPase and dock the secretory vesicles to the plasma membrane for secretion (Figure 10). The function of the exocyst complex can be elucidated by the example of glucose transporter 4 (GLUT4). Insulin stimulation leads to translocation of GLUT4 from its intracellular tubulo-vesicular compartments to the plasma membrane via dynamic

trafficking, including sorting, budding, tethering, docking and fusion. This is done through a complex containing the adapter protein Cbl, Cbl-associated protein (CAP) and the Rho-family GTP-binding protein TC10. This complex is phosphorylated and binds to flotillin which resides in membrane lipid rafts. TC10 has been shown to bind to Exo70, another component of the exocyst pathway and this interaction is necessary for the final steps in GLUT4 exocytosis.

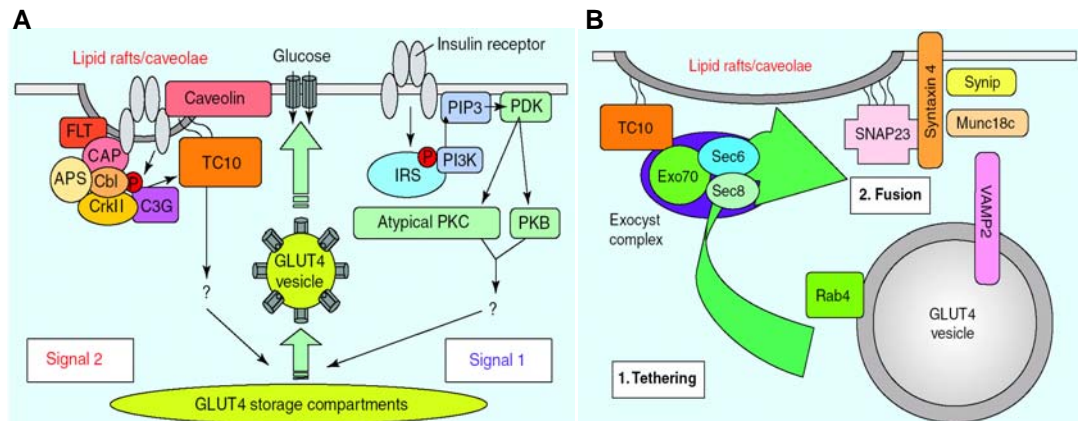


Figure 10: A: Insulin-induced GLUT4 translocation from intracellular storage compartments to the plasma membrane requires two independent signaling pathways; one is dependent on the IRS/PI3K pathway (signal 1) and the other is dependent on the CAP/Cbl/TC10 pathway (signal 2). These two distinct insulin-induced signal transduction pathways act together to elicit the translocation of GLUT4 protein mediating via membrane trafficking systems. IRS, insulin receptor; PKB, protein kinase B; FLT, flotillin; PKC, protein kinase C; APS, Adaptor protein containing PH and SH2 domains.

B: Tethering and docking of GLUT4-containing vesicles at the plasma membrane are dependent on the interaction between TC10 and the exocyst protein complex. Following insulin stimulation the lipid-raft-resident TC10 recruits Exo70 and its associated exocyst protein complex to the plasma membrane. This interaction is necessary for the final fusion step of GLUT4-containing vesicles to the plasma membrane mediated by SNARE proteins (SNAP-23, syntaxin4, synip, Munc18c and VAMP2)¹³¹.

At the final stage of exocytosis, the lipid bilayers of the vesicle and plasma membrane fuse in a reaction catalyzed by SNF-attachment proteins (SNAPs) and SNAP-Receptors (SNAREs). The formation of a stable complex between these SNAREs brings the vesicle and the target membrane to close proximity eventually leading to fusion (Figure 10).

Rabs are members of the Ras superfamily which ensure accuracy in docking and/or fusion of vesicles with their correct acceptor compartments. RAB proteins undergo regulated exchange of GTP for GDP, and slowly hydrolyze the bound GTP in a reaction regulating the timing and unidirectional nature of the fusion. The Rab5-effector EEA1 has

been shown to directly interact with syntaxin 13 demonstrating the role of Rabs in controlling membrane fusion and endosome docking ³⁹.

Cdc42, also involved in regulating the actin cytoskeletal architecture and filopodia formation, has been shown also to act as a trafficking regulator for Rabs thus playing a role in intracellular trafficking ³². Besides, the filopodia formation leads to an increase in cell surface giving a bigger area where cholesterol efflux can take place due to increased vesicle fusion.

In addition, the Rho proteins interact with the exocyst and control the localization of the docking. Finally, small Ras-related regulatory GTPases called ADP-ribosylation factors (ARFs), control the stage of vesicle budding and eventually fusion ¹⁵⁸. ARF-like proteins (ARLs) have similar functions like the Ras-family, Arl7 contributes to a vesicular transport step between the late endosome and ABCA1-accessible cholesterol pool at the plasma membrane and thereby participates in the RCT pathway which enables the cell to export cholesterol when the cellular level of cholesterol is rising and cholesterol secretion is necessary in order to protect the cell from the devastating effects resulting from cholesterol overloading. The fact that Arl7-mediated stimulation of cholesterol efflux is dependent on the presence of apoA1 makes it likely that ARL7 acts in concert with ABCA1 ⁵⁷ either by modulating apoA1 and/or ABCA1 endocytic transport or altering the half life of ABCA1 (Figure 11).

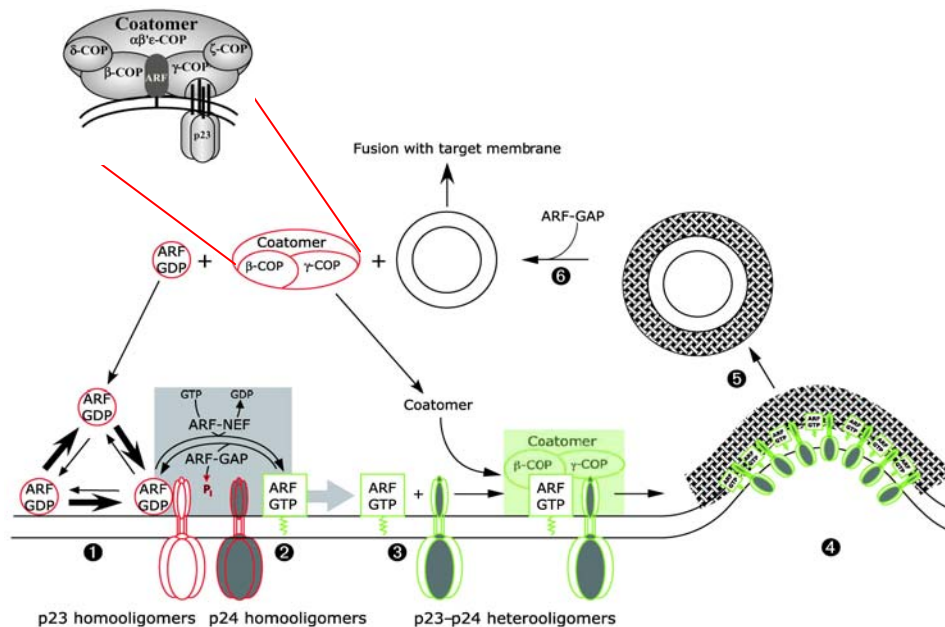


Figure 11: The core machinery of COPII recruitment to membranes, coat polymerization, vesicular budding and uncoating. [Adapted from Alberts, 2003 and Nickel et al. ¹³⁹]

A central role in this recruitment is played by the adapter related protein complex 3 (AP-3). In *Drosophila*, mutations in the AP-3 complex as well as mutations in ABCG5 and ABCG8 (both half-size ABC transporters which interact to form the functional full-size) lead to changes in the eye color, due to trafficking disturbances in lysosomes and related organelles⁸⁸.

In mice, the „mocha” and „pearl” platelet storage pool deficiency (SPD) mutants also have defects in the Ap-3 complex^{86,199}. In addition, Huang et al⁸⁶ showed that mutations in syntaxin 13 binding protein (pallidin) lead to „pallid” and „gunmetal” phenotypes. The latter mutants are defective in a more downstream event of vesicle-trafficking: namely, vesicle-docking and fusion. These mice suffer from hypo pigmentation, lung fibrosis, kidney lysosomal enzyme elevation and prolonged bleeding. AP-3 pathway constituents are: ARL7⁵⁷, Syntaxin 13 and ABCA1¹⁰, Syntaxin 13-interacting protein (pallidin), Cdc42^{83,163} ABCG1/G2/G4 (which leads to mutations: white, brown and scarlet), HPS1-7:Hermansky-Pudlak-Syndrome complex, P2-Purinergic receptors and GIRKs (G-protein coupled inward rectifying K-channels).

In human, defects of the secretory lysosome lead to a number of genetic diseases like Hermansky-Pudlak syndrome (HPS) and Chediak-Higachi syndrome (CHS), autosomal recessive disorders which lead to storage defects resulting, among others, from defects in secretory lysosomes leading to pulmonary fibrosis and prolonged bleeding.

Another family of proteins which regulate trafficking to lysosome-related organelles is the biogenesis of lysosome-related organelles complex-3 (BLOC 3); it includes the proteins HPS1 and HPS4 which lead to Hermansky-Pudlak syndrome (HPS) a genetic disorder characterized by albinism, bleeding, and lysosomal storage disorder resulting from defects of multiple cytoplasmic organelles: melanosomes, platelet-dense granules, and lysosomes, it is a parallel to the HPS disorder in mice which involves a syntaxin 13-interacting protein called pallidin as well as other genes like muted, and cappuccino, all of which are members of the BLOC1 family. The BLOC family encodes the β 3A-subunit of the adapter protein (AP) complex, AP3¹²⁵.

Table 3 summarizes the defect genes, the affected compartments and the resulting mouse mutants.

Table 3: Mouse models of lipid trafficking disorders

Human Disease	Defective cells	Defective gene	Affected complex	Mouse mutant
Hermansky-Pudlak-Syndrome	Melanocytes and platelets	HPS1	BLOC-3	"Pale ear"
Hermansky-Pudlak-Syndrome	Immunocytes, melanocytes & platelets	AP3B1 (HPS2)	AP-3	"Pearl"
Hermansky-Pudlak-Syndrome	Melanocytes and platelets	HPS3	BLOC-2	"Cocoa"
Hermansky-Pudlak-Syndrome	Melanocytes and platelets	HPS4	BLOC-3	"Light ear"
Hermansky-Pudlak-Syndrome	Melanocytes and platelets	HPS5	BLOC-2	"Ruby-Eye2"
Hermansky-Pudlak-Syndrome	Melanocytes and platelets	HPS6	BLOC-2	"Ruby-Eye"
Hermansky-Pudlak-Syndrome	Melanocytes and platelets	DTNBP1 (HPS7)	BLOC-1	"Sandy"
Hermansky-Pudlak-Syndrome	Melanocytes and platelets	AP3D1	AP-3	"Mocha"
Hermansky-Pudlak-Syndrome	Immunocytes, melanocytes & platelets	RABGGTA	Transient with Rabs	"Gunmetal"
Hermansky-Pudlak-Syndrome	Melanocytes and platelets	PLDN	BLOC-1	"Pallid"
Hermansky-Pudlak-Syndrome	Melanocytes and platelets	MU	BLOC-1	"Muted"
Hermansky-Pudlak-Syndrome	Melanocytes and platelets	CNO	BLOC-1	"Cappuccino"
Hermansky-Pudlak-Syndrome	Melanocytes and platelets	VPS33A	Unknown	"Buff"
Chediak-Higashi-Syndrome	Immunocytes and melanocytes	LYST	Unknown	"Beige"
Elejalde-Syndrome (Griscelli 1)	Melanocytes and neurons	MYO V	Rab27a/MyoV/Melanophilin	"Dilute"
Griscelli-Syndrome 2	Immunocytes and melanocytes	RAB27A	Rab27a/MyoV/Melanophilin	"Ashen"
Griscelli-Syndrome 3	Melanocytes	MLPH	Rab27a/MyoV/Melanophilin	"Leaden"

6.1. COATED VESICLE ASSEMBLY

All types of coated vesicles are formed by polymerization of cytosolic coat proteins on a donor (parent) membrane to form vesicle buds that eventually pinch off from the membrane to release a complete vesicle. Three types of coated vesicles have been characterized, each with a different type of protein coat and each formed by reversible polymerization of a distinct set of GTP-binding proteins (ARF or Sar1) belonging to the GTPase superfamily. Also, each of them transports cargo proteins from particular parent organelles to particular destination organelles:

- COPII vesicles transport proteins from the rough ER to the Golgi.
- COPI vesicles mainly transport proteins in the retrograde direction between Golgi cisternae and from the cis-Golgi back to the rough ER.
- Clathrin vesicles transport proteins from the plasma membrane (cell surface) and the trans-Golgi network to late endosomes.

After formation of vesicles by budding from a donor membrane, the coats depolymerize into their subunits, which are reused to form additional transport vesicles, this is summarized in (Figure 12).

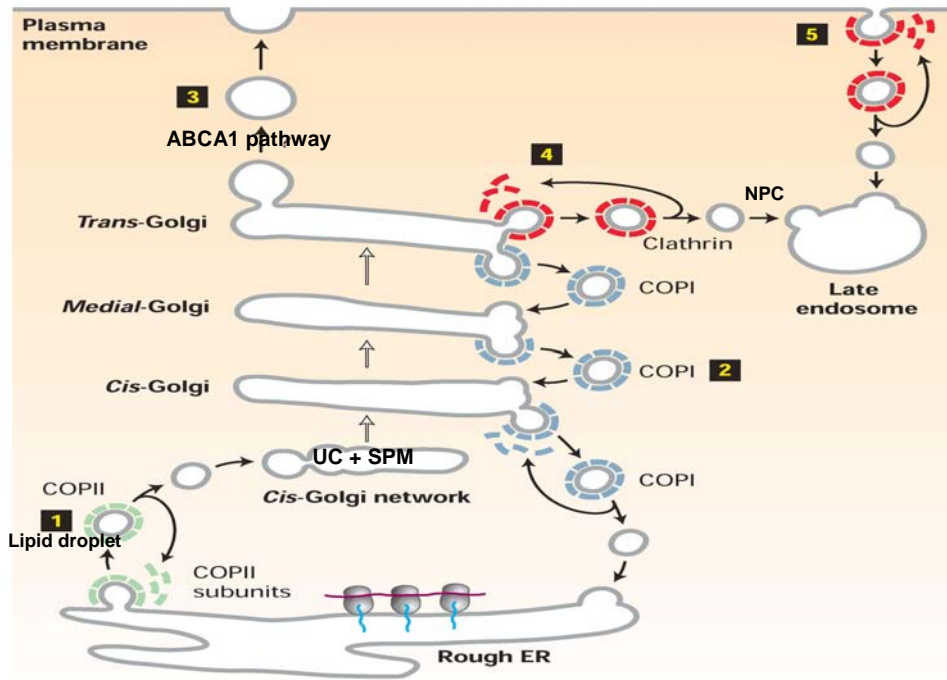


Figure 12: Involvement of the three major types of coat proteins in vesicular traffic in the secretory and endocytic pathways.

A. 1. COPII vesicles mediate anterograde transport from the rough ER to the *cis*-Golgi/*cis*-Golgi network. 2. COPI vesicles mediate retrograde transport within the Golgi and from the *cis*-Golgi/*cis*-Golgi network to the rough ER. 3. The coat proteins surrounding secretory vesicles are not yet characterized; these vesicles carry secreted proteins and plasma-membrane proteins from the *trans*-Golgi network to the cell surface. 4-5. Vesicles coated with clathrin bud from the *trans*-Golgi network and from the plasma membrane; after uncoating, these vesicles fuse with late endosomes. Adapted from Alberts 2003, pg. 719

The general scheme of vesicle budding shown in Figure 13 applies to all three known types of coated vesicles.

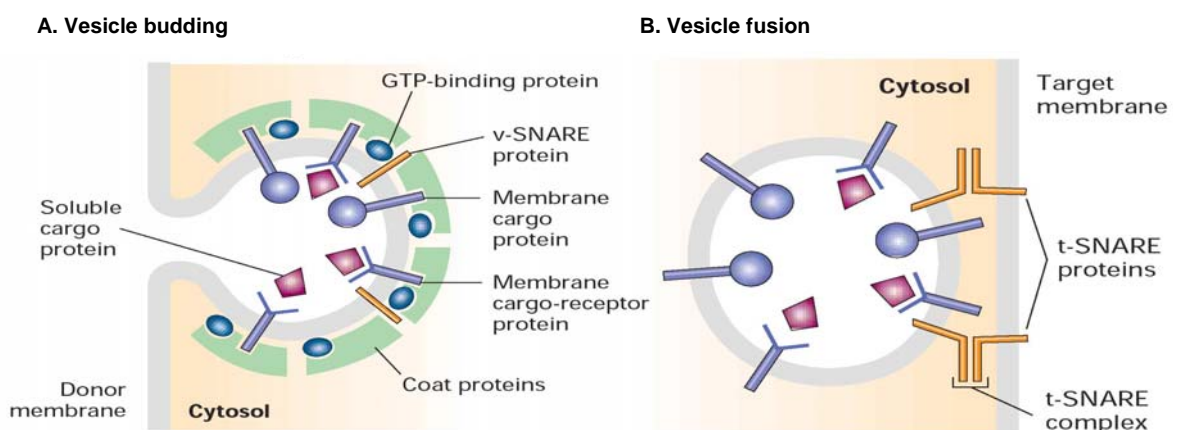


Figure 13: Budding and fusion. Overview of vesicle budding and fusion with a target membrane. (a) Budding is initiated by recruitment of a small GTP-binding protein to a patch of donor membrane. Complexes of coat proteins in the cytosol then bind to the cytosolic domain of membrane cargo proteins, some of which also act as receptors that bind soluble proteins in the lumen, thereby recruiting luminal cargo proteins into the budding vesicle. (b) After being released and shedding its coat, a vesicle fuses with its target membrane in a process that involves interaction of cognate T-SNARE proteins [Alberts, 2003].

Shortly after a vesicle buds off from the donor membrane, the vesicle coat disassembles to uncover a vesicle-specific membrane protein, a v-SNARE. Likewise, each type of target membrane in a cell contains t-SNARE membrane proteins. After Rab-mediated docking of a vesicle on its target (destination) membrane, the interaction of cognate SNAREs brings the two membranes close enough together that they can fuse. The SNARE-mediated vesicle fusion can be viewed in figure 14.

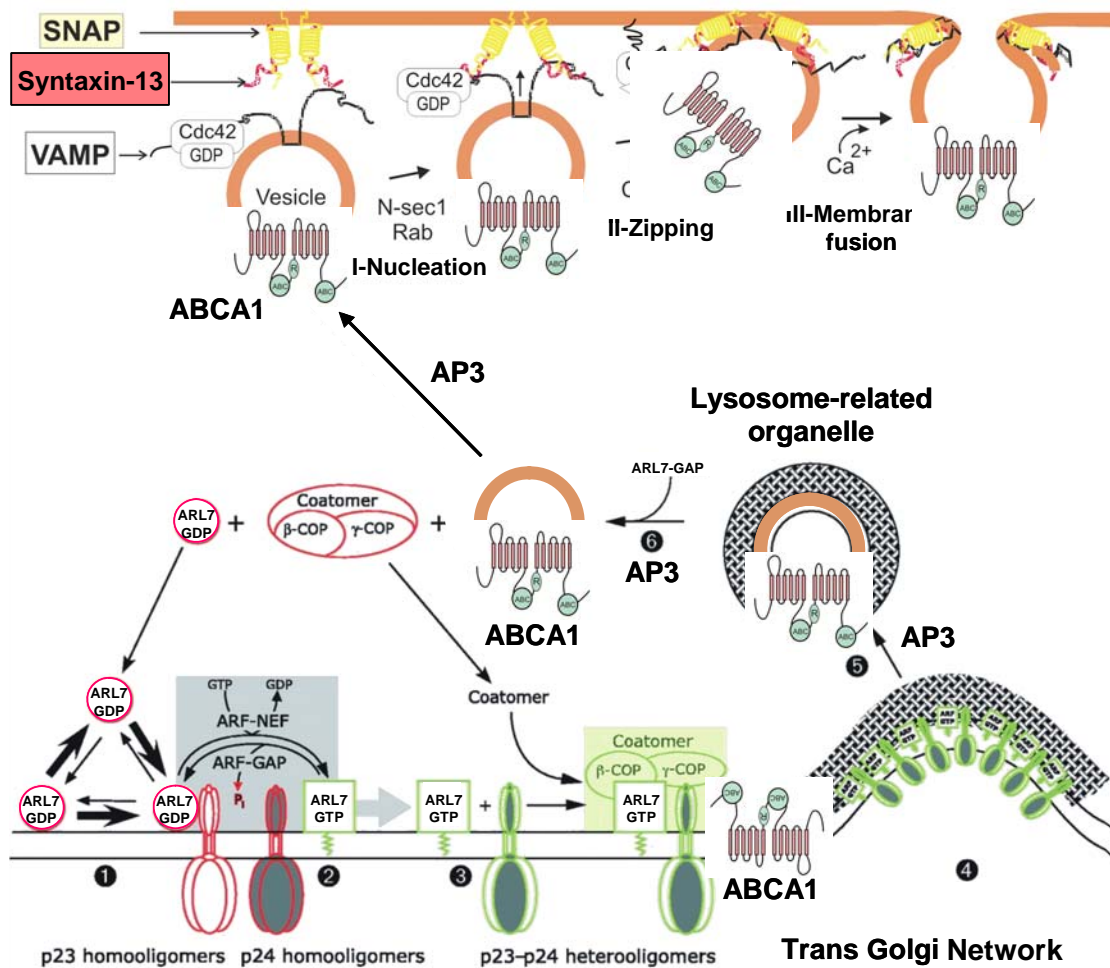


Figure 14: Syntaxins and SNAREs in vesicle fusion. A v-SNARE, known as VAMP (vesicle-associated membrane protein), is incorporated into secretory vesicles as they bud from the trans-Golgi network. Syntaxins are t-SNAREs, integral membrane protein in the plasma membrane, and SNAP-25, which is attached to the plasma membrane by a hydrophobic lipid anchor in the middle of the protein. The cytosolic region in each of these three SNARE proteins contains a repeating sequence that allows four α -helices - one from VAMP, one from syntaxin, and two from SNAP-25 to coil around one another to form a four-helix bundle. As the four-helix bundles form, the vesicle and target membranes are drawn together by the embedded transmembrane domains of VAMP and syntaxin, an effect induced by Ca^{++} ions.

6.2. SYNTAXINS AS CONSTITUENTS OF THE SNARE FAMILY

Syntaxins are SNARE proteins required in vesicular docking and fusion. All mammalian syntaxins, except syntaxin 11, are transmembrane proteins. The structure is highly conserved and consists of a transmembrane domain, several hydrophobic regions forming coiled-coil domains and a characteristic and conserved SNARE domain. Roughly, syntaxins can be divided into two categories, the first with a transmembrane domain (TMD) revealing a long amino acid TMD is predominantly located at the PM, the second, with short amino acid TMD is distributed in cell organelles. Table 4 shows the intracellular distribution of syntaxins.

Table 4: Localization and known function of syntaxins.

Syntaxin Family				
	Protein	Chrom. Loc.	Predominant Localisation	Known Function
TMD long form aa	Syntaxin-1A HPC-1;Unc-64;p35-1	7q11.23	Plasma Membrane; neuronal and secretory cells	Neuronal exocytosis
	Syntaxin-1B	16p11.2	Similar to 1A	Similar to 1A
	Syntaxin-2 Epimorphin	7	Plasma Membrane Ubiquitous	Exocytosis
	Syntaxin-3A	11cen-11q12.3	Plasma Membrane Transport Vesicles	Exocytosis
	Syntaxin-4A p35-2	16p13.13-16p12.3	Plasma Membrane Ubiquitous	GLUT4 translocation
TMD short form aa	Syntaxin-5A	11cen-q12.1	Golgi; ER COP Coated Vesicles	ER-Golgi transport
	Syntaxin-6	1	TGN; Endosomes	TGN-Endosome transport immature granule fusion
	Syntaxin-7	6	Endosome; Lysosome	Late endosome fusion
	Syntaxin-8 CARB	17p12	ER; Endosomes	Late endosome fusion
	Syntaxin-10	19p13.2	TGN	?
	Syntaxin-11	6q23.1-6q25.3	TGN; Late endosome	?
	Syntaxin-13 Syntaxin-12	1	Endosomes	Surface protein recycling Early endosome fusion
	Syntaxin-16 HSYN16	20p11.23-p11.21	Golgi	Early endosome-TGN transport
	Syntaxin-17	?	Smooth ER	Trafficking to smooth ER
	Syntaxin-18	4	ER	ER-Golgi transport

TMD= Transmembrane domain; ER= Endoplasmatic Reticulum; TGN= Trans-Golgi Network

It is this SNARE domain which mediates the interaction with the SNARE domain of other target membrane SNARE proteins to form a t-SNARE complex. The t-SNARE complex interacts with the vesicle SNARE domain forming the core fusion complex.

Syntaxins have been shown to interact with several proteins, syntaxin 1a interacts with SNAP-25³⁴, RAB27a¹⁹¹ and to Slo calcium-activated potassium channel⁴⁰, syntaxin 2 interacts with RAB3A¹⁰², syntaxin 3 interacts with Munc-18-2¹⁵³, syntaxin 4 interacts with actin⁹, syntaxin 13 interacts with EEA1¹²⁹ and with ABCA1¹⁰, only to mention a few.

6.3. THE RAB PATHWAY AND ITS INVOLVEMENT IN VESICULAR TRANSPORT

The RAS superfamily of GTP (guanosine triphosphate) hydrolysis-coupled signal transduction relay proteins can be subclassified into RAS, RHO, RAB, and ARF families. Ras family GTPases regulate cell signaling events that lead to alterations in gene transcription; Rho family GTPases (Rho, Rac and Cdc42), function as regulators of the actin cytoskeleton and can also influence gene transcription; Rab (>60 members) and (ADP-ribosylation factor) ARF (Arf1–Arf6, Arl1–Arl7) family GTPases control the formation, fusion and movement of vesicular traffic between different membrane compartments of the cell.

Multiple Rab GTPases, such as Rab1, Rab4, Rab5, Rab7 and Rab11, have been identified to regulate ER–Golgi transport as well as the endocytosis and trafficking of G-protein coupled receptors between early, late and recycling endosomes and lysosomes ¹⁷

The following figure 15 shows the distribution of Rabs throughout the cell.

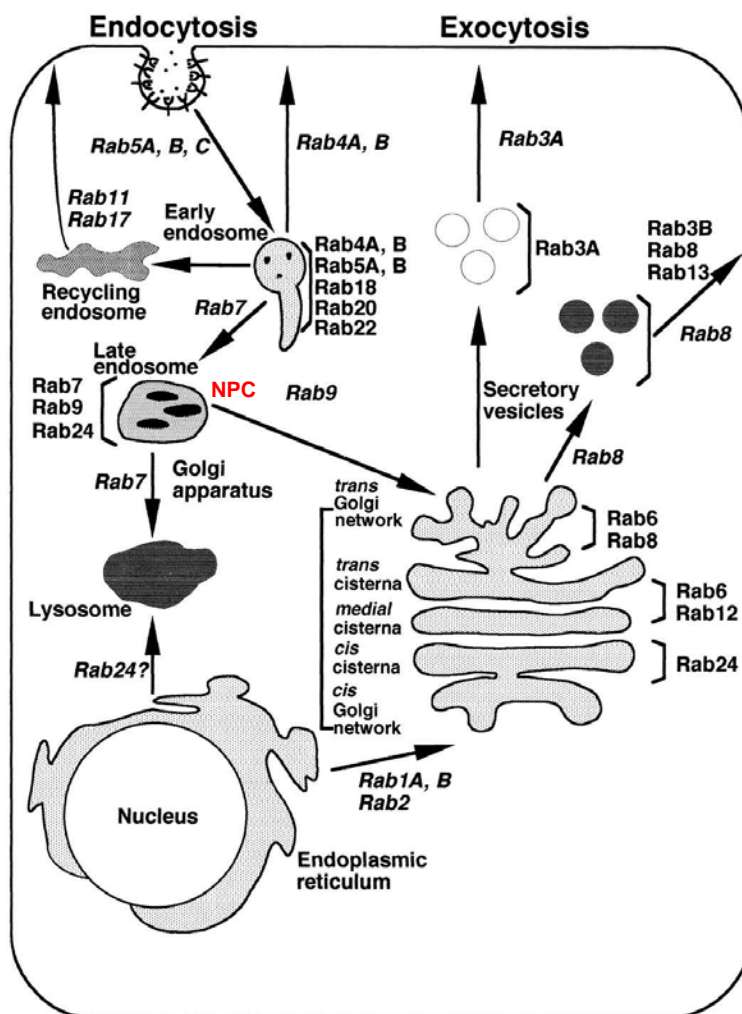


Figure 15: Distribution of Rabs throughout the cell and their influence on vesicular transport shuttling and fusion.

Rabs can be separated into two groups according to the speed they handle trafficking with. Rapidly recycling Rabs are Rab4, Rab5, Rab7, whereas Rab11 regulates slow recycling endosomes.

Zerial and co-workers²⁰⁶ have proposed that endosomes are organized as a mosaic of different Rabs. The early endosome would comprise of Rab4 and Rab5, the intermediate endosome of Rab6, the recycling endosome Rab11 and the late endosomes of Rab7 and Rab9. Cargos coming from the TGN may be able to enter any of these endosomal domains, thus, providing these pathways with newly synthesized material.

Due to mutations in either NPC1 or 2, cholesterol as well as other lipids and proteins accumulate in the different endosomal organelles³⁰.

Consequently, cholesterol homeostatic responses in the endoplasmic reticulum fail, as manifested by defective cholesterol esterification and inappropriately high cholesterol synthesis¹²¹. NPC1 is a membrane protein localized in Rab7-positive late endosomes²⁰⁹. NPC2 is a cholesterol-binding soluble protein that is also targeted to Rab7-positive late endocytic organelles. The group of Elina Ikonen has recently reported that the clearance of lysosomal cholesterol deposits can also be inhibited by Rab-GDP dissociation inhibitor (Rab GDI)⁸⁴. This protein controls multiple vesicular transport pathways by sequestering GDP bound (inactive) forms of the small GTPases of the Rab family in the cytoplasm.

In this concept, Rab11 serves as an important regulator of membrane trafficking depending upon cellular cholesterol balance and, in addition, modulates endosomal cholesterol levels independent of LDL uptake.

7. GENE ARRAYS

Gene array analysis and data validation with Taqman[®] was a major basis of this thesis. Therefore, this innovative technique will be introduced here in more detail.

Gene expression analysis is essential for obtaining a comprehensive picture of cellular mRNA levels. Whole-genome analysis made it possible to investigate the abundance of nearly all mRNAs in a cellular tissue.

Gene arrays consist of large numbers of DNA molecules spotted on a solid substrate such as a nylon membrane, a glass slide, or a silicon chip. Depending on the size of each DNA spot on the array, DNA arrays can be categorized as microarrays (each DNA spot has a diameter of <250 microns) and macroarrays (spot diameter of >300 microns). Different methods of manufacturing gene arrays have resulted in the generation of two array formats: oligonucleotide arrays and cDNA arrays.

In this thesis, we used oligonucleotide arrays from Affymetrix called “GeneChip® Human Genome U133A Arrays” to monitor the expression of approximately 14,500 human genes regulated by lipid loading and deloading.

GeneChip® arrays are manufactured through a combination of photolithography and combinatorial chemistry using technologies adapted from the semiconductor industry. GeneChip manufacturing begins with a 5-inch square quartz wafer. Initially the quartz is washed to ensure uniform hydroxylation across its surface. In the next step, silane which reacts with the hydroxyl groups of the quartz is added, providing a light activated surface. Probe synthesis occurs in parallel, resulting in the addition of either an A, C, T, or G nucleotide to multiple growing chains. To define which oligonucleotide chains will receive a nucleotide in each step, photolithographic masks are placed over the coated wafer. When ultraviolet light is shone over the mask in the first step of synthesis, the exposed linkers become deprotected and are available for nucleotide coupling (Figure 15).

Once the desired features have been activated, a solution containing a single type of deoxynucleotide with a removable protection group is flushed over the wafer's surface. The nucleotide attaches to the activated linkers, initiating the synthesis process. This process is repeated until the probes reach their full length, usually 25 nucleotides.

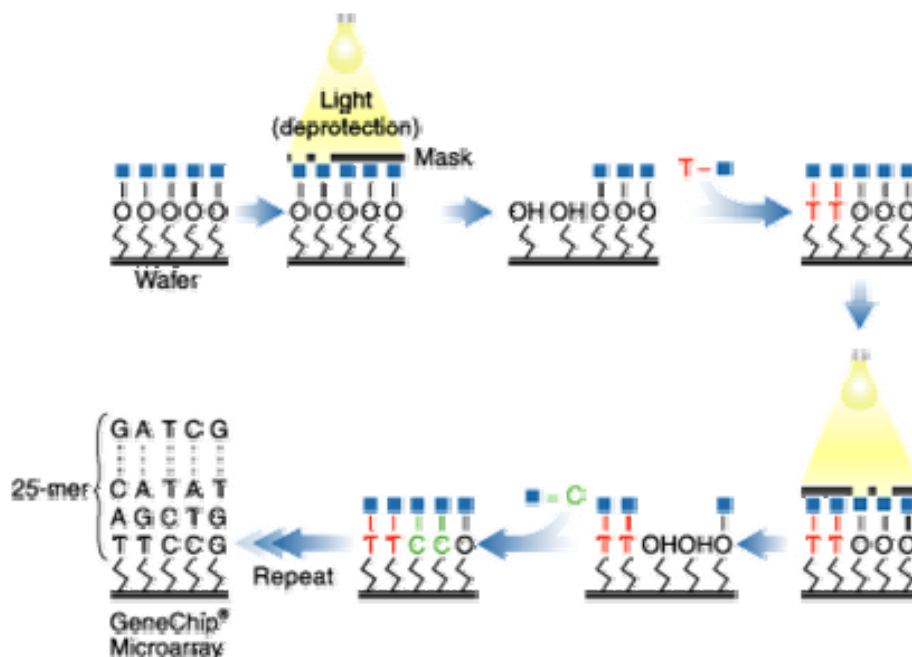


Figure 15: Lithographic manufacture of Affymetrix GeneChip® Arrays. This technology is based on oligonucleotides coupled with light sensitive hydroxyl groups. Once the first layer is attached to the silane layer, the first line of nucleotides is deprotected and exposed to light revealing a group capable of binding new oligos (See text for details) [Affymetrix homepage].

For each probe designed to be perfectly complementary to a target mRNA sequence, a partner probe is generated that is identical except for a single base mismatch in its center. These probe pairs, called the Perfect Match probe (PM) and the Mismatch probes (MM), allow the quantitation and subtraction of signals caused by non-specific cross-hybridization. In general, 11 to 16 probes are selected among all possible 25-mers to represent each mRNA transcript. In addition to choosing the probes based on their predicted hybridization properties, candidate sequences are filtered for specificity. Their potential for cross-hybridizing with similar, but unrelated sequences is correlated. The gene expression data analysis was performed by Affymetrix GeneChip® Operating Software (GCOS) which automates the control of the fluidics stations and scanners. In addition, GCOS acquires data, manages sample and experimental information.

Based on the expression algorithm, GCOS computes the detection call which defines whether a signal is absent, marginal present or present. This call is emphasized by a detection p-value and by a normalized signal which is background-subtracted and adjusted for noise. In addition, GCOS is capable of doing comparison analysis and calculating the *difference call*. Each transcript has five possible calls, *Increase*, *Decrease*, *Marginal Increase*, *Marginal Decrease*, *No Change*.

Another important result obtained is the signal log ratio (SLR) which monitors the expression level of a transcript when two experiments are being compared. This value is logarithmic and a \log_2 ratio of 1 equals a fold change of 2. Using the SLR a fold change can be calculated using the following two formulas:

$$FC = 2^{(SLR)} \text{ if } SLR \geq 0;$$

$$FC = -1 * 2^{(-SLR)} \text{ if } SLR < 0$$

8. THE YEAST TWO-HYBRID SYSTEM

The yeast two-hybrid system can identify protein-protein interactions by using a number of different proteins as potential binding partners⁶⁰.

The yeast two-hybrid technique uses two protein domains that have specific functions: a DNA-binding domain (BD), which binds to DNA, and an activation domain (AD), which activates transcription of the DNA. It is based on the principle that a protein with a DNA binding domain can activate transcription by binding to another protein containing an activation domain.

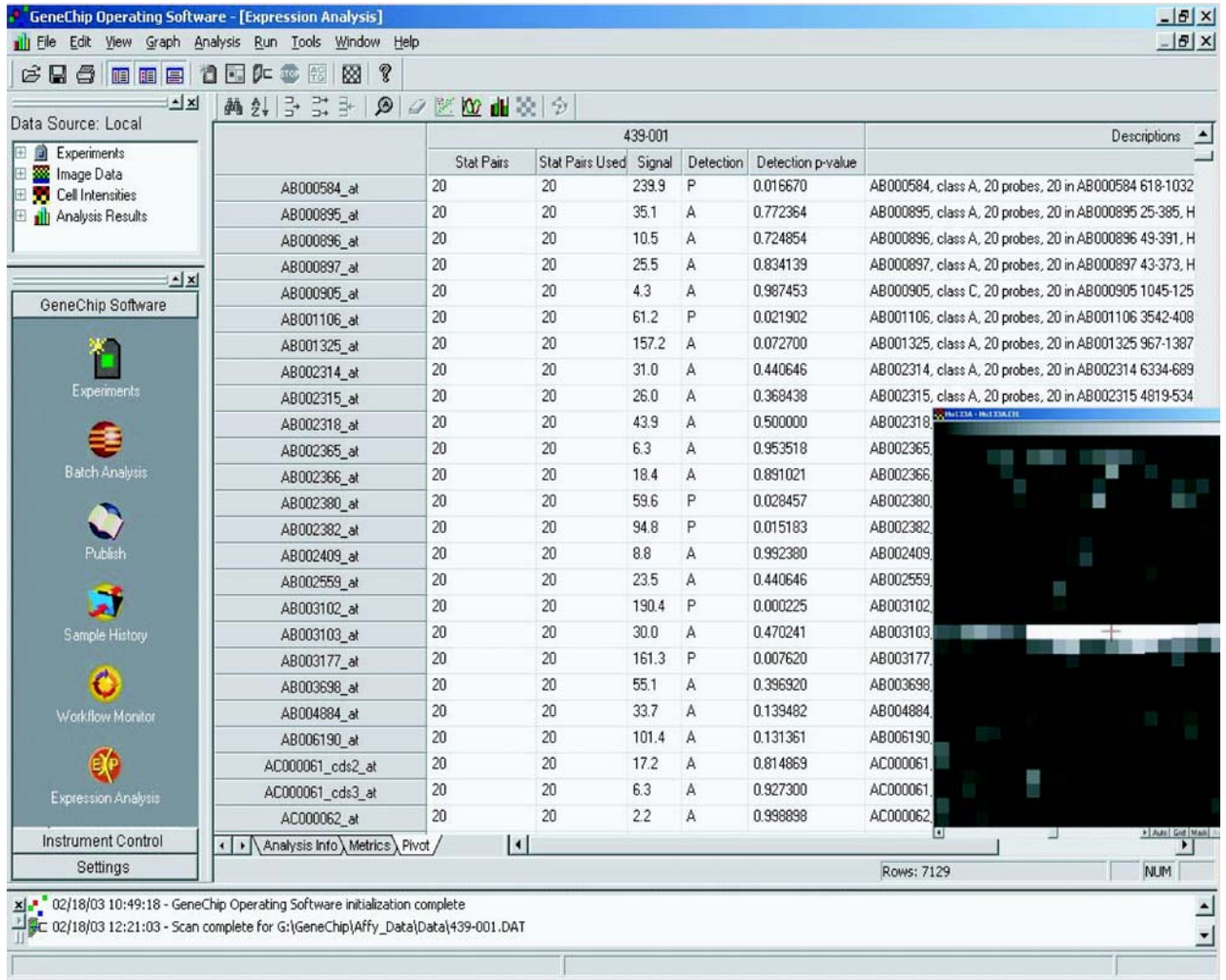


Figure 16: Screenshot of GCOS. This software controls the hardware composed of the fluidics station and the scanner, in addition to analyzing the results of hybridized arrays and calculating the expression profiles of the genes.

II. AIM OF THE THESIS

The aim of the thesis was to identify and further characterize novel genes in the ABCA1 pathway and ABCA1 interactive proteins. Therefore, a Yeast-Two-Hybrid screening was performed with parts of ABCA1 as bait. Putative ABCA1 associated proteins were identified and association in complexes was confirmed by independent approaches. Functional studies were performed to elucidate the physiological consequences of these complexes. Another goal was to identify and characterize genes that are inversely regulated by atherogenic LDL and/or HDL using gene arrays. These experiments were performed with primary human monocytes differentiated in-vitro in the presence of M-CSF to macrophages. These investigations should contribute to the understanding of ABCA1 and other macrophage-specific genes in the pathogenesis of atherosclerosis.

III. MATERIALS

1. CHEMICALS

Agarose	Biozym, Hameln, Germany
Ampicillin	Roche, Mannheim, Germany
Bacto-Agar	Difco-Laboratories, Detroit, USA
Bacto-Trypton	Difco-Laboratories, Detroit, USA
Bacto-Yeast extracts	Difco-Laboratories, Detroit, USA
Blue-dyed Phagobeads (0,8 µm)	Sigma, Deisenhofen, Germany
BSA (Lipid-free)	Sigma, Deisenhofen, Germany
DABCO (Triethylendiamin)	Sigma, Deisenhofen, Germany
EDTA (Di-sodium)	Pharmacia Biotech, Freiburg, Germany
Fluoromount-G	Southern Biotech, Birmingham, USA
Fluoesbrite microparticles	Polysciences, Eppelheim, Germany
H ₂ O Nuclease-free	Promega, Madison, AL, USA
Kanamycin	Roche, Ingelheim, Germany
L-glutamine	Gibco BRL, Berlin, Germany
Lubrol WX	Serva, Heidelberg, Germany
MEM (Non-essential Amino acid)	Gibco BRL, Berlin, Germany
Minimal SD Agar Base	Clontech, Palo Alto, USA
Nickel-Chelating Resin	GenoTech Biosciences, Lohmar, Germany
Penicillin/Streptomycin	Gibco BRL, Berlin, Germany
Polyvinyl alcohol	Sigma, Deisenhofen, Germany
Protease inhibitors	Calbiochem, Bad Soden, Germany
Protein A-Dynabeads	Dynal, Hamburg, Germany
Second strand buffer	Invitrogen, Glasgow, UK
Triton X-100	Boehringer, Mannheim, Germany
Urea	Pharmacia Biotech, Freiburg, Germany

2. STANDARDS AND KITS

1 kb Ladder, DNA	Gibco BRL, Berlin, Germany
100 bp Ladder, DNA	Pharmacia, Freiburg, Germany
AMV-Reverse Transcriptase	Promega, Madison USA
BCA Protein Assay Kit	Pierce, Rockford, IL, USA
Cell Line Nucleofector Kit	Amaxa GmbH, Cologne, Germany
ECL™ Western Blotting Analysis System	Amersham, Braunschweig, Germany
GeneChip Sample Cleanup Module	Affymetrix, Santa Clara, CA, USA

HighYield RNA Transcript Labeling Kit	Enzo Life, Farmingdale, NY, USA
Limulus endotoxin assay	Sigma, Deisenhofen, Germany
Oligotex mRNA Kit	Qiagen, Hilden, Germany
Oligolabeling Kit	Pharmacia, Freiburg, Germany
Rainbow Coloured Molecular Marker	Amersham, Braunschweig, Germany
Reverse Transcription System	Promega, Madison, AL, USA
RNA 6000 Nano Chip	Agilent, Palo Alto, CA, USA
RNeasy Mini Kit	Qiagen, Hilden, Germany
SuperScript Choice System	Invitrogen, Glasgow, UK
T7-Oligo(dT) Promoter Kit	Affymetrix, Santa Clara, CA, USA
QIAEX II Gel Extraction Kit	Qiagen, Hilden, Germany
Qiashredder	Qiagen, Hilden, Germany
Qiaprep (Miniprep) Kit	Qiagen, Hilden, Germany

3. RADIOACTIVE MATERIALS

[³ H]Choline phospholipid	Amersham, Braunschweig, Germany
[¹⁴ C]Cholesterol	Amersham, Braunschweig, Germany

4. ENZYMES

Cholesterol Esterase	Roche, Mannheim, Germany
Klenow-Enzyme	Pharmacia, Freiburg, Germany
Long Template PCR System	Roche, Mannheim, Germany
RNase A	Fluka, Deisenhofen, Germany
T4-DNA-Ligase	Gibco BRL, Berlin, Germany
T4-DNA-Polymerase	Roche, Mannheim, Germany
T4-Polynukleotidkinase	Roche, Mannheim, Germany
Taq-DNA-Polymerase	Roche, Mannheim, Germany
TaqMan PCR Mastermix	ABI, Darmstadt, Germany
Trypsin / EDTA	Sigma, Deisenhofen, Germany

5. HUMAN PRIMARY CELLS AND CELL LINES

5.1. MONOCYTES

Leukocyte-enriched apheresates were obtained from healthy, normo-lipidemic donors 25–45 years of age bearing either the apolipoprotein E3/E3 or the apolipoprotein E4/E4 genotype after informed consent. Monocytes were isolated by counterflow elutriation and cells were cultured at 37°C in 5% CO₂.

5.2. FIBROBLASTS

Human fibroblasts TD1, TD3, and TD5 were obtained from patients with documented mutations in their ABCA1 gene. Patient TD1 bears a homozygous K171X mutation, patients TD3 and TD5 display mutations that have been published previously²¹. As control, human fibroblasts obtained from healthy individuals were used. The fibroblasts were incubated in DMEM medium supplemented with 1% MEM and 10% FCS at 37°C in 5% CO₂ atmosphere.

5.3. HUMAN CELL LINES

The following cell lines have been used:

Cell line	Description	Reference
Hep-G2	Hepatocellular carcinoma	2
Meg-01	Chronic myeloid leukemia	¹⁴³
HL-60	Acute myeloid leukemia	43
THP-1	Acute monocytic leukemia	¹⁹²

6. BACTERIA (E.COLI)

One Shot[®] TOP10

F⁻, *mcrA*, $\Delta(mrr-hsdRMS-mcrBC)$, $\Phi80/lacZ\Delta M15$, $\Delta lacX74$, *deoR*, *recA1*, *araD139*, $\Delta(ara-leu)7697$, *galU*, *galK*, *rpsL(Str^R)*, *endA1*, *nupG*, Invitrogen, Glasgow, UK

7. PLASMIDS

ABCA1 TD
pAS2-1

T. Langmann
Clontech, Palo Alto USA

pACT2	Clontech, Palo Alto USA
pcDNA3.1.D/V5-His-TOPO	Invitrogen, Glasgow, UK

8. MEDIA AND BUFFERS

Bacto-Agar	Difco-Laboratories, Detroit USA
Bacto-Trypton	Difco-Laboratories, Detroit USA
Bacto-Yeast extract	Difco-Laboratories, Detroit USA
DMEM with L-Glutamin	Bio WHITTAKER, Walkersville USA
DMEM with L-Glutamin, w/o Phosphate	Bio WHITTAKER, Walkersville USA
Fetal Calf Serum (FCS)	Gibco BRL, Berlin, Germany
-Leu DO Supplement	Clontech, Palo Alto USA
-Leu/-Trp DO Supplement	Clontech, Palo Alto USA
-Leu/-Trp/-His DO Supplement	Clontech, Palo Alto USA
Luria Broth Base	Gibco BRL, Berlin, Germany
Macrophage-SFM-Medium	Gibco BRL, Berlin, Germany
PBS w/o Ca ⁺² /Mg ⁺²	Gibco BRL, Berlin, Germany
RPMI 1640	Gibco BRL, Berlin, Germany
YPD Medium	Clontech, Palo Alto USA
YPD Agar Medium	Clontech, Palo Alto USA

9. MICROARRAYS

Human Genome U95Av2 Array	Affymetrix, Santa Clara, CA, USA
Human Genome U133A	Affymetrix, Santa Clara, CA, USA
Human Genome U133 Plus 2.0 Array	Affymetrix, Santa Clara, CA, USA

10. TECHNICAL EQUIPMENTS

2100 Bioanalyzer, Caliper	Agilent, Palo Alto, CA, USA
Autoclave Steam Sterilizer Type 24	Melag, Berlin, Germany
Automatic Gamma Counter 1470 WIZARD	Berthold, München, Germany
Biofuge 15R	Heraeus, Hanau, Germany
Cell culture Incubator 6000	Heraeus, Hanau, Germany
ELISA-reader	Tecan, Stuttgart, Germany
FACScan	BD, Heidelberg, Germany
GeneQuant pro RNA/DNA Calculator	Amersham, Braunschweig, Germany

GeneChip® Fluidics Station 450	Affymetrix, Santa Clara, CA, USA
GeneChip® Scanner 3000	Affymetrix, Santa Clara, CA, USA
Horizontal Shaker GFL-3016	GFL, Großburgwedel, Germany
Hybridization Oven 640	Affymetrix, Santa Clara, CA, USA
Incubator B 6120	Heraeus, Hanau, Germany
Instant Camera MP4	Polaroid, Offenbach, Germany
Kodak X-Omat 2000 processor	Kodak, Rochester, NY, USA
LaminAir Hood	Heraeus, Hanau, Germany
Liquid Scintillation Counter Wallac 1410	Berthold, München, Germany
Lumi Imager F1	Boehringer, Mannheim, Germany
Megafuge 1.0 R	Heraeus, Hanau, Germany
Microscope (Visible) Leitz Laborlux S	Leitz GmbH, Wetzlar, Germany
Milli-Q UF Plus System	Millipore, Bradford, VT, USA
MiniSpin Plus Centrifuge	Eppendorf, Hamburg, Germany
Mini Transblot Cell	BioRad, München, Germany
Mini Protean-3 Electrophoresis Cell	BioRad, München, Germany
Mini-Sub Cell GT Electrophoresis	BioRad, München, Germany
pH-Meter pH537	WTW, Weilheim, Germany
Precision Balance Sartorius MD BA 200	Sartorius, Göttingen, Germany
Power Supply PAC 300	BioRad, München, Germany
Princeton MicroMax CCD-1317-K/1	Roper Scientific, Trenton, NJ, USA
Shaking Incubator GFL-3032	GFL, Großburgwedel, Germany
Shaking Water Bath Julabo SW-20C	Julabo, Seelbach, Germany
Spectrophotometer UV/VIS Lambda 2	Perkin Elmer, Überlingen, Germany
Stirrer with Heating Surface IKAMAG	Labor Center, Nürnberg, Germany
SpeedVaq Alpha RVC	Christ, Osterode, Germany
Sysmex Micro-Cell Counter F-300	Digitana AG, Hamburg, Germany
Thermocycler Gene Amp PCR System 9600	Perkin Elmer, Überlingen, Germany
Thermomixer Comfort	Eppendorf, Hamburg, Germany
Ultrasonic Disintegrator Soniprep 150	MSE, Watford Herts, United Kingdom
Ultracentrifuge (fixed angle) J2-21 M/E	Beckman, München, Germany
Ultracentrifuge L-70	Beckman, München, Germany
Ultracentrifuge Optima TLX	Beckman, München, Germany
Vortex-Mixer REAX 2000	Heidolph, Kelheim, Germany
Zeiss Axiovert S-100 Spectral Microscope	Carl Zeiss, Goettingen, Germany

11. SILENCING RNA

Syntaxin 13 (NM_177424) supplied by Ambion, Austin, TX, USA.

Sense sequence: 5'-ggguaucugaaaaggaaaatt-3'

Antisense sequence: 5'-uuuuccuuuucagauaccctt-3'

Non-Silencing Control siRNA: Qiagen, Hilden, Germany.

Sense sequence: 5'-UUCUCCGAACGUGUCACGUdTdT-3'

Antisense sequence: 5'-ACGUGACACGUUCGGAGAAAdTdT-3'

Positive Silencing Control siRNA: Lamin A/C, Qiagen, Hilden, Germany.

Sense sequence: 5'-CUGGACUUCCAGAAGAACAAdTdT-3'

Antisense sequence: 5'-UGUUCUUCUGGAAGUCCAGdTdT-3'

Fluorescent Neg. Control siRNA Fluorescein, Qiagen, Hilden, Germany.

Sense sequence: 5'-UUCUCCGAACGUGUCACGUdTdT-3'

Antisense sequence: 5'-ACGUGACACGUUCGGAGAAAdTdT-3'

12. GENE BANKS

Human Liver MATCHMAKER, cDNA

Clontech, Palo Alto USA

Marathon-Ready cDNA (Liver, Spleen)

Clontech, Palo Alto USA

13. FILMS AND MEMBRANES

ECL Hyperfilm

Amersham, Braunschweig, Germany

Fluorotrans Membrane (PVDF)

Pall Filtron GmbH, Dreieich, Germany

Instant Picture Film Typ 667

Polaroid, Offenbach, Germany

X-Ray Films Biomax

Kodak, Rochester, NY, USA

14. ANTIBODIES

Antibody	Host	Company
ABCA1	Rabbit	Novus, Littleton, CO, USA
β -Actin	Mouse	Sigma, Taufkirchen, Germany
β 2-Syntrophin	Rabbit	Pineda, Berlin, Germany
Caspase 8	Rabbit	Upstate Biotechnology, NY, USA
Early endosome Antigen 1	Rabbit	Abcam, Cambridge, United Kingdom
FADD	Rabbit	Upstate Biotechnology, NY, USA
Flotillin-1	Mouse	BD Biosciences, San Diego, CA, USA
MYC	Mouse	Invitrogen, Karlsruhe, Germany
Syntaxin 1	Rabbit	Calbiochem, Darmstadt, Germany

Syntaxin 2	Rabbit	Calbiochem, Darmstadt, Germany
Syntaxin 3	Rabbit	Calbiochem, Darmstadt, Germany
Syntaxin 4	Rabbit	SySy, Goettingen, Germany
Syntaxin 6	Rabbit	BD Biosciences, San Diego, CA, USA
Syntaxin 7	Rabbit	SySy, Goettingen, Germany
Syntaxin 8	Mouse	BD Biosciences, San Diego, CA, USA
Syntaxin 11	Mouse	Transduction, Lexington, KY, USA
Syntaxin 13	Mouse	Imgenex, San Diego, CA, USA
Syntaxin 13	Rabbit	SySy, Goettingen, Germany
Syntaxin 16	Rabbit	SySy, Goettingen, Germany
Rab9	Mouse	Abcam, Cambridge, United Kingdom

15. PREPARATION OF SOLUTIONS

PBS-Tween

10 l PBS

100 ml 10% Tween

Transfer-buffer (western blot)

1 l Methanol

30.3 g TRIS

144 g Glycine

Ad 10 l H₂O

5x SDS-Gel running buffer (western blot)

75 g TRIS

360 g Glycine

250 ml 10% SDS

5x sample loading buffer (Laemmli dye - western blot)

5 ml Glycerol

1 g SDS

2.56 ml β -Mercapto-Ethanol

2.13 ml 0.5M TrisHCl pH 6.8+ 0.4% SDS

Bromo-Phenol Blue Traces

Tris Base Sodium Chloride TBS-BG (Fluorescent staining)

100 ml Tris/HCl pH 7.6 200 mM

137 ml NaCL 1 M

30 ml KCl 100 mM

10 ml MgCl₂ 150 mM

5 g Glycine

5 g BSA check pH. fill up to 1 l and add:

0.5 ml Tween 20

0.5 g Na-Azid

Mounting Medium (Fluorescent microscopy)

12 g Glycerol (87% 13.8 g)

12 ml H₂O Mix and add 4.8 g Polyvinylalcohol (30-70.000). let stir overnight

Add 24 ml 0.2 M Tris pH 8-8.5 30` at 50°C. Shake occasionally and add 1.15 g DABCO

Centrifuge at 3000 g twice (5 min. RT). Remove supernatant and store in aliquots at -20°C for months or at 4°C for a week.

5 x TBE-buffer (DNA)

54 g Tris; 27.5 g Boric acid; 20 ml 0.5 M EDTA (pH 8.0); ad 1 l H₂O

6 x Sample buffer (DNA)

0.25 % (w/v) Bromphenolblue; 0.25% (w/v) Xylencyanol; 15% (w/v) Ficoll 400 in H₂O

Ethidiumbromid stock solution (DNA – RNA)

10 mg/ml Ethidiumbromide in H₂O

5 x Gel-running buffer (RNA)

0.2 M MOPS. pH 7.0; 50 mM Na-Acetate; 5 mM EDTA

10 x sample buffer (RNA)

50% (v/v) Glycerol; 0.4% (w/v) Bromphenolblue; 0.4% (w/v) Xylencyanol; 1 mM EDTA in H₂O

LB-Medium: 25 g Luria Broth Base; ad 1000 ml H₂O; autoclave

LB-Agar: LB-Medium with 1.5 % (w/v) Agar; autoclave

LB-Agar-Amp: LB-Agar; autoclave; cool to 55°C; add 100 µg/ml Ampicillin

IV. METHODS

1. PRIMARY CELLS AND CELL LINES

1.1. ELUTRIATION OF HUMAN MONOCYTES

Suspensions enriched in human peripheral blood leukocytes were isolated by leukapheresis in a Spectra cell-separator (Gambro BCT), supplemented with the anticoagulant ADCA and diluted with an equal volume of PBS (w/o Ca^{2+} , Mg^{2+}). The diluted apheresate was subjected to counterflow centrifugation (J2-MC centrifuge with JE-6B Rotor, Beckmann) using buffers and centrifuge adjustment as follows:

Running buffer:

PBS (w/o Ca^{2+} , Mg^{2+})

1.0 % (v/v) penicillin / streptomycin-solution

0.5 % (w/v) BSA

0.1 % (w/v) Glucose

Rotation: 2040 rpm		
Rotor temperature: 15°C		
	Flow rate (ml/min)	Volume of fraction (ml)
Loading	7	-
Pre-run	9	150
Fractions 1 - 4	12	50
Fractions 5 - 8	15	50
Fractions 9 - 12	18	50
Fractions 13 - 16	20	50
Fractions 17 - 19	22	50
Fractions 20 - 22	24	50

The monocyte content of each fraction was determined using flow cytometry based on the different scatter properties of lymphocytes, granulocytes and monocytes. Fractions that were devoid of granulocytes with a monocyte content of at least 95% of leukocytes were pooled, washed with PBS (w/o Ca^{2+} , Mg^{2+}) and resuspended in culture medium. The concentration of the suspension was determined with a Sysmex micro-cell counter F-300.

1.2. CULTIVATION AND DIFFERENTIATION OF HUMAN MONOCYTES

10 million monocytes revealing a purity of >95% were seeded on cell culture dishes (10 cm Ø) with a concentration of 1×10^6 monocytes/ml. The serum-free medium complemented with 50 ng/ml human M-CSF (R&D System) and monocytes were incubated for 4 days at 37°C / 5% CO₂ (Heraeus Incubator) to induce phagocytic differentiation as described¹⁸¹. Afterwards, the macrophages were lipid-loaded with either E-LDL (30 µg/ml) or Ox-LDL (100 µg/ml) for 48 h. Lipid Deloading was achieved by incubating the loaded foam cells with new SFM-medium supplemented with HDL₃ (100 µg/ml) for 24 h.

1.3. CULTIVATION OF HUMAN TUMOR CELL LINES

Pro-myelocytic HL-60 human leukemia cells were seeded at a concentration of 1×10^6 cells/ml in non-adherent cell culture flasks (green cups, NUNC, Wiesbaden, Germany) in RPMI medium supplemented with 10% FCS and 1% MEM. The medium was changed once per week and cells were splitted at a 1:3 ratio. Cells were collected by centrifugation at 270 g and resuspended in 3-4 ml medium; counting was performed with Sysmex microcell counter F-300.

Megakaryoblastic leukemia MEG-01 cells were seeded in non-adherent cell culture flasks in RPMI medium supplemented with 10% FCS and 1% MEM. Medium was changed twice weekly and splitting was performed after cells reached confluency at a ratio of 1:4.

Human acute monocytic leukemia THP-1 cells were seeded in non-adherent cell culture flasks in RPMI medium supplemented with 10% FCS and 1% MEM. Medium was changed once weekly and splitting was performed after cells reached confluency at a ratio of 1:3.

Differentiation and adhering was induced in all mentioned cell lines by 10 nM phorbol myristate acetate (PMA).

1.4. TRANSFECTION OF CELL LINES

For transfection, two different methods have been used according to the cell line transfected.

1. *Lipofectamine (Invitrogen)*: A liposome formulation which is suitable for the transfection of DNA into tissue culture cells. It interacts with DNA, forming a lipid-DNA complex, the fusion of the latter with the cells results in efficient uptake of the DNA. The transfection was performed according to manufacturer's instruction.
2. *Human Dermal Fibroblast Nucleofector Kit (Amaxa)*: A non-viral transfection method that permits high gene transfer efficiency for human fibroblasts, the DNA is

directly delivered into the nucleus during nucleofection. The cells are suspended in an appropriate electroporation buffer and put into an electroporation cuvette, DNA is added, the cuvette is connected to a power supply, and the cells are subjected to a high-voltage electrical pulse of defined magnitude and length. The electroporation was performed according to the optimized protocol from the supplier. 2 µg of DNA were transfected into 400'000 cells.

2. LIPOPROTEINS

2.1. ISOLATION OF LIPOPROTEINS

Lipoproteins and lipoprotein-deficient serum were prepared from human plasma or serum by sequential preparative ultracentrifugation in KBr gradients followed by extensive dialysis and filter sterilization. All lipoprotein concentrations mentioned are protein concentrations determined by Lowry's method¹²⁴. Lipoprotein fractions were stored at 4°C and used within two weeks from end of dialysis.

2.2. ENZYMATIC AND OXIDATIVE MODIFICATION OF LDL

Enzymatic degradation of LDL was performed by diluting LDL to 2 mg/ml protein in PBS (w/o Ca²⁺, Mg²⁺). Enzyme treatment was conducted with trypsin (6.6 mg/ml) and cholesterol esterase (40 mg/ml) for 24-36 h at 37°C until the solution was turbid. Mildly oxidative modification of LDL was performed by dialyzing purified LDL (1 mg of protein/ml) against 5 µM CuSO₄ for 48 h.

During LDL preparation and subsequent modification, general precautions were taken to avoid lipopolysaccharide (LPS) contamination. The latter was excluded by Limulus endotoxin assay (Sigma, Deisenhofen, Germany)⁵⁵.

3. PROTEIN METHODS

3.1. ISOLATION OF PROTEINS

Cells were harvested, washed 3 times with PBS, collected by centrifugation for 7 min. at 270 g. Afterwards, cells were resuspended in probe buffer (PBS, 1% Triton X-100, protease inhibitor) and homogenized by sonification on ice. The homogenate was left on ice for 30 min and centrifuged at 14000 rpm at 4°C for 30 min.

3.2. PROTEIN CONCENTRATION DETERMINATION

For protein quantification, the BCA protein assay kit (Pierce) was used. The method is based on the reduction of Cu²⁺-ions to Cu⁺-ions in alkaline environment (Biuret reaction).

The Cu⁺-ions form a complex with **b**icinchonic **a**cid (BCA) a purple colored complex with a peak absorption at 562 nm. The absorption is linear in a range of 20 - 2000 µg/ml and is proportional to the protein concentration.

BCA reagent was freshly prepared by adding 4% CuSO₄ to the protein solution at a ratio of 1:50. 25 µl of the probe or the standard were added to a microtiter plate and mixed with 200 µl of the prepared BCA solution. After incubation at 37°C for 30 min the extinction was measured in an ELISA-reader and the protein concentration was calculated.

3.3. SDS-PAGE AND WESTERN BLOTTING

Proteins are separated by SDS-PAGE (**P**oly**A**crylamide **G**el **E**lectrophoresis) according to their size regardless of any other physical feature.

For gel electrophoresis, pre-cast gradient gels (Bio-Rad) were used. Protein samples were diluted in 5x samples loading buffer (Laemmli dye) and incubated at 85°C for 10 min. The samples were loaded to the gel and separated by Bio-Rad apparatus at 25 mA per gel for 90 min at RT.

After electrophoresis, the gel was transferred to a PVDF Fluotrans transfer membrane using a Mini Trans-Blot electrophoretic transfer cell (Bio-Rad). The transfer conditions were 4°C, 350 mA for 2 h.

After blotting, the membrane was blocked using 5% non-fat dry milk in PBS-Tween (0,1%) at RT for 30 min. Afterwards, primary antibodies were applied at different dilutions (refer to antibodies) for 1 h. After washing 3 times with PBS-Tween 0,1%, the secondary peroxidase-conjugated antibody was diluted 1: 2000 -10000 and incubated at RT for 1 h. Signal detection was performed using ECL plus detection system according to manufacturer's instruction.

3.4. ISOLATION OF PHAGOSOMES WITH PHAGOBEADS

Human macrophages were cultivated with SFM medium supplemented with M-CSF for 4 d for phagocytic differentiation. Blue-dyed latex phagobeads (0,8 µm diameter, 10% aqueous suspension) were diluted at ratio 1:100 in SFM medium and incubated with 10x10⁶ macrophages. After a 1 h pulse (internalization), cells were washed with PBS and further incubated at 37°C for 2, 3, 6, 12 and 20 h (chase) before homogenization. Isolation of phagosomes was performed using a modification of a method described by Desjardins et al.⁵⁰. Cells were washed in cold PBS (3 x 5 ml) and scraped with a rubber Policeman at 4°C. The cells were pelleted and washed in homogenization buffer (250 mM sucrose, 3 mM imidazole, pH 7.4) at 4°C. They were then pelleted again, resuspended in 1 ml of homogenization buffer and homogenized in a homogenizer using ball bearings.

The homogenization was carried out until about 90% of cells were broken without major breakage of the nucleus, as monitored by light microscopy. Unbroken cells were pelleted in a 15 ml Falcon tube at 270 g for 5 min at 4°C and the supernatant, containing the phagosomes, was recovered. The phagosomes were then isolated by flotation on a sucrose step gradient (all sucrose solutions are wt/wt in 3 mM imidazole, pH 7.4) as follows: The supernatant from five subconfluent 10 cm dishes (about 1 ml) was brought to 40% sucrose by adding the same volume of a 62% sucrose solution. This 40% sucrose supernatant was loaded on top of a 1ml cushion of 62 % sucrose. We then added 2 ml of 35 % sucrose, 2 ml of 25 % sucrose, and 2 ml of 10% sucrose solutions. Centrifugation was done in swinging bucket rotor (SW40; Beckman Instruments, Palo Alto, CA) for 1 h at 100,000 g at 4°C. The phagosomes band was collected from the interface of the 10 and 25 % sucrose solutions and resuspended in 12 ml of cold PBS. The phagosomes were finally pelleted by a 15 min centrifugation at 40,000 g in an SW 40 rotor at 4°C.

An important advantage of this flotation method is that the latex beads float the membranes enclosing them to a density on the gradient where no protein was detectable in the absence of beads.

3.5. SUCROSE GRADIENT CENTRIFUGATION AND ISOLATION OF RAFTS

After incubation and the removal of culture media, cells were scraped in PBS and subsequently centrifuged for 10 min at 700 g. The cell pellets (100 ± 30 mg of protein) were lysed for 30min on ice in 500 µl ice-cold TNE-lysis buffer containing 50 mM TRIS, 150 mM NaCl, 5 mM EDTA, 200 mM aminoethylbenzylsulfonamide, 160 mM aprotinin, 10 mM bestatin, 3 mM E64-protease inhibitor, 4 mM leupeptin, 2 mM pepstatin A and either 1% Triton X-100 or 1% Lubrol WX. The lysates were brought to 1,2 M sucrose by adding 300 µl of 2,4 M sucrose in TNE-buffer placed on the bottom of a SW55 TI tube (Beckmann) and overlaid with 1,2 ml of 0,9 M, 0,6 ml of 0,8 M, 1,2 ml of 0,7 M, 1,2 ml of 0,1 M sucrose in TNE-buffer. Samples were ultracentrifuged at 335,000 g at 4°C for 16 h. After centrifugation, 600 µl fractions were collected from the top to the bottom and the pellet was resuspended in Triton X-100 at RT. Then the fractions were either subjected directly to further analysis or pooled to yield the following fractions: fractions 1-5 representing the low-density fraction (LDF), fractions 6-8 representing the high-density fraction (HDF) and the pellet. In a subset of experiments, fractions 6 and 7 obtained after lysis in Lubrol WX were diluted 1:20 with TNE buffer and centrifuged at 100,000 g for 1 h.

3.6. CO-IMMUNOPRECIPITATION

For co-immunoprecipitation, cells were lysed in 1% Triton X-100 in PBS with a protease inhibitor mixture for 30 min at 4°C followed by centrifugation at 15,000 x g for 10 min. The supernatant was incubated overnight with primary antibodies linked to magnetic protein-A beads. The beads were washed three times with the lysis buffer and were eluted by 100 mM triethylamine, pH 11, supplemented with 10% dioxane. The eluates were analyzed by immunoblots. In addition, extracts were lysed in 50 mM Tris, 150 mM NaCl, 1% Nonident P-40, and 0,5% Na deoxycholate in PBS with protease inhibitor (RIPA buffer) and then incubated with primary antibodies linked to magnetic beads for 1h, washed with RIPA buffer three times at RT, and further processed as described above.

3.7. IMMUNOFLOUORESCENT STAINING AND MICROSCOPY

Cells were grown on slides or cover-slips, after removing the medium, the cells were washed with PBS 3 times for 5 min and fixed either with methanol (-20°C) or paraformaldehyde supplemented with glutaraldehyde. The slides were air dried and permeabilised by covering the cells with PBS, 1% Triton X-100 for 5-30 min at RT according to cell type. Afterwards, the cells were blocked with TBS-BG (Tris Base Sodium Chloride) for at least 15 min. The primary antibody was diluted in PBS with 0,1% Triton X-100 and 0,5% BSA, the dilutions ranged from 1:50 to 1:500. For double stains, the antibodies were simply combined (only Ab's from different species), the incubation was performed for at least 1h at RT or over night at 4°C. After that the slides were washed 3 times for 5 min in PBS and secondary antibody was added for 1 hour at RT in the dark.

The antibody solution was prepared by diluting the secondary antibody 1:500 in PBS (0,1% detergent, 0,5% BSA and 0,5 µg/ml DAPI).

Slides were washed 3 x 5 min in PBS, briefly dried and mounted by adding a drop of mounting medium right onto the cells and covered with a cover slip for at least 1h prior to microscoping. Non-confocal fluorescent images were collected on a Zeiss Axiovert S-100 spectral microscope using a CCD camera from Princeton Instruments MicroMax RTE/CCD-1317-K/1 controlled by Metamorph software (Universal Imaging, Downingtown, PA, USA) with excitation and emission conditions chosen to clearly resolve Texas Red- and FITC-labeled secondary antibodies. The nuclear shape was determined from the DAPI staining.

3.8. FLOW CYTOMETRY

Flow cytometry of surface exposed antigens, 5×10^5 cells in 100 µl PBS, 0,5% BSA were incubated for 15 min on ice with saturating concentrations of the antibodies. Thereafter

two washing steps with PBS 0,5% BSA were performed. The cellular light-scatter signals and the fluorescence signals of 20 000 cells per sample were analyzed in list mode at a channel resolution of 1024 with forward scatter as the trigger parameter on an FACSCalibur flow cytometer (excitation: 488 nm (argon) / 635 nm (diode); emission filters: 530/30 nm band pass (channel 1) / 585/47 nm band pass (channel 2) / 670 nm long pass (channel 3): 661/16 nm band pass (channel 4); The photomultiplier gains were calibrated with polychromatic fluorescent reference beads (Polysciences). Compensation was adjusted with fluorochrome-coated microbeads (Becton Dickinson, Heidelberg, Germany). Gating of cultivated fibroblasts was based on forward- and side-scatter dot plots. Antibodies used for detection were directly fluorochrome conjugated. Mean fluorescence values were corrected for background by subtraction of cellular auto fluorescence. For analysis of the list files the software CellQuest 2.0 (Becton Dickinson, Heidelberg, Germany) was used on a Macintosh G3.

4. RADIOACTIVE LIPID EFFLUX

Efflux of [³H]-choline phospholipids from cells was measured by the appearance of radioactive label in the medium after incubation with either apoA-I or HDL₃. Lipids in the medium were extracted according to the method of Bligh and Dyer²⁰, and the radioactivity was measured by liquid scintillation counting. Lipid efflux was calculated by subtracting the radioactivity secreted in the supernatant from total radioactivity. Specific lipid efflux was determined as lipid efflux in the presence of apoA-I or HDL₃ subtracted by the efflux in the absence of a nonspecific acceptor (BSA).

5. CULTIVATION OF ESCHERICHIA COLI

E. coli cultures were cultivated either on agar plates or in liquid medium over night at 37°C in an incubator. Cultures were obtained by inoculating a single colony or suspension of bacteria from a glycerol culture into LB-medium. Liquid cultures are incubated in a shaker at 37°C and 240 rpm over night. It is necessary to add an appropriate antibiotic (Ampicillin) to select a specific plasmid.

E. coli cultures were permanently stored in glycerol, to achieve this 500 µl liquid culture was mixed with 500 µl sterile glycerol (30%) in a Cryo-tube and were shock frozen in liquid nitrogen and stored at -80°C.

6. NUCLEIC ACID METHODS

6.1. RESTRICTION ENZYME DIGESTION OF DNA

The restriction digest can either be performed analytically to analyze the DNA or

preparatively to prepare DNA for further cloning. The incubation is performed with buffers obtained from Roche (10x buffers: A, B, L, M, H) for 2 h at the according temperature in a thermo block.

For the analytical approach, 1 µg DNA is digested with 10 units of restriction enzyme in 20 µl total volume. For preparative digestions, 20 µg of DNA were digested with 30 units of enzyme at a total volume of 80 µl.

6.2. DNA GEL ELECTROPHORESIS AND DNA EXTRACTION FROM AGAROSE GELS

Different length DNA-molecules can be separated in agarose gels according to their mobility and the negative total charge of the DNA-double helix.

The electrophoretic mobility of the DNA is inversely proportional to the logarithm of base pairs. Polyacrylamid gels are capable of separating DNA fragments up to 1 kb of size, whereas agarose gels separate fragments up to 20 kb. In order to achieve a maximum of separation capacity gels are cast in following concentrations:

DNA fragment size < 1kb	1,5% - 4% gel
DNA fragment size 1 – 10 kb	0,7% - 1% gel
DNA fragment size > 10kb	0,5% gel

The applied voltage varied between 80 – 100 V. To visualize the DNA in the gel, ethidium bromide was incorporated in the gel, and this mutagen substance binds to the DNA double helix, staining it with an orange colored fluorescent light when observed under UV (365nm). The gel was photographed with a MP-4 camera (Polaroid) or scanned with a Lumi-imager (Boehringer-Mannheim).

DNA-fragments were extracted from agarose gels by selectively adsorbing them to a special matrix. This was accomplished using the „QIAEX II Gel Extraction Kit” (Qiagen). In this method, DNA is bound to a silica-matrix at a high salt concentration and then eluated in water at low salt concentrations. The agarose piece is diluted with 10 times of its volume with QX1 buffer and 10µl QIAEX II suspension is added and incubated at 50°C for 10 min in a shaking thermo block. After centrifugation (18000 g, 2 min) the pellet was washed with PE-buffer, dried and the DNA was resuspended in 20 µl of sterile water.

6.3. CLONING OF DNA FRAGMENTS

Prior to transfection, the DNA fragment must be ligated to the plasmid, this is done by the T4-DNA-ligase enzyme in presence of ATP and Mg²⁺ ions. The optimal ratio between the

plasmid and the insert-DNA is 1:3.

Plasmid-DNA (200 ng/μl)	2,0 μl
Insert-DNA (200 ng/μl)	6,0 μl
5 × Ligase buffer	4,0 μl
T4-DNA-Ligase (5 U/μl)	1,0 μl
H ₂ O (Millipore)	7,0 μl

The ligation is performed over night at 14°C.

Prior to transfection, the chemically competent *E. coli* were thawed on ice and the selection plates (LB +Amp) were pre-warmed to 37°C on the bottom shelf of an incubator. The ligation mixture was added to the cells and left on ice for 30 min followed by 30 sec at 42°C. The cells were spread onto the pre-warmed plates, air dried for 5 min and cultured over night at 37°C.

6.4. SMALL INTERFERENCE RNA (SIRNA)

RNA interference is based on the observation that the presence of double stranded RNA in a cell eliminates the expression of a gene having the same sequence, whereas expression of other unrelated genes are left undisturbed.

Double stranded RNA (dsRNA) is recognized and bound within the cell by the Dicer-RDE-1 (RNAi deficient-1) protein complex. This protein complex cleaves long dsRNA into 19-22 bp siRNA oligonucleotides. The antisense strand of the siRNA is used by an RNA-induced silencing complex (RISC) to guide mRNA cleavage, therefore promoting mRNA degradation. Knockdown of the syntaxin 13 expression was achieved by transfection of cells with siRNA. The siRNA was designed and supplied by Ambion (Austin, TX). A sequence of 19 nucleotides starting at position 421 of syntaxin 13 (NM_177424) was targeted; the sense sequence was 5'-ggguaucugaaaaggaaaatt- 3', and the antisense sequence was 5'- uuuuccuuuucagauaccctt-3'. Transfection was done using RNAiFect reagents (Qiagen, Hilden, Germany), according to the manufacturer's instructions. As control a nonsilencing siRNA was used (Qiagen). The knockdown of syntaxin 13 expression reached its maximum 3 d after transfection.

6.5. RNA ISOLATION

The method of choice is the Trizol method. Cells are washed with PBS and 1 ml Trizol is added for 10×10^6 cells. The RNA is now protected from degradation and can be stored at -80°C for several months. Before processing, the solution was pressed through a syringe for homogenization. A volume of 200 μl chloroform was added to 1 ml Trizol, vigorously shaken and, after incubation at RT for 3 min, centrifuged at 12,000g for 15 min at 4°C.

The upper aqueous phase with the RNA was collected and placed in a new cup. 500 μ l isopropanol were added and left on ice for 15 min. After precipitation, the cup is centrifuged at 12,000 g for 30 min at 4°C. The pellet was washed twice with ethanol (75%) and the pellet was air-dried and afterwards resuspended in 100 μ l of RNase-free water.

Note: Phenol, which also absorbs light at 260 nm, can greatly affect the quality and quantitation of total RNA sample, it further inhibits or reduces the efficiency of a RT-PCR reaction.

6.6. QUALITY ASSESSMENT AND QUANTIFICATION OF RNA (AGILENT)

After the RNA has been resuspended in water, it is left at -80°C over night for complete solubilization. 1 μ l was diluted at a ratio of 1:10 and measured at 260 nm. The concentration is calculated according to the following formula:

$$C \text{ } \mu\text{g/ml} = E_{260} \cdot k / d \quad k = 40 \text{ for RNA, } k = 20 \text{ for ss DNA, } k = 50 \text{ for ds DNA}$$

$$d = \text{Path length of cuvette [cm]}$$

The quality was assessed by using the Agilent 2100 bioanalyzer in combination with the 6000 Nano LabChip® according to manufacturer's instructions.

6.7. RNA GEL ELECTROPHORESIS

Total RNA is separated in a formaldehyde-containing agarose gel after the secondary structure of RNA has been denaturated at 56°C; the formaldehyde keeps the RNA from renaturating.

For a 100 ml gel, 1,2 g agarose were boiled in 63 ml of Millipore water. After cooling to 60°C, 20 ml 5 x Gel Running Buffer (see material) and 17,8 ml formaldehyde were added.

The RNA-probes were prepared as follows:

10 μ g total-RNA	4,5 μ l
5 x Gel Running Buffer	2,0 μ l
Formamid	10,0 μ l
Formaldehyde (37 % v/v)	3,5 μ l

After denaturation of RNA (15 min, 56°C), 2 μ l 10 x RNA sample buffer were added and the sample was applied to the gel. Electrophoresis was performed in 1 x gel running buffer at 13 V over night. The gel was washed in Millipore water for 60 min and stained for 10 min in 250 ml Millipore water + 10 μ l ethidium bromide, washed again in water and photographed with a fluorescent ruler.

6.8. REVERSE TRANSCRIPTION PCR (RT-PCR)

AMV reverse transcription system from Promega was used to synthesize single-stranded cDNA from total RNA.

For 4 µg of total RNA the following reaction mixture has been prepared: MgCl₂ 16 µl, RT-buffer 8 µl, dNTP mix 8 µl, RNAsin 2 µl, AMV reverse transcriptase 3 µl, oligo dT 4 µl, in a total volume of 40 µl.

The RNA is placed in a cup and incubated at 70°C for 10 min, then the mix is added and the cup is incubated at 42°C for 60 min. After heat-inactivation at 95°C, the reaction is cooled on ice for 5 min.

6.9. REAL-TIME PCR

In conventional PCR, quantification either requires multiple samples or several aliquots must be taken from a single sample at certain intervals. The accuracy of this method is limited because the amplification product has to be detected by ethidium bromide staining, a procedure which lacks sensitivity and specificity and is time consuming. These drawbacks can be eliminated by using a novel method which uses online-detection of fluorescence as a marker for the ongoing PCR. Two different methods are used in Real-Time-PCR, both of which can be practiced either on the LightCycler system (Roche) or on the Taqman (ABI).

6.9.1. GENE EXPRESSION MONITORING WITH SYBR-GREEN-I DYE (LIGHTCYCLER)

The fluorescent dye SYBR-Green I binds to the minor groove of the DNA double helix. In solution, the unbound dye exhibits very little fluorescence, this is greatly enhanced upon DNA-binding.

At the beginning of amplification, the reaction mixture contains the denatured DNA, the primers, and the dye and only a weak fluorescence is detectable (Figure 17 A).

After annealing of the primers and beginning of the elongation step, SYBR-Green molecules bind to the dsDNA, resulting in increased light emission upon excitation (Figure 17 B). During elongation, more and more dye molecules bind to the newly synthesized DNA (Figure 17 C). By continuous monitoring of the reaction, an increase in fluorescence is determined in real-time. Upon denaturation of the DNA for the next heating cycle, the dye molecules are released and the fluorescence signal falls. Fluorescence measurement at the end of the elongation step of every PCR cycle is performed to monitor the increasing amount of amplified DNA.

The advantages of this method are the easy way of conducting it, in addition to its low cost. The disadvantages lie in the relatively low specificity, since SYBR-Green will bind to any double stranded DNA regardless if it is the targeted DNA or not.

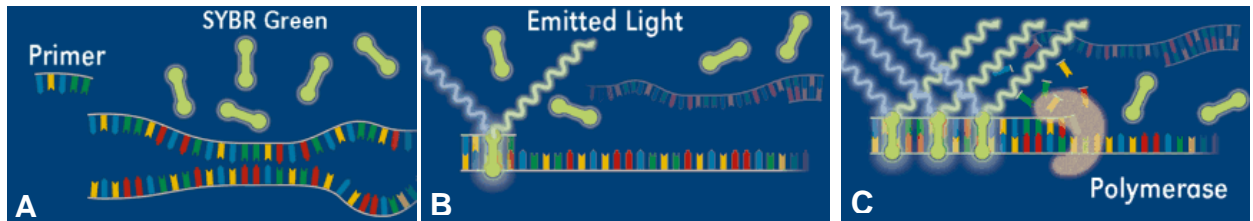


Figure 17: Steps of real-time PCR in the Light Cycler. A. SYBR-Green dye does not bind to the denaturated single strand DNA. B. after elongation process, the double strand DNA begins to bind SYBR-Green. C. Increasing fluorescence is measured at the end of the elongation step every cycle. Roche applied science online site [Roche homepage].

The LightCycler experiments were performed with the hot-start DNA Master SYBR-Green I kit provided by Roche Molecular Biochemicals (Mannheim, Germany). Specific primer pairs were used for PCR amplification.

Each reaction (20 μ l) contained 2 μ l cDNA, 2.5 mM $MgCl_2$, 1 pmol of each primer and 2 μ l of Fast-Start Mix (containing buffer, dNTPs, SYBR-Green dye and Taq polymerase). The amplification program consisted of 1 cycle of 95°C with a 5 min hold ('hot start') followed by 45 cycles of 95°C with a 15 second hold, 60°C annealing temperature with a 5 second hold and 72°C with a 10-second hold. Amplification was followed by melting curve analysis to verify the correctness of the amplicon. A negative control without cDNA was run with every PCR to assess the specificity of the reaction. Analysis of data was performed using LightCycler software version 3.5. PCR efficiency was determined by analyzing a series of 2-fold dilutions of cDNA. Using the analysis mode of the LightCycler software, the slope of log concentrations of the cDNA dilutions was calculated. Efficiency was calculated as follows: $Eff. = 10^{-1/slope}$. For quantification, we only used primer pairs showing amplification efficiency between 1.92 and 2.04. The measured efficiencies were used for calculation. GAPDH was analyzed in parallel as a housekeeping gene.

6.9.2. GENE EXPRESSION MONITORING WITH HYDROLYSIS PROBES (TAQMAN)

The hybridization probe format is used for DNA detection and quantification and provides a maximal specificity for product identification. In addition to the reaction components used for conventional PCR, a specially designed, sequence specific oligonucleotide is applied in this detection method. This oligonucleotide is called Taqman probe, it is labelled with two fluorescent dyes: one is the emitting fluorescent dye (FAM, VIC) and the other is

either a fluorescent (TAMRA) or a non-fluorescent quencher. As long as the two dyes are in close proximity, the light emitted from the first dye, is quenched by the other, but as elongation occurs, the probe is hydrolyzed and the two dyes are separated from each other allowing a fluorescence emission. The increasing amount of measured fluorescence is proportional to the increasing amount of DNA generated during the ongoing PCR process (Figure 18).

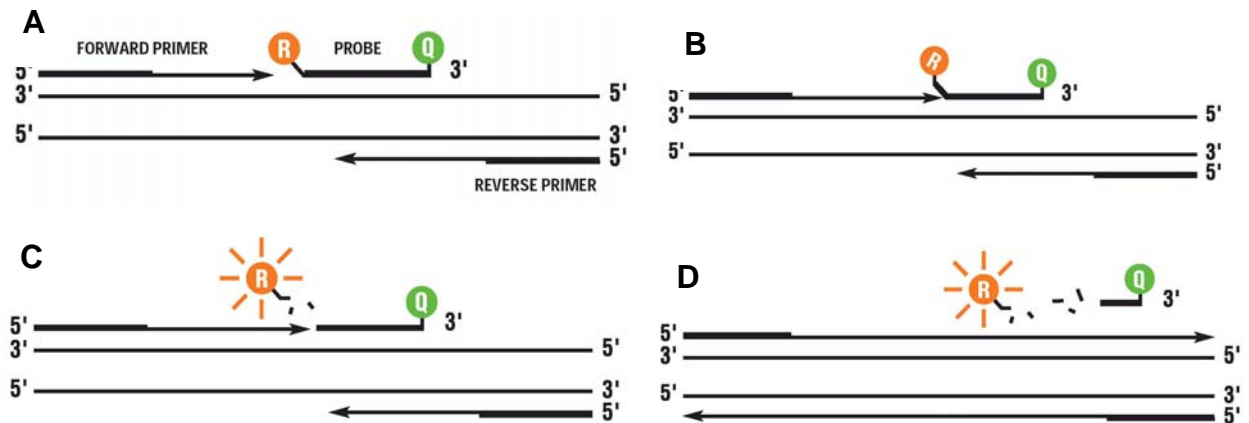


Figure 18: Steps of real-time PCR in the Taqman. A. fluorescent reporter (R) dye and a quencher (Q) are attached to the 5' and 3' ends of a TaqMan probe. B. When the probe is intact, the reporter dye emission is quenched. C. During each extension cycle, the DNA polymerase cleaves the reporter dye from the probe. D. Once separated from the quencher, the reporter dye emits its characteristic fluorescence [Applied Bioscience homepage].

7. AFFYMETRIX® MICROARRAYS

10 µg of total RNA were reverse transcribed by the Invitrogen Life Technologies SuperScript Choice system using T7-oligo-dT primer (50 µM) and the SuperScript II RT (400 U) for 75 min. After that a second strand cDNA is synthesized by T4 DNA polymerase (10 U).

cDNA was synthesized by a Superscript II kit (Life Technologies) using T7-oligo(dT) primer. The cDNA is cleaned by the Gene Chip Sample Cleanup Module supplied by Affymetrix. The antisense cRNA strand is amplified and biotin-labeled by Enzo BioArray HighYield RNA Transcript Labeling Kit based on the manufacturer's protocol. The Biotin-labeled cRNA was purified, fragmented and quantified by measuring the

spectrophotometric absorbance at 260 nm; the purity was determined by the use of the 2100 Bioanalyzer (Agilent technologies).

After addition of control oligonucleotide B2 (3 nM) and 20x Eukaryotic Hybridization Controls (bioB, bioC, bioD, cre) the cRNA was hybridized to Affymetrix H-U133A GeneChips (Santa Clara, CA) for 16 h at 45°C. The chips were stained with Streptavidin Phycoerythrin (SAPE), and washed in the Fluidics Station 450 with protocol EukGE-WS2 which includes an antibody amplification step. The arrays were scanned on the Affymetrix array scanner and the gene expression data analysis was performed according to instructions and recommendations provided by Affymetrix using the Affymetrix statistical data analysis software, Affymetrix Microarray Suite (MAS, version 5.0), which controls the fluidics stations and scanners. In addition, MAS acquires data, manages sample and experimental information.

For each gene, the gene expression of the treated cells and the control was compared. The comparison was based on a statistical analysis of probe sets consisting of 16 oligos recognizing different portions of the target gene. Based on the expression algorithm, MAS computes the detection call which defines whether a signal is absent, marginal or present. This call is emphasized by a detection p-value and by a normalized signal which is background-subtracted and adjusted for noise. In addition, MAS is capable of doing comparison analysis, calculating the difference call. Each transcript has five possible calls, Increase, Decrease, Marginal Increase, Marginal Decrease, No Change. The probe sets were excluded if the detection call for both target and reference was absent; or if the change call gave no change (NC) in comparison analysis or if the signal log ratio (SLR) between target and reference was between -1 and 1.

The SLR monitors the expression level of a transcript between a baseline and an experiment array. This value is logarithmic and a log₂ ratio of 1 equals a fold change of 2. Using the SLR a fold change can be calculated using the following formula:

$$\begin{aligned} FC &= 2^{(SLR)} && \text{if } SLR \geq 0 \\ FC &= -1 * 2^{(-SLR)} && \text{if } SLR < 0 \end{aligned}$$

8. YEAST-TWO-HYBRID SYSTEM

This part of work was done as described in ^{27,154}, therefore, it will not be explained here in detail. Shortly, the last 144 C-terminal amino acids of ABCA1 were cloned into pAS2.1

9. MASS SPECTROMETRY

This part of work was done as cooperation with Dr. G. Liebisch as described in ¹¹⁸ therefore, it will not be explained here in detail. Shortly, sera from 4 pallidin knock-out mice and 4 wild-type mice were collected and pooled in each category. The sera were separated by fast protein liquid chromatography (FPLC) and subsequently lipoproteins were analyzed by electrospray ionization - tandem-mass spectrometry (ESI-MS/MS).

V. RESULTS

1. IDENTIFICATION OF ABCA1 INTERACTIVE PROTEINS BY YEAST-TWO-HYBRID SYSTEM

Since ABCA1 plays a central role in the reverse cholesterol transport, we aimed to identify proteins which interact with ABCA1. These proteins may contribute to the stability and processing of ABCA1. The yeast-two-hybrid system was used to screen a human liver library. Since the C-terminal region of several ABC-transporters like CFTR are involved in protein-protein interactions, the C-terminal region of ABCA1 was used as bait.

Therefore, we constructed a fusion construct of the Gal4 DNA-binding domain with the C-terminus of human ABCA1 (bp 6292–6723) which resembles the 144 carboxy-terminal amino acids. The alignment of the ABCA1 C-terminus with ABCR shows the high conservation of several amino acids and a number of mutations and polymorphisms found in this region, further supporting the functional importance of these amino acids (Figure 19).

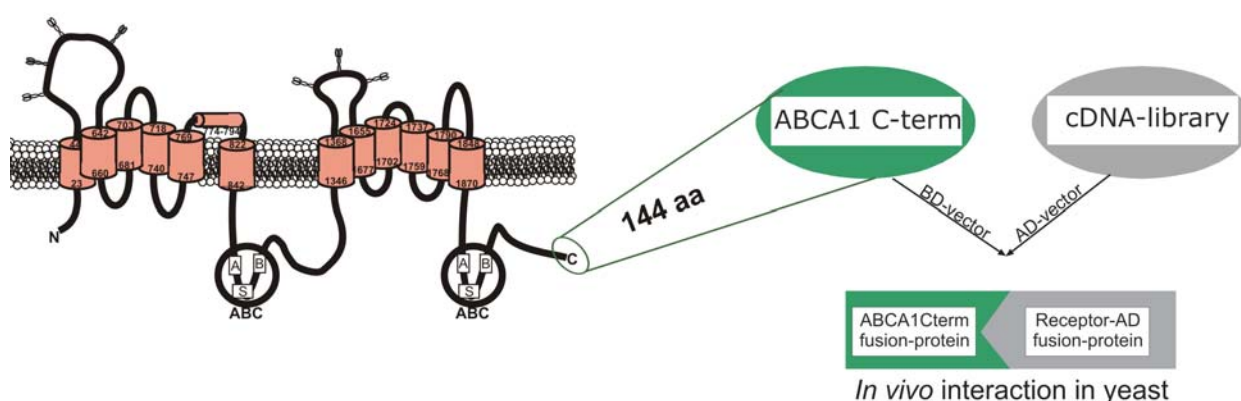


Figure 19: Model of ABCA1 protein and Yeast-Two-Hybrid approach. The coloured cylinders resemble the transmembrane domains, the two circles the walker motifs. The last 144 amino acids were used as bait for a Yeast-Two-Hybrid approach to identify ABCA1 interacting proteins in human liver library.

This was used as bait with which we screened a human liver yeast-two-hybrid cDNA library, to identify proteins which may interact with ABCA1.

Table 5: Proteins identified to interact with ABCA1. The name, the human unigene number (Hs.) and the number of clones identified are given.

Identified gene	Unigene	Number of clones
Fas-associated death domain (FADD)	Hs.86131	3
β 2-syntrophin (SNTB2)	Hs.461117	3
RET finger protein (RFP)	Hs.440382	4
PRP8 splicing factor	Hs.181368	4

UDP-glucose pyrophosphorylase (UGP2)	Hs.516217	4
Succinate dehydrogenase (SDHB) (Iron-sulphur protein subunit)	Hs.465924	2
Aldehyde oxidase 1 (AOX1)	Hs.406238	14
Unknown		5

2. CHARACTERIZATION OF THE ABCA1-FADD COMPLEX

One of the positive clones identified to interact with the ABCA1 C terminus encoded the 98 C-terminal amino acids of FADD (amino acid positions 111–208) as a Gal4 activation domain fusion protein. The identified ABCA1-interacting FADD fragment contains almost the complete death domain of FADD (amino acids 97–161).

To further confirm the association of ABCA1 and FADD, pull-down assays were performed.

His-tagged full-length human FADD bound to nickel-chelating resin (GenoTech Biosciences, Lohmar, Germany) was incubated with *in-vitro* translated ABCA1 C-terminus with an N-terminal Myc-tag. The ABCA1 C-terminus was pulled down by FADD-agarose and detected on the immunoblot using a Myc antibody, whereas FADD-agarose (Upstate Biotechnologies, NY, USA), with Myc-tagged aldehyde oxidase as control gave no signal on western blots (Figure 20 A).

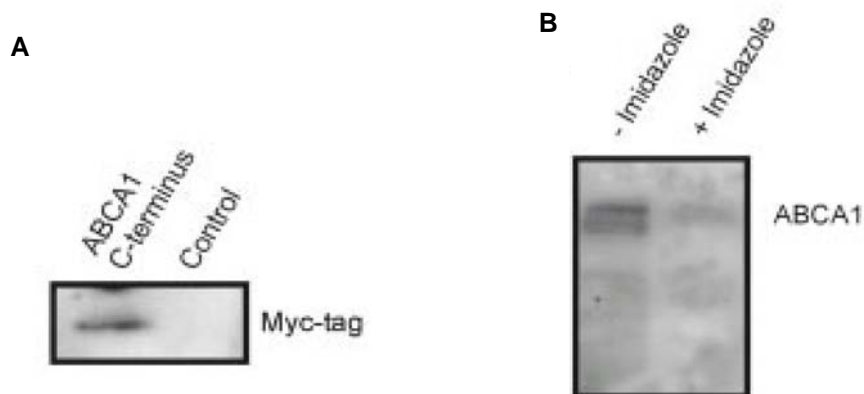


Figure 20: Interaction of ABCA1 with FADD. (A) *In-vitro* translated ABCA1 C-terminus with an N-terminal Myc tag (*left*) and Myc-tagged aldehyde oxidase (*right*) as control was precipitated by FADD-agarose. The precipitates were analyzed on immunoblots using a Myc antibody. (B) FADD-agarose (*-imidazole*) and agarose where FADD has been eluted with 100 mM imidazole (*+imidazole*) were incubated with cell lysates of the human hepatoma cell line HepG2, precipitates were analyzed on immunoblots using ABCA1 antibody.

To verify the validity of ABCA1-FADD interaction in human cell lines, we repeated the pull-down of ABCA1 with FADD-agarose from cell lysates of the human hepatoma cell line

HepG2. As a control for this experiment we eluted FADD from the agarose by washing it with 100mM imidazole prior to loading it to the cell lysate and, as presumed, ABCA1 was not detected in the precipitate (Figure 20 B).

To elucidate whether the amount of precipitated ABCA1 correlates with the amount of FADD used, the procedure was repeated in the megakaryoblastic leukaemia cell line Meg01 which reveals a high expression of ABCA1, but this time with increasing quantities of cell lysate (10, 20, and 30 μ g). As result, increasing amounts of ABCA1 were pulled down by FADD agarose (Figure 21).

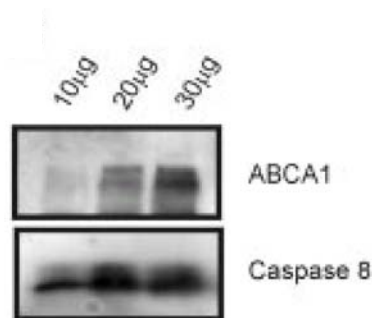


Figure 21: Interaction of ABCA1 with FADD in Meg-01 cell line. FADD-agarose was incubated with 10, 20, and 30 μ g of cell lysate prepared from the megakaryoblastic leukaemia cell line Meg-01. The precipitates were analyzed on immunoblots with ABCA1 and caspase 8 antibodies.

All these experiments strongly supported our initial finding that ABCA1 interacts with FADD. Furthermore, caspase 8, a protein described to interact with FADD, was also detected in the FADD-agarose precipitates by immunoblotting in both Meg-01 and HepG2 cells (Figure 22A). Although caspase 8 is not associated with FADD in non-apoptotic cells, caspase 8 was precipitated by FADD-agarose. With this approach potentially

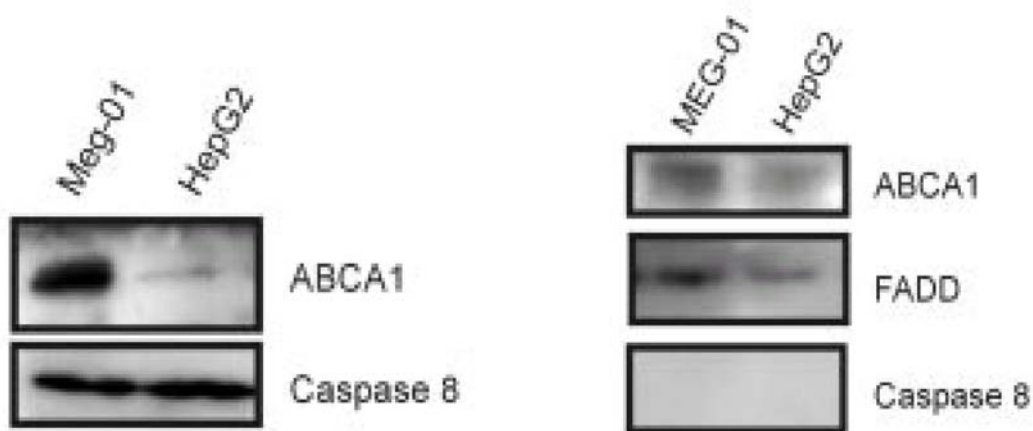


Figure 22: Co-immunoprecipitation of FADD with ABCA1 in cell lines. A. Immunoblot of ABCA1 and caspase 8 precipitated from Meg-01 and HepG2 cell lysates using FADD-agarose. B. ABCA1 antibody was covalently linked to magnetic beads and incubated with lysates from Meg-01 and HepG2. The precipitates were analyzed for ABCA1, FADD, and caspase 8 using the respective antibodies.

interacting proteins can be identified, but this alone does not prove that FADD and ABCA1 are really associated in these cell lysates. Therefore, to investigate the presumptive endogenous association of ABCA1 with FADD, ABCA1 antiserum was covalently linked to magnetic beads. Upon incubation of the beads with cell lysates, the ABCA1 antibody was able to precipitate ABCA1 and endogenous FADD from lysates of the hepatoma cell line HepG2 and Meg-01 cells, caspase 8 was not co-immunoprecipitated (Figure 22 B).

To verify this interaction in primary cells, human fibroblasts from two different healthy donors (F1 and F2) were lysed and ABCA1 and FADD but not caspase 8 were also precipitated from this lysates using ABCA1 antiserum (Figure 23).

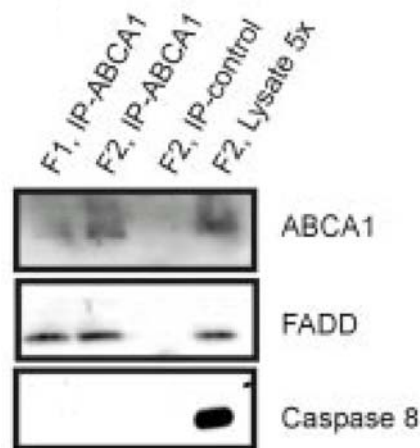


Figure 23: Co-immunoprecipitation of FADD with ABCA1 in human fibroblasts. Lysates of fibroblasts were used for immunoprecipitation using ABCA1 antibody (*F1, IP-ABCA1; F2, IP-ABCA1*). Immunoblots with the precipitates or the lysate were performed and probed with ABCA1, FADD, and caspase 8 antibodies. F1: Fibroblast 1; F2: Fibroblast 2; IP: Immunoprecipitation; IP-control: unrelated antibody.

A control antiserum failed to immunoprecipitate ABCA1 and FADD from the lysate of F2 (Figure 23). The supernatant of the lysate F2 after incubation with ABCA1 antibody was 5-fold concentrated, and the immunoblot indicates that about 50% of ABCA1 and FADD and nearly 100% of caspase 8 remain in the supernatant.

This indicates that caspase 8 does not interact with FADD associated with ABCA1 or that the amount of caspase 8 associated with ABCA1 and FADD is beyond the sensitivity of the western blot.

Since ABCA1 is known to facilitate the transfer of phospholipids to apoA-I, whereas FADD is mainly described as an adaptor molecule in death receptor-induced apoptosis, the association of ABCA1 with FADD may imply a response of fibroblasts to lipid loading.

Therefore we investigated the protein expression of FADD in fibroblast from controls incubated with E-LDL for 24 h, in serum-starved cells for 3 days and in cells incubated with HDL₃ for 24 h to promote lipid efflux (Figure 24).

FADD expression was not altered under these culture conditions indicating that FADD expression is not sensitive to lipid loading or deloading.

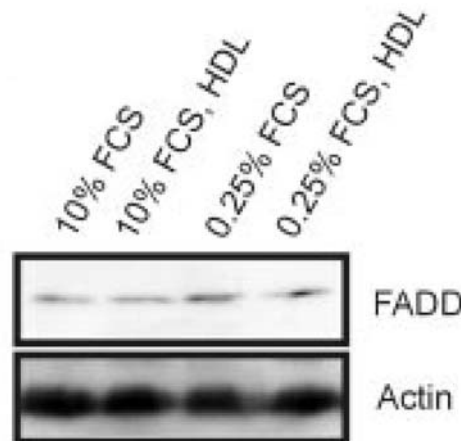


Figure 24: FADD is not sensitive to lipid-loading. FADD and actin immunoblot using whole cell lysates from human fibroblasts cultivated with 10% FCS for 4 d (10% FCS), and additionally 24 h in 10% FCS with 100 $\mu\text{g/ml}$ HDL₃ (10% FCS, HDL), or the same conditions with 0,25% FCS

To analyze whether inhibition of FADD may modulate ABCA1 function; a dominant negative form (FADD-DN)⁸⁷ was cloned into pcDNA3.1/NT-GFP and expressed with a N-terminal GFP fusion in HepG2 cells. In addition, a GFP fusion with the 144-amino acid C terminus of ABCA1 was generated to analyze a possible inhibitory function of the ABCA1 C terminus. Stable clones were selected, and expression of GFP was monitored by fluorescence microscopy and flow cytometry. Nearly 95% of the transfected HepG2 cells were GFP-positive with both methods.

Immunoblot analysis with GFP antiserum revealed that the ABCA1 C-terminal construct was weakly expressed, whereas FADD-DN was expressed at a much higher level. In the transfected cells expression of ABCA1, FADD, and caspase 8 was investigated by immunoblots. Recombinant FADD-DN was much more abundant than native FADD, which was similarly expressed in the transfected cells (Figure 25 A).

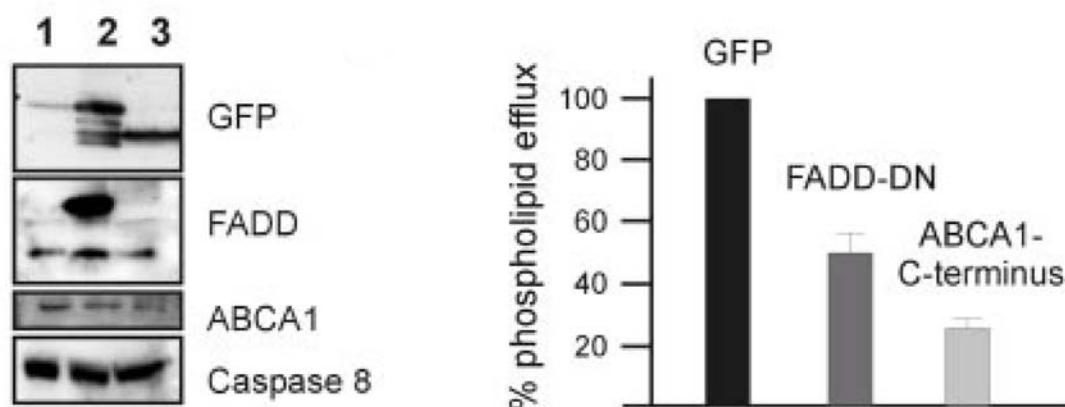


Figure 25: Expression of FADD-DN and ABCA1 in HepG2 cells and its effect on lipid efflux. A. HepG2 cells were stably transfected expressing ABCA1 C-terminus with an N-terminal GFP tag (lane 1), FADD-DN fused to GFP (lane 2), or GFP alone as control (lane 3). B. specific choline phospholipid efflux from stably transfected HepG2 cells expressing GFP as control, FADD-DN fused to GFP, or ABCA1 C terminus with an N-terminal GFP tag. The efflux of the GFP-transfected cells was set to 100%.

The transfected cells were further analyzed for choline phospholipid efflux to apoA-I. Cells were labeled with [³H]-choline for 34 h and subsequently incubated in the presence of bovine serum albumin or bovine serum albumin plus apoA-I as an acceptor.

After incubation, the media were removed and centrifuged at 800g to precipitate any detached cells. Cells were rinsed 3 times with PBS and lysed with 0,2% SDS. Lipids were extracted from supernatant media and cell lysates according to the method of Bligh and Dyer ³H-radioactivity was measured by liquid scintillation counting in total lipid extracts from cell lysates and in the incubation media. Lipid efflux in response to HDL₃ is expressed as the percentage of “total radioactivity” that appeared in the medium after the chase period.

The efflux of the GFP-transfected cells was set to 100%. Specific efflux in FADD-DN expressing cells was 46,2 ± 9.5% and 26,2 ± 7.4% in cells with recombinant ABCA1 C terminus. Four assays with triplicate determinations were performed. Specific efflux was calculated by subtraction of efflux without acceptor from apoA-I-mediated efflux. Reduction of efflux is significant for FADD-DN and ABCA-1 C terminus with p<0.001 (Student’s t test). As result, expression of the ABCA1 C-terminus inhibited apoA-I-inducible phospholipid efflux 4-fold and the expression of FADD-DN reduced efflux by 50% thereby confirming that full length FADD has relevance for ABCA1 function (Figure 25 B).

FADD-DN protected HepG2 cells from TNF- α /CHX-induced apoptosis, whereas HepG2 cells expressing GFP or the ABCA1 C-terminus revealed a similar response as detected by the release of histone-bound DNA fragments and trypan blue staining of dead cells.

3. CHARACTERIZATION OF THE ABCA1 - β 2-SYNTROPHIN COMPLEX

β 2-syntrophin is a protein previously shown to interact with utrophin¹⁵¹, it has a PSD95 Disc large Zo1-domain and two functional pleckstrin-homology (PH) domains, which are often found in cytoskeletal or signalling proteins where they mediate protein-protein or protein-lipid interactions¹⁷⁵.

Initially we searched for a cell line highly expressing ABCA1 by immunoblotting cell lysates from fibroblasts, platelets and Meg-01 cell line (Figure 26)

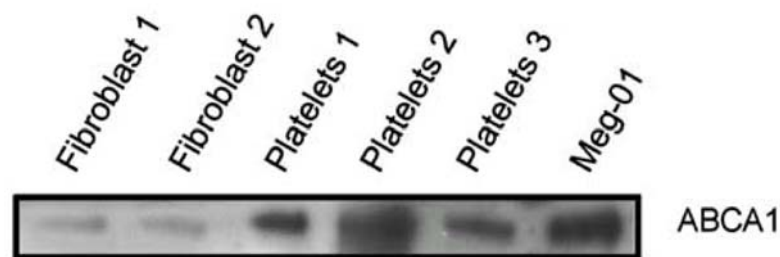


Figure 26: ABCA1 blot in various cell lysates. Immunoblot with 30 μ g cell lysates from human primary fibroblasts (donor 1 and 2), 5 μ g lysate from human platelets (3 donors), and 5 μ g from the Meg-01 cell line using ABCA1 antibody.

To verify the interaction of β 2-syntrophin with ABCA1, we performed Co-immunoprecipitation. ABCA1 antibodies were covalently linked to magnetic protein-A beads and incubated with Meg-01 cell lysates. The eluted protein was analyzed on immunoblots. β 2-syntrophin was detected in ABCA1 immunoprecipitates whereas magnetic protein A beads coupled with a control antiserum did not bind the β 2-syntrophin (Figure 27 A).

Furthermore, the β 2-syntrophin antiserum covalently linked to magnetic protein A beads precipitated ABCA1 in Meg-01 lysates (Figure 27 A).

These results confirmed the finding of the yeast two-hybrid screening and demonstrate that ABCA1 and β 2-syntrophin are associated with each other in megakaryocytes. We further demonstrated that the ABCA1 antibody also precipitates β 2-syntrophin in 4 d differentiated macrophages and in macrophages loaded with E-LDL for 24 h (Figure 27 B).

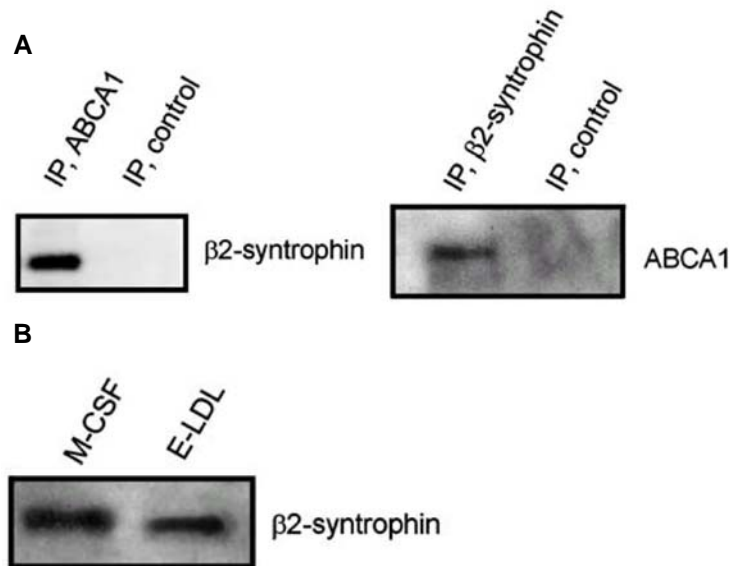


Figure 27: ABCA1 interacts with β 2-syntrophin. A. ABCA1 (IP, ABCA1) and a control (IP, control) antiserum covalently linked to beads were incubated with cell lysate from Meg-01 cells and β 2-syntrophin was detected in the precipitate by immunoblotting. β 2-syntrophin antiserum (IP, β 2-syntrophin) precipitates ABCA1 from Meg-01 cell lysates. ABCA1 was not detected in the control incubation (IP, control). B. β 2-syntrophin is detected in ABCA1 precipitates from macrophages differentiated 4 d with M-CSF and subsequently incubated with E-LDL.

Another protein detected in the ABCA1 precipitate was utrophin and the amount of ABCA1 associated with β 2-syntrophin and utrophin is similar in control and foam cells, indicating that cholesterol-induced ABCA1 expression is not associated with an altered formation of ABCA1/ β 2-syntrophin/utrophin complexes (Figure 28).

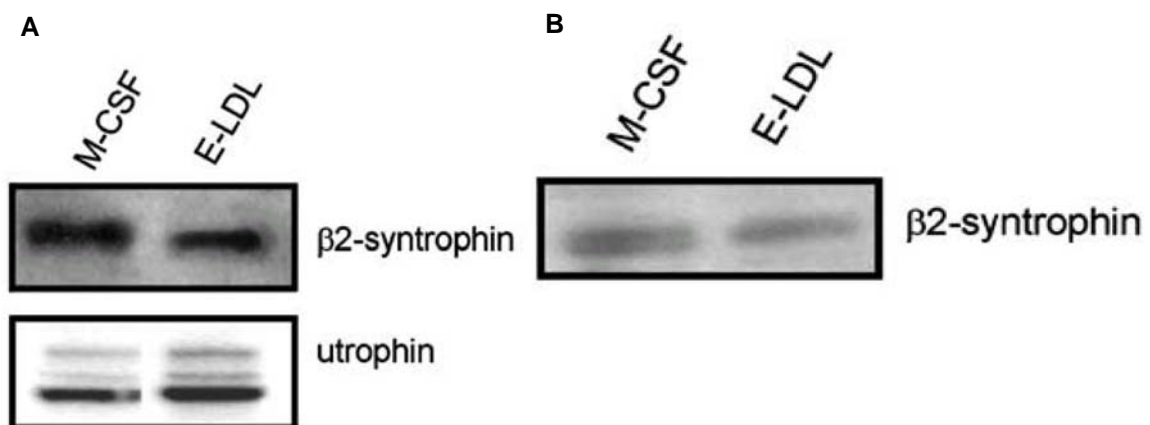


Figure 28: ABCA1/ β 2-syntrophin complex interacts with utrophin. A. ABCA1 antiserum precipitates similar amounts of β 2-syntrophin and utrophin in 4 d differentiated macrophages (M-CSF) and foam cells (E-LDL). B. Similar amounts of β 2-syntrophin are precipitated with β 2-syntrophin antibody (IP, β 2-syntrophin) in control (M-CSF) and E-LDL incubated macrophages.

The ABCA1/ β 2-syntrophin/utrophin complex is bound to the cytoskeleton by the interaction of utrophin to actin, a mechanism which could link ABCA1 and β 2-syntrophin to the intracellular shuttling of ABCA1 (Figure 29)

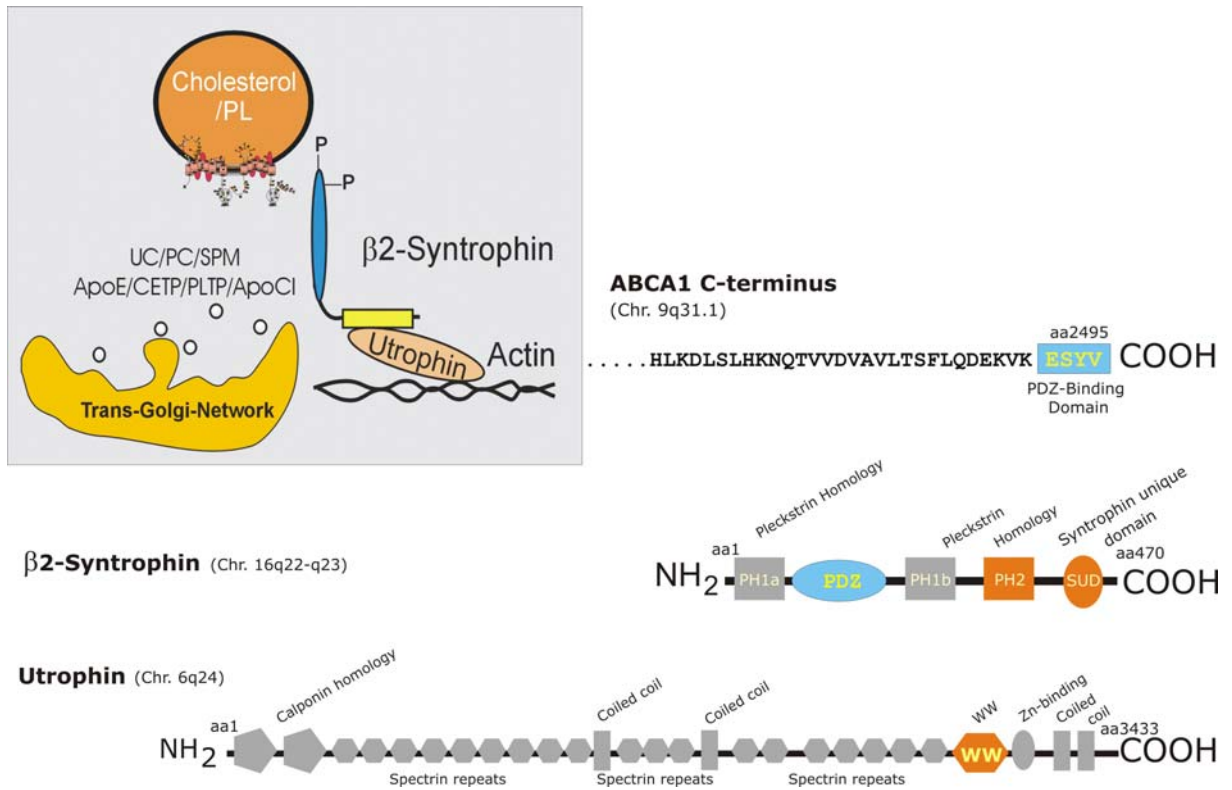


Figure 29: Interaction of ABCA1 C-terminus with β 2-syntrophin and utrophin. The figure shows the domains expressed on each protein. The last four amino acids in the ABCA1 sequence are a PDZ-binding domain, they interact with the PDZ-domain in β 2-syntrophin. In addition, β 2-syntrophin reveals a pleckstrin homology (PH) domain and a syntrophin unique domain (SUD) which are capable of interacting with the two conserved tryptophans (WW) found in utrophin. Utrophin, in turn, interacts with actin and thus to the cytoskeleton.

To further elucidate the distribution of ABCA1/ β 2-syntrophin complex throughout the cell, we isolated Lubrol rafts from whole cell lysates and blotted for both ABCA1 and β 2-syntrophin. E-LDL-loaded macrophages were solubilized in 1% Lubrol and fractionated by sucrose gradient centrifugation. Immunoblots using ABCA1 antiserum revealed a faint signal in the microdomain fractions; however, ABCA1 is found mainly in the soluble fraction (Figure 30, lanes 7, 8) not associated with rafts. Furthermore, β 2-syntrophin is not associated with microdomains whereas utrophin is detectable in all Lubrol density fractions with the majority in the soluble fraction (Figure 30, lanes 7, 8), followed by a

similar abundance in the high density fractions (Figure 30, lanes 5, 6) and the microdomains represented by the low density fractions (Figure 30, lanes 2–4).

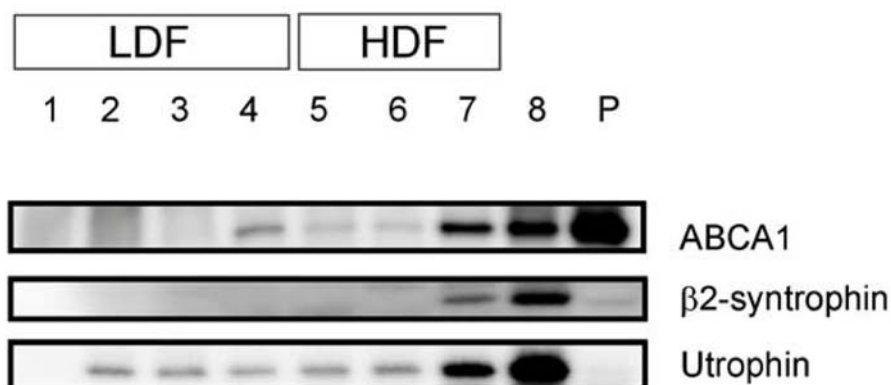


Figure 30: Microdomain localization of ABCA1 and associated proteins. Immunoblots were performed with ABCA1, β2-syntrophin, and utrophin antiserum. LDF indicates microdomains, whereas the high density fraction (HDF) is not associated with rafts. Fraction 8 represents the soluble membrane proteins and P is the insoluble pellet.

4. PROTEIN-PROTEIN INTERACTIONS OF SYNTAXIN 13, ABCA1 AND FLOTILLIN-1

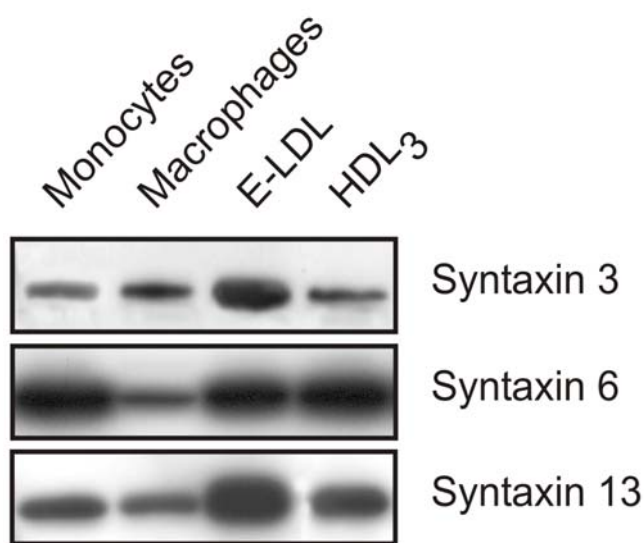
PDZ proteins also bind to the C-terminus of the ABC-transporter CFTR. The N-terminal region of CFTR is associated with syntaxin 1a. We investigated whether ABCA1 also binds to members of the syntaxin family, which play a vital role in vesicular transport and membrane budding and fusion events.

In order to identify ABCA1 interactive syntaxins we first examined the mRNA expression and protein levels of syntaxins in monocytes, macrophages, E-LDL loaded and subsequently HDL₃-deloaded foam cells. Fifteen members of the syntaxin family are present in the human genome with different subcellular locations of the corresponding proteins¹⁸⁸. We focused on syntaxins with relevance for endocytosis, phagocytosis and secretion namely the syntaxins 2, 3 and 4 located at the plasma membrane, syntaxin 8 and 13 associated with the early endosome, syntaxin 7 that plays a role in the biogenesis of lysosomes and syntaxin 6 that is involved in the release of vesicles from the Trans Golgi Network (TGN). Syntaxin 1 is not expressed in macrophages⁷³ and therefore was not analyzed.

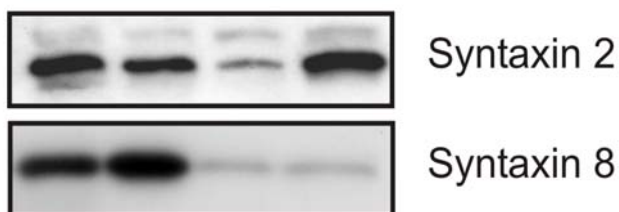
ABCA1 is induced during monocytic differentiation and further upregulated by sterol loading of these cells. Therefore, we investigated the expression of syntaxins in monocytes, in *in-vitro* differentiated macrophages, in macrophages incubated with

enzymatically modified LDL (E-LDL) for 24 h and in E-LDL loaded cells subsequently treated with HDL₃ for 24 h to allow cholesterol efflux. Syntaxin 4, 6 and 7 are down regulated during phagocytic differentiation whereas the expression of syntaxin 2, 3, 4, 8 and 13 was unchanged. Incubation with E-LDL induced syntaxin 3, 6 and 13 and the subsequent addition of HDL₃ reversed this upregulation for syntaxin 3 and 13. Syntaxin 2 and 8 were found reduced in E-LDL loaded macrophages and HDL₃ treatment again upregulated syntaxin 2 expression whereas syntaxin 8 levels were not altered (Figure 31).

A. Syntaxin levels induced by E-LDL loading



B. Syntaxin levels reduced by E-LDL loading



C. Syntaxins not regulated by E-LDL loading

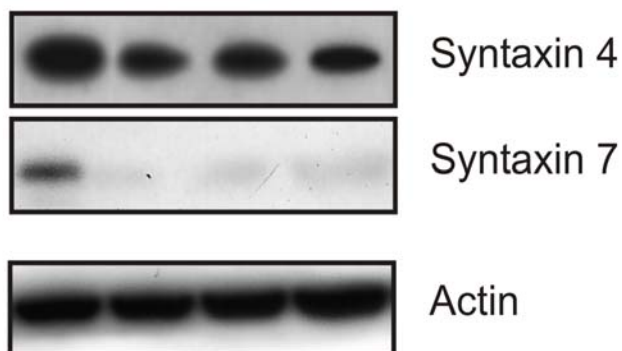


Figure 31: Analysis of syntaxin expression in primary human monocytes and macrophages.

The expression of syntaxin 2, 3, 4, 6, 7, 8, and 13 was investigated in monocytes, M-CSF differentiated macrophages, macrophages incubated for 24 h with 40 µg/ml ELDL, and E-LDL-loaded cells subsequently treated with 100 µg/ml HDL₃ for additional 24 h using immunoblots. A. Syntaxin 3, 6, and 13 were induced by E-LDL. B. Syntaxin 2 and 8 were down-regulated by E-LDL. C. Syntaxin 4 and 7 are not regulated by E-LDL. β-actin was used as a loading control.

To determine whether these changes in protein expression are transcriptionally or post-transcriptionally regulated we established TaqMan® assays for syntaxin 2, 3, 4, 6, 8 and 13. The mRNA expression was determined in monocytes, macrophages, foam cells and E-LDL loaded cells treated with HDL₃. The mRNA abundance of the syntaxins investigated was unchanged under the conditions described above (Figure 32) and therefore the differential expression of syntaxins is most likely related to altered protein stability and regulatory mechanism at the post-transcriptional level.

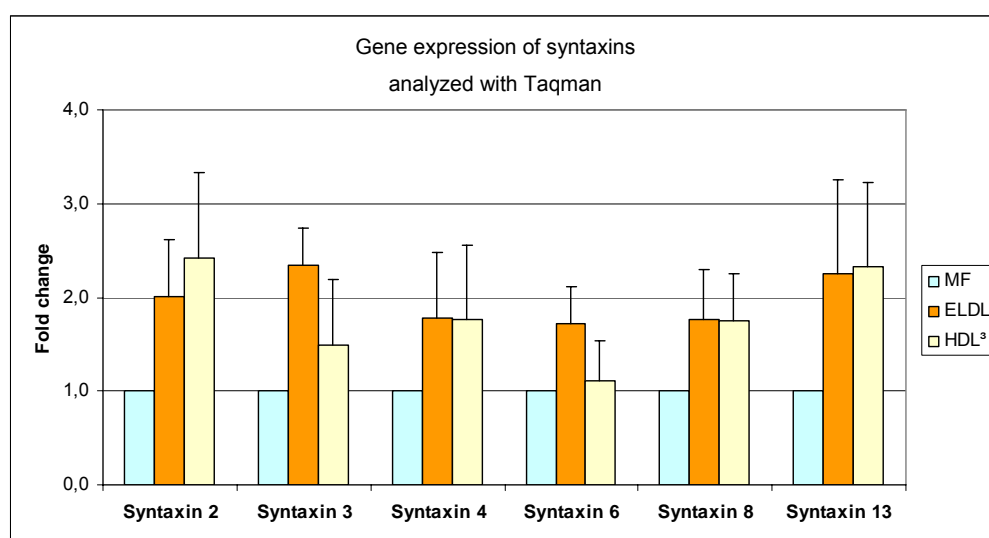


Figure 32: mRNA expression of syntaxins. mRNA was analysed by TaqMan®, normalized to 18s RNA and related to macrophages as calibrator. Fold-changes below 2,5-fold were considered as non significant.

The similar upregulation of ABCA1, syntaxin 3, 6 and 13 by sterols and the downregulation by HDL₃ for ABCA1, syntaxins 3 and 13 may indicate a functional association of these syntaxin and ABCA1.

Therefore, we further performed immunoprecipitation experiments using cell lysates from differentiated and E-LDL treated macrophages and were able to precipitate syntaxin 13 with ABCA1 antibodies (Figure 33 A). to confirm for this result, we co-immunoprecipitated ABCA1 from the lysates using syntaxin 13 antibodies (Figure 33 B). Although syntaxin 3 and 6 and ABCA1 were co-ordinately regulated, we could not identify an interaction in macrophages or foam cells (not shown). In E-LDL loaded cells, an increased amount of ABCA1 interactive syntaxin 13 was detected when compared to macrophages. This could be explained by the enhanced expression of ABCA1 and syntaxin 13 in E-LDL treated macrophages.

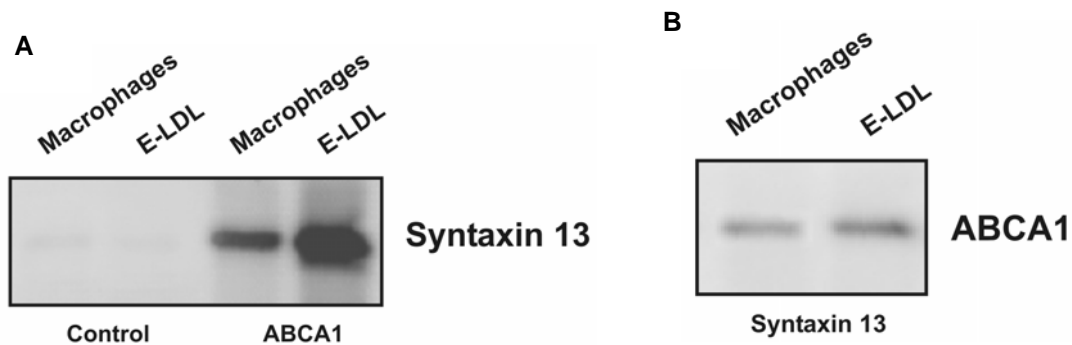


Figure 33: Interaction of ABCA1 with syntaxin 13 demonstrated by immunoprecipitation.

A. Immunoblot of syntaxin 13 precipitated with control (lanes 1 and 2) and ABCA1 antibody (lane 3 and 4) from cell lysates prepared from 4 d differentiated macrophages and E-LDL-loaded cells. B. Immunoblot of ABCA1 precipitated with syntaxin 13 antibody from cell lysates prepared from 4 d differentiated macrophages and E-LDL-loaded cells.

To confirm this interaction in living cells, immunofluorescence microscopy was performed with HL-60 cell line and monocyte-derived macrophages. The cells were differentiated and fixed with a mixture of paraformaldehyde and glutaraldehyde in order to gain a better staining for the intracellular localized proteins. Prior to staining the cells with the primary antibodies, the cells were permeabilized with PBS containing Triton X-100 and SDS. The antibodies were diluted 1:100 for syntaxin 13 antibody and 1:300 for ABCA1 antibody and applied to the cells for 1 h. After washing the cells with PBS, the secondary antibody was added and incubated for 1 h. Texas Red-labeled anti-rabbit for ABCA1 and FITC-labeled anti-mouse for syntaxin 13. The slides were further processed for immunofluorescent microscopy and DAPI was used to stain the nuclei (Figure 34).

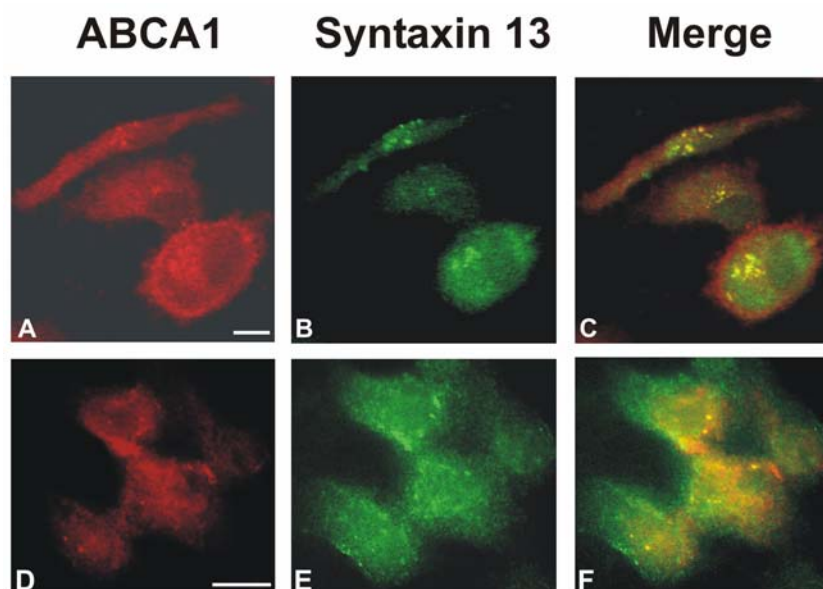


Figure 34: Syntaxin 13 colocalizes with ABCA1. Human monocytes (A, B, C) and differentiated HL-60 cells (D, E, F) were fixed and incubated with ABCA1 (A and D) or syntaxin 13 (B and E) antibodies. The merged images are shown in C and F. Yellow area resembles the overlap. Bars represent 10 μ m.

To gain insight into the functionality of this interaction, we aimed to knock-out syntaxin 13 and measure choline-phospholipid efflux to apoA-I and HDL₃.

In order to have a suitable model for transfection experiments, the myelomonocytic HL-60 cell line which can be induced to differentiate to macrophages by PMA³⁸, was employed. The cells were transfected with siRNA targeting syntaxin 13 (NM_177424).

Successful knock-out of syntaxin 13 was confirmed by western blotting. Cells treated with syntaxin 13 siRNA also revealed a reduced ABCA1 protein level, indicating a disturbed ABCA1 function (Figure 35 A).

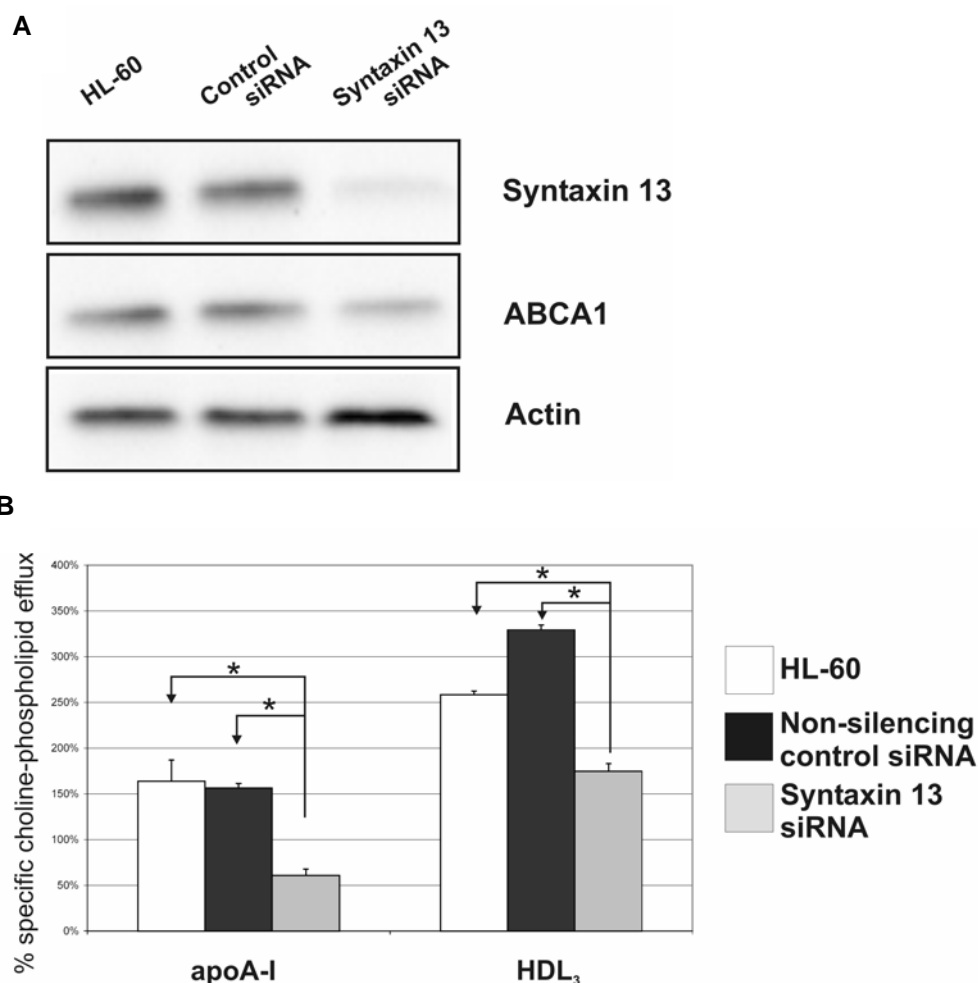


Figure 35: Knock-down of syntaxin 13 and [³H]choline-phospholipid efflux in HL-60 cells.

A. Lysates of PMA-differentiated HL-60 cells, differentiated HL-60 cells transfected with syntaxin 13 siRNA and HL-60 cells transfected with a non-silencing control siRNA were blotted and membranes were incubated with syntaxin 13, ABCA1 and actin antibody.

B. The cells were loaded with [³H]choline-phospholipid efflux and deloaded with apoA-I or HDL₃. The lipid efflux relative to the unspecific efflux from three independent experiments is given in percent. The significance of the decrease in efflux between syntaxin 13-silenced cells and control cells was calculated using *t* test; **p* < 0.05.

Choline-phospholipid efflux was determined in PMA differentiated HL-60 cells, in cells transfected with a control siRNA and cells where the expression of syntaxin 13 was silenced by a syntaxin 13 specific siRNA.

The knockdown of syntaxin 13 RNA and protein in HL-60 cells led to a significant decrease in choline-phospholipid efflux to apoA-I and HDL₃; whereas lipid efflux was not affected in the control transfected cells (Figure 35 B).

Syntaxin 13 has been reported to mediate endosomal cycling of plasma membrane proteins and is required for the interaction of endosomes with the phagosome⁴². ABCA1 has been found on endosomes¹³⁸ but its association with phagosomes has never been investigated.

Therefore, macrophages were fed with 0,8 µm blue-dyed latex phagobeads for 1 h, washed and the internalization of the phagobeads into phagosomes was allowed for 2, 4, 6, 12 and 20 h. Immunoblots using purified phagosomal proteins were performed. Both ABCA1 and syntaxin 13 were similarly detectable in the 2 h and 4 h fraction, reaching their peak after 6 h and decreasing afterward (Figure 36).

The phagosomal markers flotillin-1 and Rab-9 as well as the lysosomal marker LAMP1 were also detected in order to gain insight into the maturation of phagosomes throughout time and the increasing merge of phagosomes with lysosomes.

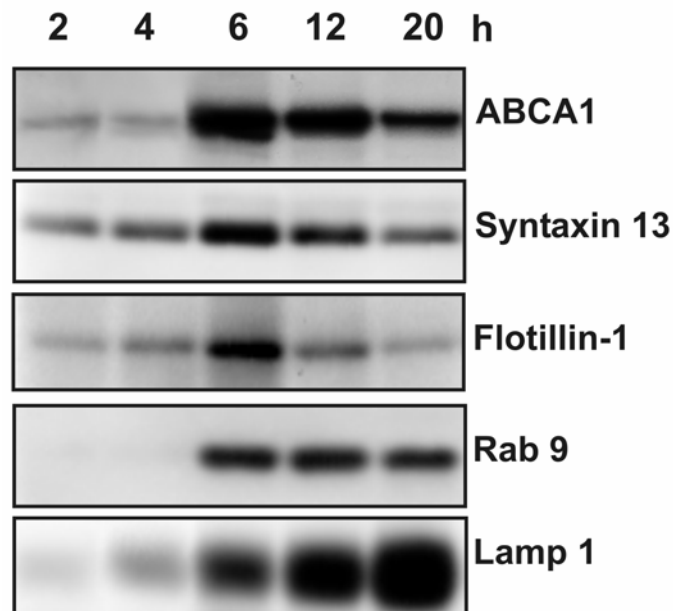


Figure 36: Phagosomal localization of ABCA1 interactive proteins. Phagosomes were purified from 4 d differentiated macrophages incubated with latex beads for 2, 4, 6, 12, and 20 h. Purified phagosomal proteins were used for immunoblotting. The expression of ABCA1, syntaxin 13, flotillin-1, Rab 9, and LAMP1 was analyzed.

To investigate whether ABCA1 and syntaxin 13 interact in phagosomes, we performed additional co-immunoprecipitation assays with stringent RIPA buffer (Figure 37) and found that syntaxin 13 antibodies co-immunoprecipitated ABCA1 and, for confirmation, ABCA1 antibodies co-immunoprecipitated syntaxin 13 from phagosomal lysates. For negative control a rabbit antibody was used.

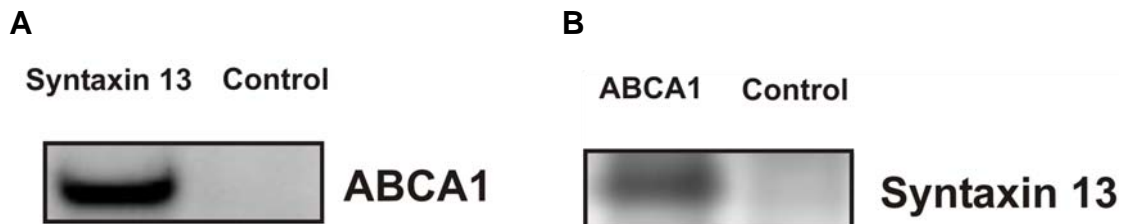


Figure 37: ABCA1 interacts with syntaxin 13 in phagosomes. A. Immunoblot of ABCA1 precipitated with syntaxin13 antibody from phagosomal protein fraction (6 h). B. Syntaxin 13 precipitated with ABCA1. Control rabbit antibody was used as negative control.

To further support the hypothesis that ABCA1 may regulate phagocytosis, the phagocytic activity of fibroblasts from control donors and fibroblasts isolated from the Tangier patients TD1 (yielding a mutation at K171X), TD3 II:4 and TD5 III:4²¹ was measured by flow cytometry using fluorescent yellow green-labeled phagobeads. Fibroblasts from Tangier patients with ABCA1 mutations had a significantly higher internalization rate compared

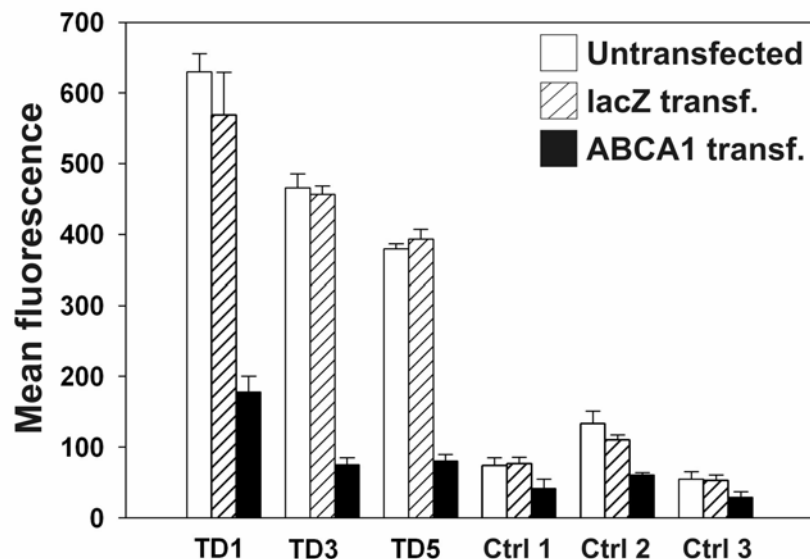


Figure 38: The phagocytic activity of fibroblasts was determined in human fibroblasts with functional, recombinant ABCA1 or lacZ as control after 4 h incubation with fluoresbrite yellow green microspheres by flow cytometry. Both, the increased phagocytosis of Tangier compared with normal fibroblasts as well as the reduced phagocytic activity of ABCA1-transfected cells when compared with lacZ-transfected fibroblasts were statistically significant ($p < 0.05$). TD1, 3, and 5: fibroblasts from TD patients. Ctrl1, 2, and 3: fibroblasts from healthy individuals.

with controls, further supporting a function of ABCA1 in the phagocytic uptake of particles (Figure 38). Recombinant expression of wild-type ABCA1 in Tangier fibroblasts led to a decreased phagocytosis rate as was seen in control fibroblasts. These findings indicate that ABCA1 is located at the plasma membrane and in the phagosome. Both compartments are involved in phagocytosis and may also be important in ABCA1-dependent lipid efflux.

Flotillin-1⁴⁹ and ABCA1⁵⁴ are raft-associated proteins. A wide variety of detergents have been used to isolate rafts and significant differences exist among the preparations. Flotillin-1 is enriched in Triton X-114-insoluble microdomains, and 5–10% of ABCA1 are located in Lubrol WX rafts, whereas it is absent from Triton X-100 rafts. Using whole cell lysates, we examined whether flotillin-1 and syntaxin 13 colocalize in Lubrol WX-insoluble microdomains in E-LDL-loaded macrophages solubilized in 1% Lubrol WX and fractionated by sucrose gradient centrifugation. Immunoblots using ABCA1 antibodies confirmed our previous data reported by Drobnik et al.⁵⁴ (Figure 39 A).

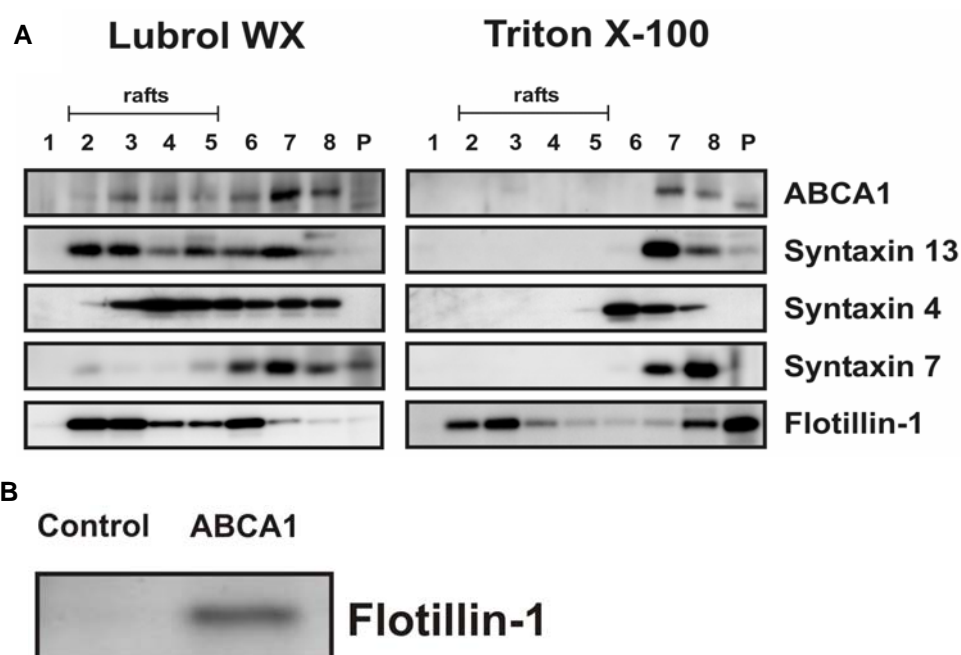


Figure 39: Microdomain localization of ABCA1-associated proteins and ABCA1 interaction with flotillin-1. A. E-LDL-loaded macrophages were solubilized in 1% Lubrol WX or Triton X-100 and fractionated by sucrose gradient centrifugation. Immunoblots were performed with ABCA1, syntaxin 13, syntaxin 4, syntaxin 7, and flotillin-1. The fractions 2–5 indicate rafts, whereas lanes 6–8 are not associated with rafts. Fraction 8 represents soluble membrane proteins and P is the insoluble pellet. B. Immunoblot of flotillin-1 precipitated with control and ABCA1 antibody from cell lysates prepared from 4 d differentiated macrophages.

Syntaxin 13 was highly abundant in Lubrol WX rafts but not detectable in Triton X-100 rafts and flotillin-1 co-purifies with Triton X-100 and Lubrol WX rafts. Syntaxin 4, localized at the plasma membrane, was also identified in Lubrol WX microdomains, whereas syntaxin 7, a marker of late endosomes, was not detected. The abundance of ABCA1 and flotillin-1 at the plasma membrane and phagosomes together with their colocalization in Lubrol WX rafts may indicate a direct interaction of ABCA1 and flotillin-1. Subsequent immuno-precipitation confirmed that flotillin-1 is directly associated with ABCA1 (Figure 39 B).

5. LIPOPROTEIN ANALYSIS OF THE PALLIDIN KO MICE

Since syntaxin 13 interacts in vivo with syntaxin 13-interacting protein (pallidin), sera from pallidin knock-out mice were analyzed for their lipoprotein profile in order to study the potential influence of syntaxin 13 on HDL metabolism.

Sera from 4 pallidin knock-out mice and 4 wild-type mice were collected and pooled in each category. The sera were separated by fast protein liquid chromatography (FPLC) and subsequently lipoproteins were analyzed by electrospray ionization - tandem-mass spectrometry (ESI-MS/MS). The results show that the syntaxin 13-interacting protein deficient pallidin mouse has less free cholesterol and sphingomyelin in the HDL fraction. HDL phosphatidylcholine is also slightly impaired while lysophosphatidylcholine is increased in the pallid mouse when compared to wild type, an observation possibly related to an enhanced esterification rate mediated by LCAT which catalyzes the formation of cholesterol esters on HDL particles. This is further supported by the increased CE/FC-ratio in the HDL fraction. VLDL-triglycerides were also found decreased which may indicate that syntaxin 13-interacting protein is also operative in the VLDL secretory pathway and thus a reduced SPM leads to increased LCAT activity in the pallid mouse (Figure 40).

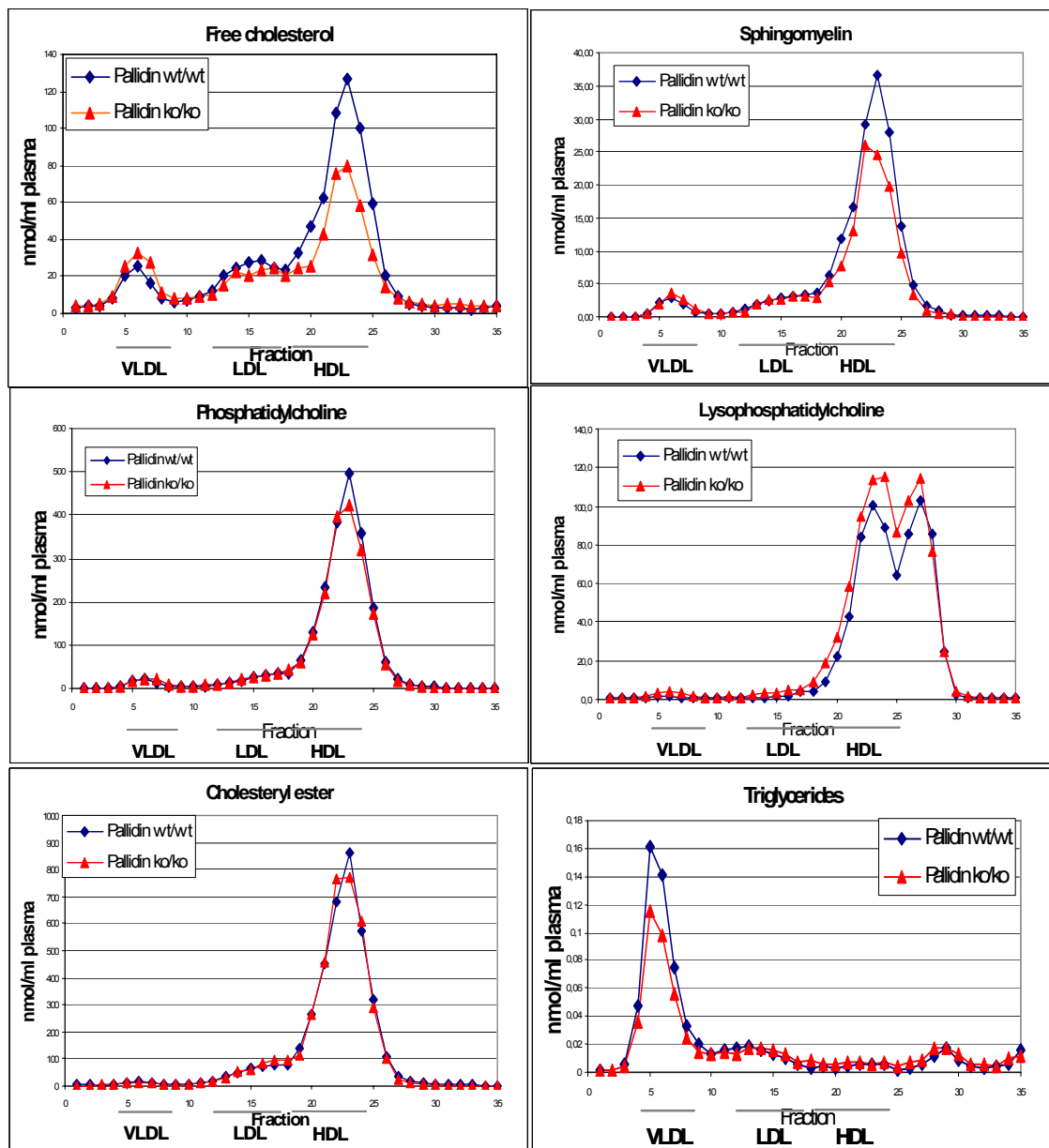


Figure 40: Lipoprotein analysis of pallidin ko mice (yellow) in comparison to wild type mice (Blue) the pallidin mouse has increased lysophosphatidyl choline and reduced triglycerides, free cholesterol and sphingomyelin.

6. IDENTIFICATION OF MACROPHAGE-SPECIFIC GENES INVOLVED IN LIPID TRAFFICKING USING GENE-CHIPS

The second aim of this thesis was to identify cholesterol and phospholipid traffic genes differentially expressed during loading of macrophages with different atherogenic lipids, namely: E-LDL and Ox-LDL. For this approach, oligonucleotide gene arrays were used. Monocytes were incubated in-vitro and RNA samples were taken as is shown in figure 39.

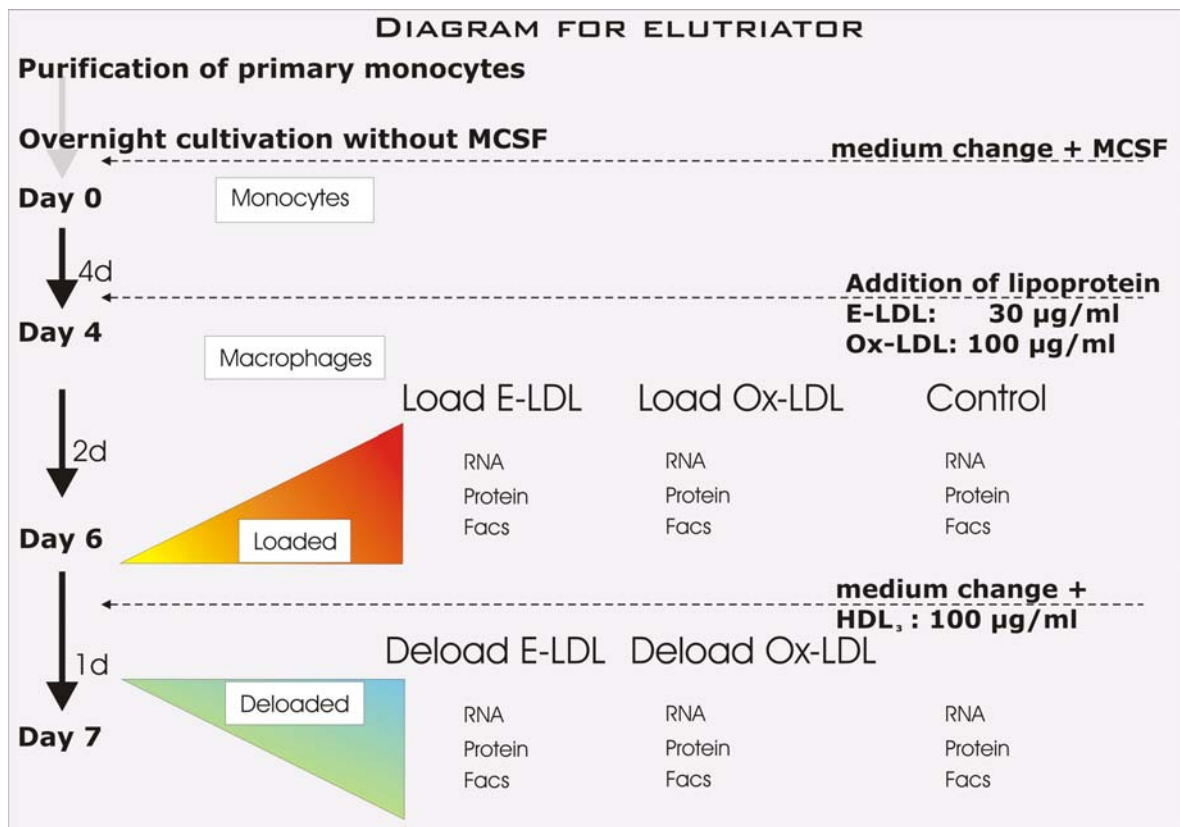


Figure 41: Incubation protocol. Differentiation, loading and deloading of monocytes/macrophages to isolate RNA and protein for subsequent experiments.

Total RNA from monocytes of 6 healthy donors bearing the Apo E3/E3 phenotype were pooled, reverse transcribed, fluorescently labeled with streptavidin-phycoerythrin and hybridized to Affymetrix Gene chips U133A, the results were analyzed with the Affymetrix Microarray Suite 5.0™. Genes with significant up- and down-regulation by loading, deloading or differentiation were sorted accordingly. This led to fourteen gene lists which rendered a percentage distribution for the E3/E3 phenotype as shown in table 6.

Table 6: Number of genes regulated by incubation with lipoproteins an ApoE3/E3 macrophages.

Category	Number of genes		Percentage	
	E-LDL	Ox-LDL	E-LDL	Ox-LDL
Load Specific Up	20	178	0,5%	4,2%
Load Specific Down	497	105	11,7%	2,5%
Deload Specific Up	625	166	14,7%	3,9%
Deload Specific Down	54	38	1,3%	0,9%
Genes regulated during differentiation	1443		34,0%	
Total significantly reglated genes	4240			
Category	Number of genes		Percentage	
	Load	Deload	Load	Deload
Common Up	29	31	0,7%	0,7%
Common Down	129	1	3,0%	0,0%
Inversly regulated	16	113	0,4%	2,7%
Genes regulated during differentiation	1443		34,0%	
Total significantly reglated genes	4240			

To verify whether our obtained array data are reliable, we compared our results with results from literature on well characterized genes like ABCA1, LDL-R, CD36 and adipophilin. The expression patterns were concordant.

Table 7: The regulation of four described genes in ApoE3/E3 phenotype, which correlated well with the expected regulation published.

Unigene	Gene title	Short	E3		E3		E3		E3		E3		E3			
			Mono		MF		E-LDL		Ox-LDL							
			Mono		Diff		Load		Deload		Load		Deload			
			Sg	p-val.	Fold	Chng	Fold	Chng	Fold	Chng	Fold	Chng	Fold	Chng	Fold	Chng
Hs.147259	ATP-binding cassette, sub-family A (ABC1), member 1	ABCA1	130	++	9,2	I	2,0	I	-1,4	D	2,0	I	-1,2	D		
Hs.3416	Adipose differentiation-related protein	ADFP	1966	++	1,5	I	2,3	I	1,0	D	3,5	I	-1,1	D		
Hs.443120	CD36 antigen (collagen type I receptor, thrombospondin receptor)	CD36	2978	++	-2,6	D	2,8	I	1,1	NC	2,5	I	1,7	NC		
Hs.213289	Low density lipoprotein receptor (familial hypercholesterolemia)	LDLR	990	++	-2,0	D	-8,6	D	3,2	I	-4,0	D	1,4	I		

The expression profile obtained for ABCA1, adipophilin and CD36 with DNA chip experiments went along well with the pattern expected, since it has been published previously that all of these genes are being upregulated by lipid loading with either E-LDL or Ox-LDL^{76,115,197}. The LDL-R was significantly downregulated by lipid loading and upregulated by deload also a result previously published by Hussein et. al.⁹¹ (Table 7).

This comparison shows that the incubation of the cells with lipoproteins, the modification of lipoproteins, the isolated RNA, the hybridization of arrays and the analysis of the data resulted in reliable results reflecting the processes occurring in-vivo.

To evaluate mRNA expression profiles in macrophages loaded with two different modified lipoproteins, on the basis of biologically coherent functional and/or structural units, we established defined categories that rely on systematic literature surveys, data base

analyses and unpublished data sets from our laboratory. Using this approach, a total of 73 categories of interest were defined. These are listed in table 8.

Table 8: Pathways assembled according to literature survey, data base analysis and unpublished data sets in our institute.

Nr.	Name of pathway	Nr.	Name of pathway
1	Wnt/Frizzled	38	Proteoglycans / Mucins / Defensins / Trefoils / IgA
2	Notch/Hedgehog/Stem cell genes	39	Hyaluronan
3	CD genes / Receptors / Tetraspans / Pentaspans / Ligands	40	Elastin/Fibrillin/Keratin/Fibulin
4	Vesicular trafficking / lipid droplet	41	Connective tissue disease
5	ABC Transporter/ATPases/Walker motif family	42	EGF family
6	Ion Channels/Porins/solute carriers	43	Junctional control
7	Phagosome/Annexins/Connexins/Copins	44	other ECM proteins
8	Rab/Ras pathway	45	G protein receptors and G proteins
9	Rac/Cdc42 regulatory pathways	46	Kinases + Phosphatases
10	Lamellar body/GPI-anchored/Golgi	47	NFkB signaling/NFkB target genes
11	Adapter proteins/PDZ family/Domain proteins/coiled coil	48	ZNF202 target genes and coregulators
12	Cytoskeleton/Actin/Tubulin/Myosin/Spectrin/Migration/polarization	49	POLII/TAFs/CDK/Cyclins/CDCs
13	ABCA1/ABCA7/NPC/Cav associated	49	/CDT-kinases in transcriptional control
14	Purin & Pyrimidin metabolism/FAD/NAD/Nucleotide/Nucleoside	50	Nucleosome/Nuclear matrix
15	TNF receptor signaling	51	Nuclear receptors
16	TNF/PI3 kinase coupling	52	PPAR/LxR/PxR/RxR/FxR nuclear receptor target genes
17	Apoptosis/Proteasome	53	ZNF TCFs
18	Mitochondrion/Peroxisome	54	Homeobox
19	Insulin/Glukose/Glutathione/Glucuronides/Energy/b-Oxidation	55	RNA-Polymerases I and III
20	Thrombosis/Haemostasis	56	Other specific transcription factors
21	Detoxifikation: Phase I / Cytochromes	57	Splicing
22	Detoxifikation: Phase II	58	Translation machinery
23	Heat shock	59	IL-1b/Cytokines/Chemokines/Poetins
24	NO/Thioredoxin/Metallothionins/Selenoproteins	60	IFNg regulated genes
25	Cholesterol metabolism / SREBP1/2 / bile acid	61	Homocysteine
26	Fatty acid metabolism / Retinoids / S100	62	Lipid sensitive genes in C. elegans
27	Glycerophospholipids	63	complement, defensins, Granzymes
28	Phosphatidylinositol and Ca ⁺⁺ metabolism / GPI biosynthesis	64	IBD candidate loci
29	Sphingolipids	65	Colon expressed genes
30	Gangliosides	66	not yet classified to pathways
31	Sulfatides/Cholesterol sulfate	67	unknowns
32	Glykosylation/Sialation/CTP/UTP/GTP/ITP	68	Replikation
33	Proteinases/Serpins/MMPs/ADAMS/Kallikreins/Calpains/Cytostatins	69	Apos/Lipid binding proteins
34	Integrins	70	Lysosome/CLNsSTART
35	TGFb-family/BMP/TGFb/Activins/Inhibins and signaling	71	CD13 / Ezetrol pathway
36	Collagens	72	HNF1a / CDX2 / GATA4
37	Laminins	73	Placenta/Prostate/Sperm/Testes

The number of 31.941 genes resembles the total number of genes that were listed in all categories. This "search list" contained redundancies due to the fact that numerous genes could be assigned to more than one category. A total of 4240 genes from the search list displayed significant regulation in apoE3/E3 macrophages under conditions of E-LDL or Ox-LDL mediated cholesterol uptake followed by cholesterol efflux.

The percentage distribution of genes in the 73 pre-defined pathways is shown in table 9.

Table 9: percentage of genes regulated by differentiation, E-LDL or Ox-LDL loading and subsequent HDL₃ deloading were the different regulations are given different colors (red for up- and blue for down-regulation).

PW	Pathway	Sum	E-LDL Load		E-LDL Deload		Ox-LDL Load		Ox-LDL Deload	
			Up %	Dwn %	Up %	Dwn %	Up %	Dwn %	Up %	Dwn %
	Apo E3/E3									
1	Wnt/Frizzled	214	4.2	15.9	10.7	7.5	2.8	9.3	6.5	6.1
2	Notch/Hedgehog/Stem cell genes	402	2.7	15.4	9.2	7.0	2.5	9.2	6.2	5.5
3	CD genes / Receptors / Tetraspans / Pentaspan / Ligands	216	6.0	19.4	12.5	9.7	7.9	20.4	11.1	8.8
4	Vesicular trafficking / lipid droplet	743	4.0	14.3	7.9	6.1	3.5	13.7	8.2	5.2
5	ABC Transporter/ATPases/Walker motif family	82	13.4	12.2	15.9	8.5	9.8	6.1	4.9	7.3
6	Ion Channels/Porins/solute carriers	405	2.5	9.9	6.2	3.5	3.5	4.9	3.5	5.4
7	Phagosome/Annexins/Connexins/Copins	523	10.5	11.5	12.8	11.3	8.6	11.7	14.5	10.3
8	Rab/Ras pathway	192	8.3	7.8	8.9	11.5	6.8	8.3	9.9	6.3
9	Rac/Cdc42 regulatory pathways	37	10.8	21.6	0.0	10.8	5.4	13.5	10.8	8.1
10	Lamellar body/GPI-anchored/Golgi	473	6.6	12.3	12.1	8.7	6.8	7.4	8.0	8.9
11	Adapter proteins/PDZ family/Domain proteins/coiled coil	461	6.1	12.1	10.2	5.9	6.5	8.0	7.4	8.9
12	Cytoskeleton/Actin/Tubulin/Myosin/Spectrin/Migration/polarization	217	3.7	9.2	10.6	5.5	3.7	7.4	6.0	5.1
13	ABCA1/ABCA7/NPC/Cav associated	371	5.7	15.6	14.6	5.7	8.9	11.1	8.1	8.6
14	Purin & Pyrimidin metabolism/FAD/NAD/Nucleotide/Nucleoside	60	8.3	13.3	15.0	16.7	6.7	16.7	15.0	10.0
15	TNF receptor signaling	158	5.1	17.1	10.8	8.9	7.0	10.1	5.7	9.5
16	TNF/PI3 kinase coupling	38	15.8	21.1	7.9	10.5	18.4	5.3	5.3	5.3
17	Apoptosis/Proteasome	591	4.2	9.8	10.0	4.9	9.5	6.8	5.4	10.0
18	Mitochondrion/Peroxisome	329	9.1	10.0	21.3	8.2	14.9	2.4	8.5	10.3
19	Insulin/Glukose/Glutathione/Glucuronides/Energy/b-Oxidation/Fucose	381	5.5	11.5	12.6	5.8	10.0	5.8	6.8	6.8
20	Thrombosis/Haemostasis	39	0.0	23.1	12.8	10.3	2.6	15.4	2.6	5.1
21	Detoxifikation: Phase I / Cytochromes	125	3.2	12.8	8.0	4.0	8.8	7.2	4.0	7.2
22	Detoxifikation: Phase II	74	5.4	13.5	14.9	8.1	5.4	12.2	6.8	6.8
23	Heat shock	58	8.6	5.2	12.1	8.6	8.6	5.2	6.9	8.6
24	NO/Thioredoxin/Metallothionins/Selenoproteins	242	5.0	14.9	16.1	6.2	7.9	10.3	7.4	6.2
25	Cholesterol metabolism / SREBP1/2 / bile acid	34	14.7	41.2	29.4	11.8	20.6	32.4	29.4	8.8
26	Fatty acid metabolism / Retinoids / S100	206	8.3	12.6	13.6	5.3	13.6	7.8	8.3	7.8
27	Glycerophospholipids	14	0.0	7.1	7.1	14.3	21.4	0.0	14.3	14.3
28	Phosphatidylinositol and Ca++ metabolism / GPI biosynthesis	229	2.2	14.4	7.9	5.2	5.2	6.1	5.7	7.4
29	Sphingolipids	14	7.1	0.0	7.1	14.3	21.4	7.1	7.1	14.3
30	Gangliosides	49	10.2	12.2	6.1	10.2	6.1	10.2	8.2	4.1
31	Sulfatides/Cholesterol sulfate	13	0.0	0.0	23.1	0.0	7.7	7.7	7.7	0.0
32	Glykosylation/Sialation/CTP/UTP/GTP/ITP	203	4.4	15.3	9.4	3.9	6.9	8.4	9.4	7.4
33	Proteinases/Serpins/MMPs/ADAMS/Kallikreins/Calpains/Cytostatin	193	3.6	14.0	11.4	6.2	4.7	11.4	5.2	5.2
34	Integrins	31	6.5	3.2	16.1	9.7	12.9	6.5	6.5	9.7
35	TGFb-family/BMP/TGFb/Activins/Inhibins and signaling	173	1.7	12.7	8.7	4.0	1.2	8.1	4.6	3.5
36	Collagens	84	4.8	8.3	7.1	6.0	6.0	9.5	7.1	6.0
37	Laminins	31	0.0	6.5	9.7	6.5	0.0	9.7	6.5	6.5
38	Proteoglycans / Mucins / Defensins / Trefolins / IgA	60	1.7	15.0	11.7	5.0	1.7	3.3	0.0	6.7
39	Hyaluronan	96	4.2	8.3	8.3	9.4	6.3	7.3	7.3	5.2
40	Elastin/Fibrillin/Keratin/Fibulin	103	2.9	13.6	9.7	8.7	2.9	8.7	3.9	2.9
41	Connective tissue disease	202	4.5	14.4	15.3	8.4	6.4	10.9	5.4	7.4
42	EGF family	112	2.7	19.6	7.1	8.0	1.8	15.2	8.9	2.7
43	Junctional control	113	1.8	10.6	3.5	2.7	1.8	5.3	3.5	3.5
44	other ECM proteins	96	3.1	18.8	11.5	5.2	5.2	12.5	3.1	5.2
45	G protein receptors and G proteins	412	2.2	12.6	7.3	2.4	1.7	7.3	2.4	2.4
46	Kinases + Phosphatases	592	3.0	11.0	10.3	7.3	4.9	6.3	6.8	7.8
47	NFkB signaling/NFkB target genes	84	6.0	13.1	9.5	13.1	7.1	14.3	14.3	7.1
48	ZNF202 target genes and coregulators	26	7.7	11.5	19.2	3.8	11.5	19.2	11.5	15.4
49	POLII/TAFs/CDK/Cyclins/CDCs/CDT-kinases in transcriptional control	250	4.0	14.0	16.4	5.6	9.2	5.6	4.0	9.2
50	Nucleosome/Nuclear matrix	114	1.8	9.6	6.1	1.8	0.9	1.8	0.9	8.8
51	Nuclear receptors	54	1.9	14.8	9.3	5.6	3.7	3.7	3.7	3.7
52	PPAR/LXR/PxR/RxR/FxR nuclear receptor target genes	721	7.4	16.2	12.1	8.0	8.2	15.0	10.0	7.6
53	ZNF TCFs	228	0.9	6.1	5.3	4.8	1.8	2.6	3.1	6.1
54	Homeobox	63	0.0	7.9	1.6	1.6	0.0	1.6	1.6	3.2
55	RNA-Polymerases I and III	18	5.6	0.0	16.7	0.0	5.6	0.0	0.0	5.6
56	Other specific transcription factors	334	1.2	12.9	7.8	6.0	1.5	9.0	4.5	4.8
57	Splicing	61	3.3	8.2	14.8	3.3	4.9	3.3	4.9	3.3
58	Translation machinery	237	6.8	19.4	33.3	6.8	15.2	4.6	5.1	29.5
59	IL-1b/Cytokines/Chemokines/Poetins	72	2.8	13.9	9.7	4.2	4.2	12.5	5.6	4.2
60	IFNg regulated genes	201	7.5	14.9	9.0	10.4	9.0	16.4	8.5	12.9
61	Homocysteine	30	3.3	6.7	10.0	10.0	10.0	3.3	0.0	13.3
62	Lipid sensitive genes in C. elegans	229	4.4	10.9	11.8	6.6	6.1	5.7	6.1	9.2
63	Complement, defensins, Granzymes	110	4.5	17.3	11.8	2.7	5.5	18.2	7.3	4.5
64	IBD candidate loci	810	4.0	13.0	10.6	4.8	6.2	7.9	5.4	7.0
65	Colon expressed genes	1484	7.7	14.9	12.9	9.6	8.8	10.5	8.9	10.8
66	not yet classified to pathways	1452	3.2	9.2	8.1	5.2	4.7	5.6	5.2	6.2
67	unknowns	3038	2.1	9.6	8.4	3.8	3.9	4.1	3.3	6.5
68	Replication	109	1.8	10.1	11.0	3.7	4.6	3.7	2.8	3.7
69	Apolipoproteins / Lipid binding proteins	23	4.3	13.0	13.0	4.3	4.3	0.0	13.0	4.3
70	Lysosome/CLNsSTART	42	7.1	16.7	11.9	7.1	9.5	11.9	4.8	9.5
71	CD13 / Ezetrol pathway	771	6.2	10.5	12.2	7.0	9.7	7.9	7.5	6.7
72	HNF1a / CDX2 / GATA4	66	1.5	13.6	3.0	3.0	1.5	1.5	4.5	1.5
73	Placenta/Prostate/Sperm/Testes	32	0.0	0.0	18.8	0.0	15.6	6.3	6.3	15.6
74	HNF1a / CDX2 / GATA4 target genes	623	6.3	11.6	8.7	8.3	7.4	8.8	9.6	7.2
	Sum	20773	958	2538	2209	1313	1300	1669	1343	1553

It is noticeable that differentiation of monocytes to macrophages has a great influence on the gene expression, leading to severe upregulation in many pathways. Moreover, it is

noticed that loading the cells with E-LDL leads to downregulation, subsequent deload to upregulation of many genes.

6.1. E-LDL MEDIATED CHOLESTEROL FLUX

Our statistical analysis of apoE3/E3 macrophages revealed that n=167 (1.3%) of the genes are upregulated during E-LDL mediated cholesterol uptake whereas the number of downregulated genes during E-LDL loading was n=1,640 (13.2%).

As for the consequent deload of macrophages with HDL₃, the E-LDL-loaden macrophages displayed an increase for n=2074 (17%). The genes downregulated by HDL₃-deload after E-LDL loading were: n=311 (2.5%). The genes that showed most pronounced regulation in apoE3/E3 individuals in E-LDL loading include various members of the cholesterol metabolism pathway including PPARs, vesicular transport genes, the wingless-frizzled pathway and genes from the detoxification machinery.

In contrast, deloading led to a significant regulation in the ABCA1-related genes, α -oxidation, mitochondrial genes and the laminins, also striking was the upregulation of the RNA polymerase II complex (RNA polymerase II peptides A, E, F, H, I, and L) as well as various members of the cyclin and cyclin-dependent kinase (cdk) families (cyclins D1, D2, D3, E1, F, cdk10, cdk inhibitor 2A, cdk inhibitor 2C, cdk inhibitor 1C) and multiple components of the translation machinery (figure 42A).

Cholesterol efflux in apoE3/E3 macrophages following E-LDL mediated cholesterol uptake induced the upregulation of a strikingly large portion among the regulated translation machinery associated genes (n=84). The vast majority of these genes included structural elements of the 40S and 60S ribosomal subunits suggesting that cholesterol efflux from macrophages has a profound effect on the expression of integral components of the ribosome complex (figure 42B). The genes that showed strongest upregulation include the members of the large subunit of ribosomal proteins (RP) RPL36, RPL28, RPLP2 and RPL14 respectively. Beside structural ribosomal proteins members of the translation initiation complex were upregulated during cholesterol export. These included the majority of the subunits of the eukaryotic translation initiation factor (EIF)-3 (EIF3S4, EIF3S5, EIF3S9, EIF3S6IP, EIF3S3, EIF3S7, EIF3S8) and members of the EIF-2 and EIF-4 complexes (EIF2B5, EIF2C1, EIF4EL3) (Table 10 and Figure 42C).

Table 10: Expression analysis of genes relevant for the translation machinery.
(blue:downregulation, red:upregulation, (marked only when fold change >=2)).

Unigene	Gene name	Short	Mono		E-LDL				Ox-LDL				
			Sig	p-val.	Load	Del.	Fold	p-val.	Load	Del.	Fold	p-val.	
0	Translation machinery												
Hs.334798	Eukaryotic translation elongation factor 1 delta	EEF1D	652	++ ++	-1,7	++	3,7	+	1,7	++	+	-1,7	
Hs.283551	Eukaryotic translation initiation factor 2B, subunit 5 epsilon, 82kDa	EIF2B5	211	++ +	-1,2	++	3,0	++	2,0	+	+	-1,1	
Hs.309452	Eukaryotic translation initiation factor 2C, 1	EIF2C1	206	++ +	-1,5	++	2,3	+	1,2	+	+	1,1	
Hs.127149	Eukaryotic translation initiation factor 3, subunit 3 gamma, 40kDa	EIF3S3	1084	++ +	-1,6	++	2,5	+	1,2	+	+	-1,1	
Hs.28081	Eukaryotic translation initiation factor 3, subunit 4 delta, 44kDa	EIF3S4	373	++ ++	-1,9	++	3,2	+	1,6	+	+	-1,1	
Hs.381255	Eukaryotic translation initiation factor 3, subunit 5 epsilon, 47kDa	EIF3S5	786	++ ++	-1,9	++	2,6	+	1,4	+	+	-1,2	
Hs.119503	Eukaryotic translation initiation factor 3, subunit 6 interacting protein	EIF3S6IP	1470	++ +	-1,6	++	3,2	+	1,5	+	+	-1,3	
Hs.55682	Eukaryotic translation initiation factor 3, subunit 7 zeta, 66/67kDa	EIF3S7	1179	++ ++	-1,9	++	2,5	+	1,3	+	+	-1,2	
Hs.371001	Eukaryotic translation initiation factor 3, subunit 9 eta, 116kDa	EIF3S9	877	++ +	-1,6	++	3,5	+	1,7	+	+	-1,5	
Hs.211823	Eukaryotic translation initiation factor 4E-like 3	EIF4EL3	376	++ +	1,2	++	2,5	++	1,9	+	+	-1,2	
Hs.310621	Eukaryotic translation initiation factor 5A	EIF5A	304	++ ++	-2,0	++	3,7	+	1,0	+	+	1,1	
Hs.448396	Ribosomal protein L10a	RPL10A	1430	++ +	-1,7	++	2,5	+	1,2	+	+	1,1	
Hs.388664	Ribosomal protein L11	RPL11	1667	++ +	-1,5	++	2,1	+	1,4	+	+	-1,1	
Hs.408054	Ribosomal protein L12	RPL12	2267	++ +	-1,4	++	2,5	+	1,2	+	+	-1,1	
Hs.410817	Ribosomal protein L13	RPL13	2225	++ +	-1,5	++	2,8	+	1,6	+	+	-1,6	
Hs.449070	Ribosomal protein L13a	RPL13A	5210	++ +	-1,5	++	2,8	+	1,2	+	+	-1,2	
Hs.446522	Ribosomal protein L14	RPL14	1245	++ +	-1,4	++	3,2	+	1,7	+	+	-1,4	
Hs.409634	Ribosomal protein L18	RPL18	2370	++ ++	-2,3	++	3,0	+	1,2	+	+	-1,3	
Hs.381123	Ribosomal protein L21	RPL21	2908	++ +	-1,3	++	2,1	+	1,3	+	+	-1,3	
Hs.406300	Ribosomal protein L23	RPL23	2069	++ ++	-1,9	++	3,0	+	1,4	+	+	1,0	
Hs.419463	Ribosomal protein L23a	RPL23A	6816	++ +	-1,2	++	2,3	+	1,4	+	+	-1,1	
Hs.184582	Ribosomal protein L24	RPL24	2134	++ +	-1,2	++	3,2	+	1,5	+	+	-1,3	
Hs.405528	Ribosomal protein L27	RPL27	3415	++ +	-1,1	++	2,3	+	1,5	+	+	-1,2	
Hs.356342	Ribosomal protein L27a	RPL27A	5175	++ +	-1,5	++	2,8	+	1,4	++	+	-1,2	
Hs.356371	Ribosomal protein L28	RPL28	2490	++ ++	-2,0	++	3,5	+	1,3	+	+	-1,2	
Hs.430207	Ribosomal protein L29	RPL29	1623	++ ++	-2,1	++	2,6	+	1,1	+	+	-1,1	
Hs.119598	Ribosomal protein L3	RPL3	3778	++ +	-1,5	++	2,1	+	1,2	+	+	-1,1	
Hs.400295	Ribosomal protein L30	RPL30	3642	++ +	-1,3	++	2,1	+	1,3	+	+	-1,1	
Hs.265174	Ribosomal protein L32	RPL32	3443	++ +	-1,2	++	2,3	+	1,4	+	+	-1,1	
Hs.250895	Ribosomal protein L34	RPL34	1566	++ +	-1,5	++	3,0	+	1,4	+	+	-1,3	
Hs.182825	Ribosomal protein L35	RPL35	2023	++ +	-1,5	++	2,5	+	1,3	+	+	1,1	
Hs.408018	Ribosomal protein L36	RPL36	835	++ ++	-2,1	++	3,7	+	1,1	+	+	-1,5	
Hs.454495	Ribosomal protein L36a	RPL36A	2577	++ ++	-2,1	++	2,8	+	1,1	+	+	-1,1	
Hs.444749	Ribosomal protein L36a-like	RPL36AL	1325	++ +	-1,3	++	2,5	+	1,5	+	+	-1,3	
Hs.80545	Ribosomal protein L37	RPL37	1757	++ +	-1,4	++	2,5	+	1,4	+	+	-1,2	
Hs.433701	Ribosomal protein L37a	RPL37A	7167	++ +	-1,2	++	2,1	+	1,4	+	+	-1,1	
Hs.380953	Ribosomal protein L38	RPL38	3084	++ +	-1,5	++	3,0	+	1,2	+	+	-1,2	
Hs.300141	Ribosomal protein L39	RPL39	4550	++ +	-1,1	++	2,3	+	1,3	+	+	-1,2	
Hs.381172	Ribosomal protein L41	RPL41	6742	++ +	-1,1	++	2,1	+	1,3	+	+	-1,1	
Hs.469653	Ribosomal protein L5	RPL5	2222	++ +	-1,1	++	2,5	+	1,4	+	+	-1,3	
Hs.421257	Ribosomal protein L7	RPL7	6157	++ +	-1,2	++	2,1	+	1,4	+	+	-1,1	
Hs.416801	Ribosomal protein L7a	RPL7A	4661	++ +	-1,6	++	2,3	+	1,3	+	+	-1,1	
Hs.178551	Ribosomal protein L8	RPL8	2281	++ ++	-1,9	++	2,8	+	1,0	+	+	1,1	
Hs.412370	Ribosomal protein L9	RPL9	4474	++ +	-1,2	++	2,0	+	1,6	+	+	-1,1	
Hs.406620	Ribosomal protein S10	RPS10	5835	++ +	-1,6	++	2,5	+	1,2	+	+	-1,2	
Hs.433529	Ribosomal protein S11	RPS11	3094	++ ++	-1,9	++	3,0	+	1,1	+	+	-1,1	
Hs.380956	Ribosomal protein S12	RPS12	2741	++ +	-1,2	++	2,5	+	1,5	+	+	-1,1	
Hs.446588	Ribosomal protein S13	RPS13	3722	++ +	-1,1	++	2,0	+	1,2	+	+	-1,1	
Hs.381126	Ribosomal protein S14	RPS14	3849	++ +	-1,7	++	2,3	+	1,1	+	+	1,0	
Hs.406683	Ribosomal protein S15	RPS15	4183	++ +	-1,5	++	2,6	+	1,2	+	+	-1,1	
Hs.370504	Ribosomal protein S15a	RPS15A	3485	++ +	-1,4	++	2,3	+	1,3	+	+	-1,1	
Hs.397609	Ribosomal protein S16	RPS16	2770	++ +	-1,4	++	2,8	+	1,4	+	+	-1,1	
Hs.433427	Ribosomal protein S17	RPS17	4328	++ +	-1,1	++	2,1	+	1,5	+	+	-1,1	
Hs.275865	Ribosomal protein S18	RPS18	4336	++ +	-1,7	++	2,6	+	1,2	+	+	-1,1	
Hs.381184	Ribosomal protein S19	RPS19	3129	++ +	-1,6	++	2,6	+	1,2	+	+	-1,1	
Hs.498569	Ribosomal protein S2	RPS2	6637	++ +	-1,7	++	2,3	+	1,1	+	+	1,1	
Hs.8102	Ribosomal protein S20	RPS20	3624	++ +	1,1	++	2,0	+	1,5	+	+	-1,2	
Hs.372960	Ribosomal protein S21	RPS21	2174	++ +	-1,7	++	3,2	+	1,2	+	+	-1,2	
Hs.534369	Ribosomal protein S23	RPS23	5152	++ +	-1,2	++	2,1	+	1,3	+	+	-1,1	
Hs.356794	Ribosomal protein S24	RPS24	4359	++ +	-1,4	++	2,3	+	1,2	+	+	-1,1	
Hs.512676	Ribosomal protein S25	RPS25	1646	++ +	-1,7	++	3,0	+	1,4	+	+	-1,2	
Hs.355957	Ribosomal protein S26	RPS26	1346	++ ++	-2,0	++	2,5	+	1,1	+	+	-1,1	
Hs.337307	Ribosomal protein S27	RPS27	3710	++ +	-1,5	++	2,8	+	1,3	+	+	-1,1	
Hs.311640	Ribosomal protein S27a	RPS27A	2736	++ +	-1,1	++	2,6	+	1,6	++	+	-1,4	
Hs.108957	Ribosomal protein S27-like	RPS27L	1160	++ +	-1,1	++	2,1	++	2,3	+	+	-1,1	
Hs.153177	Ribosomal protein S28	RPS28	3836	++ +	-1,6	++	3,0	+	1,4	+	+	-1,3	
Hs.539	Ribosomal protein S29	RPS29	3557	++ +	-1,4	++	3,0	+	1,2	+	+	-1,1	
Hs.387576	Ribosomal protein S3	RPS3	2820	++ ++	-1,7	++	2,8	+	1,3	+	+	-1,2	
Hs.446628	Ribosomal protein S4, X-linked	RPS4X	3003	++ +	-1,5	++	2,6	+	1,4	+	+	-1,1	
Hs.149957	Ribosomal protein S6 kinase, 90kDa, polypeptide 1	RPS6KA1	1811	++ ++	-2,0	++	2,5	+	-1,1	+	+	1,1	
Hs.444012	Ribosomal protein S7	RPS7	2473	++ +	-1,1	++	2,1	+	1,4	+	+	-1,2	
Hs.139876	Ribosomal protein S9	RPS9	1484	++ ++	-2,3	++	3,0	+	1,1	+	+	-1,1	
Hs.437594	Ribosomal protein, large P2	RPLP2	2814	++ ++	-2,3	++	3,5	+	1,1	+	+	-1,1	
Hs.443796	Ribosomal protein, large, P0	RPLP0	5451	++ +	-1,5	++	2,8	+	1,5	+	+	-1,1	
Hs.356502	Ribosomal protein, large, P1	RPLP1	4300	++ +	-1,2	++	2,3	+	1,4	+	+	-1,2	
Hs.461178	Eukaryotic translation initiation factor 1A, Y-linked	EIF1AY	92	++ ++	1,7	++	-3,5	++	-3,5	+	+	1,4	
Hs.151777	Eukaryotic translation initiation factor 2, subunit 1 alpha, 35kDa	EIF2S1	689	++ ++	2,1	+	1,0	++	2,5	+	+	1,5	
Hs.102506	Eukaryotic translation initiation factor 2-alpha kinase 3	EIF2AK3	143	++ ++	2,0	++	-2,8	+	1,6	+	+	-1,2	
Hs.173987	Eukaryotic translation initiation factor 3, subunit 1 alpha, 35kDa	EIF3S1	613	++ +	1,6	+	1,2	++	2,0	+	+	1,5	
Hs.79306	Eukaryotic translation initiation factor 4E	EIF4E	622	++ ++	2,1	++	-2,5	+	1,3	++	+	2,1	
Hs.433702	Eukaryotic translation initiation factor 5	EIF5	1454	++ +	-1,1	++	-2,0	+	-1,3	++	+	2,0	
Hs.158688	Eukaryotic translation initiation factor 5B	EIF5B	370	++ ++	3,2	++	-3,7	+	-1,1	+	+	1,5	
Hs.180911	Ribosomal protein S4, Y-linked 1	RPS4Y1	1126	++ +	-1,1	-	-1,2	++	-8,6	+	+	-1,4	

Interestingly, only one gene from the upregulated ribosomal genes during E-LDL deload (n=84) was significantly regulated during Ox-LDL deload and the majority of these genes (n=83) did not exhibit any regulation. These findings indicate dramatic differences in the regulation of ribosomal genes in response to cholesterol export when cholesterol efflux from E-LDL and Ox-LDL loaded macrophages is being compared.

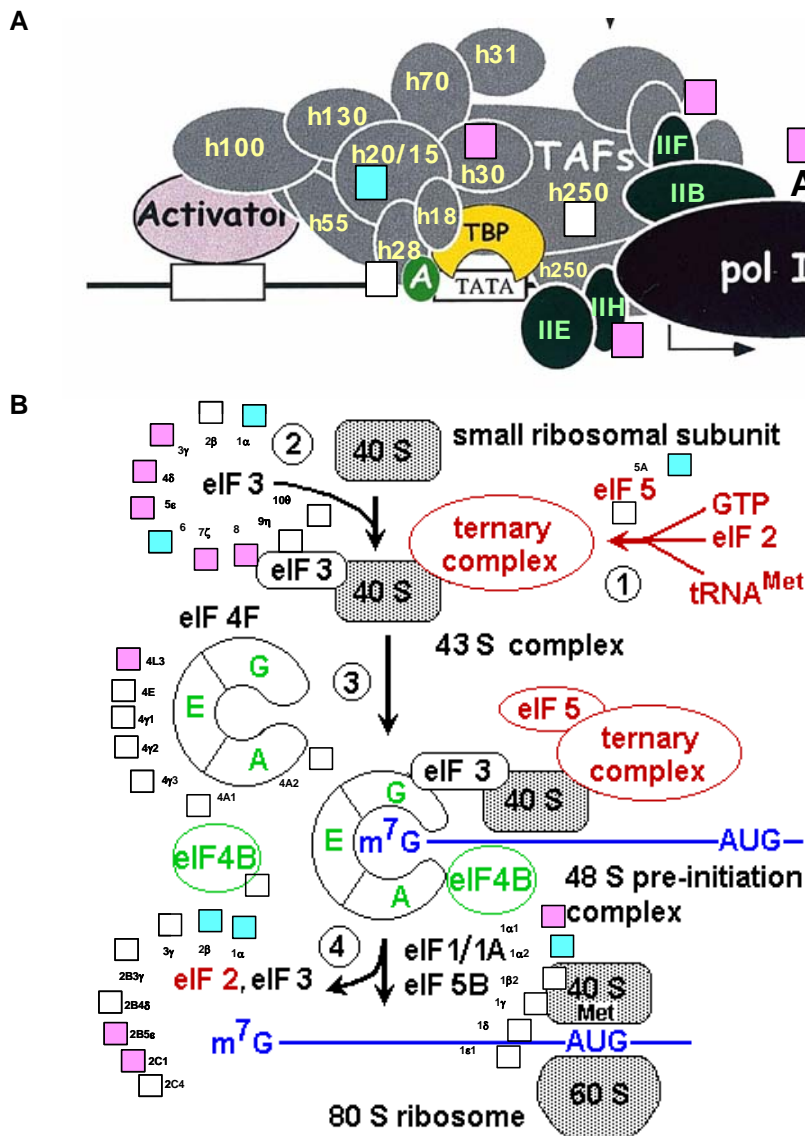


Figure 42: **A.** Regulation of multiple components of the RNA polymerase II complex in apoE3/E3 macrophages during cholesterol deloading following E-LDL mediated cholesterol influx. **B.** Regulation of translation initiation and elongation factors of the ribosome complex in apoE3/E3 macrophages in response to cholesterol deloading

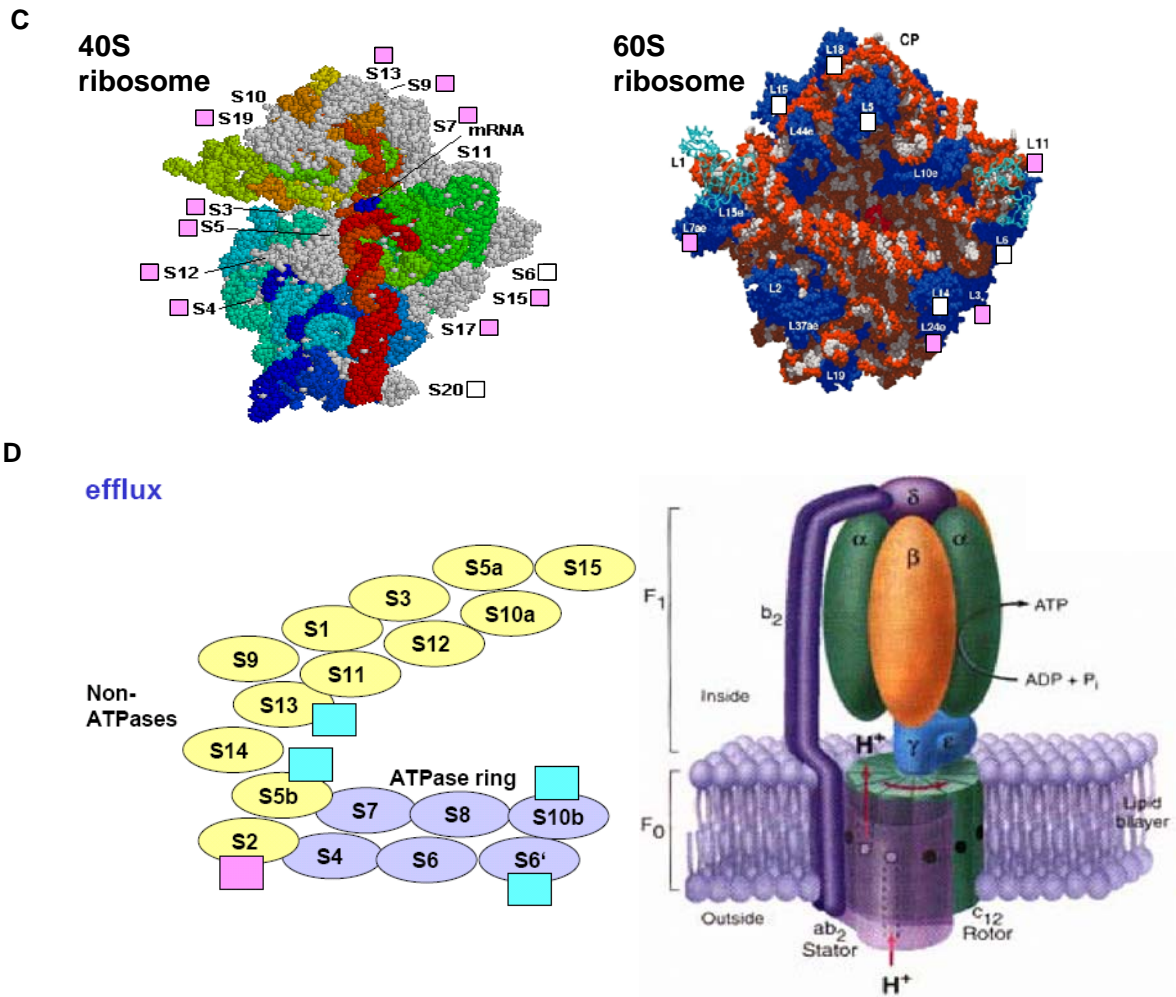


Figure 42: C. Regulation of integral components of the ribosome complex in apoE3/E3 macrophages in response to cholesterol deload with HDL₃. **D.** Regulation of ATPase and non-ATPase factors of the ATP-synthase during E-LDL deload.

6.2. OX-LDL MEDIATED CHOLESTEROL FLUX

Loading the macrophages with Ox-LDL resulted in the upregulation of $n=757$ (6.1%) and a downregulation of $n=671$ (5.4%) genes. Export of cholesterol following Ox-LDL loading increased $n=1022$ (8.2%) genes and only $n=133$ (1.1%) were downregulated. The genes regulated during Ox-LDL load are more distributed and show only pronounced regulation in the cholesterol metabolism pathway and the extracellular matrix pathway.

Genes related to the apolipoproteins and their binding proteins were regulated similarly both in E-LDL and Ox-LDL deloading, as well as genes from the ZNF202 pathway and the PPARs. In controversy to E-LDL deloading, cholesterol efflux following loading with Ox-LDL did not result in statistically significant regulation of translation machinery associated genes in apoE3/E3 macrophages.

In conclusion, numerous genes of the nuclear machinery are involved in the macrophage response to E-LDL cholesterol loading, whereas Ox-LDL loading of macrophages had only a moderate effect on this pool of genes. This reflects the existence of two different regulatory pathways that control the trafficking of E-LDL and Ox-LDL in apoE3/E3 macrophages.

6.3. BIOCHEMICAL PATHWAYS AND CANDIDATE GENES WITH RELEVANCE TO LIPID TRAFFIC IN MACROPHAGES

To further decipher the genes obtained in the previous list, we focused on more defined pathways which describe endocytosis, intracellular processing and exocytosis of lipids. In addition, certain intracellular machineries have been exploited i.e. phagosomes, vesicular trafficking genes and ABCA1-related genes. The percentage of genes regulated is displayed in table 11.

Table 11: Percentage distribution of genes in the defined pathways

Pathway	# genes	ApoE3/E3							
		E-LDL				Ox-LDL			
		Load		Deload		Load		Deload	
		Up	Dwn	Up	Dwn	Up	Dwn	Up	Dwn
1 Endocytosis	19	21,1	21,1	26,3	10,5	15,8	31,6	36,8	0,0
2 Coated vesicle	94	1,1	4,3	14,9	4,3	3,2	3,2	12,8	1,1
3 Vesicle transport	53	1,9	15,1	11,3	1,9	5,7	1,9	7,5	0,0
4 Phagosome	211	1,4	6,6	13,3	4,7	8,1	6,6	14,2	0,5
5 Budding / Fusion	62	1,6	6,5	12,9	0,0	3,2	0,0	9,7	0,0
6 Ca ⁺² transport	100	0,0	17,0	21,0	1,0	6,0	6,0	10,0	0,0
7 Exocytosis ABCA1-related	196	1,5	18,4	17,3	1,5	6,1	6,1	9,7	1,0

The four categories: endocytosis, coated vesicles, phagosome and budding / fusion show a similar regulation pattern with E-LDL and Ox-LDL concerning the number of regulated genes. However, the genes in the three pathways: vesicular transport, calcium transport and exocytosis were primarily regulated by E-LDL and only to a small extent by Ox-LDL. Both calcium transport and exocytosis-related genes were down-regulated by E-LDL load and up-regulated by E-LDL deload. These results are significant but still have to be verified by independent experiments.

6.3.1. REGULATION OF GENES IN THE ENDOCYTIC AND PHAGOCYTTIC PATHWAY IN MACROPHAGES

A pool of 20 non redundant genes was compiled that have been associated with cell endocytosis in general, those genes are mainly scavenger receptors and LDL related genes. Among those, 3 genes were up-, 8 genes were downregulated in apoE3/E3 macrophages during E-LDL or Ox-LDL mediated cholesterol flux respectively, whereas only CD163 (a member of the scavenger receptor cysteine-rich (SRCR) superfamily, which is exclusively expressed by monocytes and macrophages) was up-regulated by HDL3 deloading both in E- and Ox-LDL-loaded macrophages, another 3 genes (SCARB2, PPARG and LDL receptor adaptor protein) were regulated inversely by HDL3 deloading (Table 12).

Table 12: Genes related to the endocytosis pathway that are regulated by E-LDL and Ox-LDL loading and successive HDL₃-mediated deloading.

Unigene	Gene name	Short	Mono	E-LDL		Ox-LDL						
				Load	Del.	Load	Del.					
0	Endocytosis receptors											
Hs.213289	Low density lipoprotein receptor (familial hypercholesterolemia)	LDLR	990	++	++	-8,6	++	3,2	++	-4,0	++	1,4
Hs.184482	LDL receptor adaptor protein	ARH	219	++	++	-1,9	++	2,8	++	1,2	++	-2,2
Hs.162757	Low density lipoprotein-related protein 1	LRP1	177	++	++	-1,5	++	2,6	++	-1,2	++	1,3
Hs.210343	Low density lipoprotein receptor-related protein 6	LRP6	53	+	+	-3,0	+	2,6	+	-1,1	+	-1,2
Hs.410784	Low density lipoprotein receptor-related protein 8, Apo-E receptor	LRP8	277	++	+	-2,0	+	1,7	++	-1,2	++	-2,0
Hs.534325	Fc fragment of IgG, high affinity Ia, receptor for (CD64)	FCGR1A	208	++	++	-1,3	++	1,0	++	-3,7	++	4,0
Hs.352642	Fc fragment of IgG, low affinity IIa, receptor for (CD32)	FCGR2A	285	++	++	-1,5	++	1,5	++	-2,1	++	1,4
Hs.372679	Fc fragment of IgG, low affinity IIIb, receptor for (CD 16)	FCGR3B	158	++	++	-2,5	+	1,1	++	-10,6	+	13,9
Hs.443120	CD36 Thrombospondin receptor	CD36	2978	++	++	2,8	++	1,1	++	2,5	++	1,7
Hs.349656	Scavenger receptor class B, member 2	SCARB2	512	++	++	2,0	++	-2,8	++	-2,3	++	-6,1
Hs.436887	Macrophage scavenger receptor 1	CD204	147	++	++	2,6	++	-1,1	++	1,9	++	1,6
Hs.74076	CD163 antigen	CD163	1354	++	++	-1,7	++	2,1	++	-2,8	++	2,1
Hs.519624	CD14 antigen	CD14	1174	++	++	-3,5	++	3,5	++	-2,8	++	1,1
Hs.444310	CD83 antigen (activated B lymphocytes superfamily)	CD83	996	++	++	2,0	++	1,0	++	2,3	++	1,1
0	RAB - Traffic genes											
Hs.227327	RAB1A, member RAS oncogene family	RAB1A	352	++	++	1,1	+	-3,0	++	1,1	++	4,0
Hs.78305	RAB2, member RAS oncogene family	RAB2	453	++	++	1,0	++	-2,3	++	-1,3	++	2,6
Hs.27744	RAB3A, member RAS oncogene family	RAB3A	12	-	-	-2,0	+	4,9	-	-1,1	-	1,1
Hs.296169	RAB4A, member RAS oncogene family	RAB4A	172	++	++	-1,2	++	-1,1	++	1,1	++	2,0
Hs.73957	RAB5A, member RAS oncogene family	RAB5A	180	++	++	-1,6	+	1,1	+	-1,7	++	2,3
Hs.479	RAB5C, member RAS oncogene family	RAB5C	505	++	++	-2,5	++	1,7	++	-2,8	++	2,1
Hs.75618	RAB11A, member RAS oncogene family	RAB11A	94	++	++	1,0	++	1,4	++	-1,1	++	2,0
Hs.151536	RAB13, member RAS oncogene family	RAB13	946	++	++	-1,4	++	2,5	++	1,4	++	-1,4
Hs.5807	RAB14, member RAS oncogene family	RAB14	611	++	++	1,3	++	-2,0	++	1,1	++	2,8
Hs.281117	RAB22A, member RAS oncogene family	RAB22A	216	++	++	1,2	++	-1,6	++	1,1	++	2,0
Hs.298530	RAB27A, member RAS oncogene family	RAB27A	186	++	++	-1,1	++	-2,0	++	1,0	++	1,2
Hs.108923	RAB38, member RAS oncogene family	RAB38	31	-	+	1,1	++	2,5	++	2,5	++	1,5
Hs.302498	RAB40B, member RAS oncogene family	RAB40B	28	-	-	1,5	+	13,9	+	3,7	-	-3,0
0	Lipid droplet genes											
Hs.496383	Acyl-Coenzyme A: cholesterol acyltransferase 1	SOAT1	188	++	++	2,0	++	-1,7	++	2,1	++	1,5
Hs.406678	Acyl-CoA synthetase long-chain family member 1	ACSL1	883	++	++	2,0	++	-1,1	++	1,9	++	1,1
Hs.3416	Adipose differentiation-related protein (Adipophilin)	ADFP	1966	++	++	2,3	++	1,0	++	3,5	++	-1,1
Hs.376046	Butyrophilin, subfamily 3, member A2	BTN3A2	173	++	++	-2,1	++	2,3	++	-1,1	++	1,6
Hs.83190	Fatty acid synthase	FASN	153	++	++	-2,8	++	2,0	++	-1,1	++	-1,1
Hs.187579	Hydroxysteroid (17-beta) dehydrogenase 7	HSB17B7	391	++	++	-2,3	+	2,5	++	-1,2	+	1,0
Hs.180878	Lipoprotein lipase	LPL	1377	++	++	2,0	++	1,9	++	-2,1	++	3,0
Hs.439776	Stomatin	STOM	660	++	++	2,3	++	-2,0	++	2,5	++	-1,2
Hs.179986	Flotillin 1	FLOT1	564	++	++	-2,0	++	1,7	++	1,0	++	1,0
Hs.18799	Flotillin 2	FLOT2	528	++	++	-2,0	++	2,1	++	-1,2	++	1,4

A total number of n=211 genes were compiled in the phagosomal list, from which 85 were significantly regulated during load and/or deload. These genes were assembled according

to the phagosomal identity gene list, nicely reviewed by the group of Desjardins²⁶. It was noticeable that a significant number of genes were upregulated by deload after E-LDL loading n=28 (13.3%) and Ox-LDL loading n=30 (14.2%). Nevertheless, only one gene (major histocompatibility complex, class II, DQ beta 1) was regulated in an identical manner in E-LDL and Ox-LDL deloaded macrophages. The genes, upregulated during deload of E-LDL-loaded macrophages, include solute carrier family members (SLC12A9, SLC25A5 and SLC25A6) and major histocompatibility members (HLA-A and HLA-B) but were not regulated in Ox-LDL deloaded cells. On the other hand, deloading Ox-LDL-loaded macrophages mainly induced ATPases (ATP6V1G1, ATP6V1D and ATP6V1C1), cathepsins (C, S, and Z) and RABs (2, 3A, 5A, 5C, 11A, 14 and 22A). Rab4, 5 A, 5C and 11 are involved in the early endosome fusion and regulate ER-Golgi transport, their exclusive upregulation upon Ox-LDL deload whereas E-LDL deload does not lead to such a massive increase, only 2 genes from 13 are upregulated. This shows the involvement of different pathways when the cells is being loaded by different particles. Thus, the transport of Ox-LDL is more reliant on the coated-pit pathway.

As an additional difference between E- and Ox-LDL deloading, we mention the ATPases (ATP6V1G1, ATP6V1C and ATP6V1D1) which are inversely regulated.

LDL-receptor mediated cholesterol uptake downregulates intracellular cholesterol synthesis by inhibition of HMGCoA reductase and inhibition of LDL-receptor by feedback mechanism. This cholesterol sensitive regulatory system leads to subsequent deloading of E-LDL whereas Ox-LDL is trapped inside.

6.3.2. REGULATION OF GENES IN THE COATED VESICLE PATHWAY IN MACROPHAGES

From a total number of n=94 genes, 43 were significantly regulated. During loading no significant changes could be observed, but again during deloading n=14 genes (14.9%) from the E-LDL loaded macrophages are upregulated and only n=4 (4.3%) downregulated. The Ox-LDL deloading shows a similar picture: n=12 (12.8%) are upregulated, only one gene (1.1%) is downregulated (Table 13).

Interestingly, about half of these genes n=6 (6.4%) are regulated inversely by E-LDL and Ox-LDL deloading, those genes are: adaptor-related protein complex 1, adaptor-related protein complex 3, cathepsin S, LDL receptor adaptor protein and RAB14. All these genes mediate vesicle coating through the adapter protein pathway. Cathepsin S has been shown to block HDL₃-induced cholesterol efflux and cathepsin secreting cells seem to promote foam cell formation¹²⁰. Moreover, the AP-2 pathway is exclusively regulated by

E-LDL since it includes the LDL-related protein, in contrast to the AP-4 pathway which genes are upregulated only during Ox-LDL deload.

The AP-3 pathway which is linked to syntaxin 13 is more E-LDL sensitive, since this pathway is involved in vesicle fusion, a more downstream event of vesicle-trafficking.

Table 13: Genes related to the adapter protein1-4 pathway that are regulated by E-LDL and Ox-LDL loading and successive HDL₃-mediated deloading.

Unigene	Gene name	Short	Mono	E-LDL		Ox-LDL						
				Load	Del.	Load	Del.					
0	AP-1 pathway											
Hs.418710	adaptor-related protein complex 1, sigma 1 subunit	AP1S1	164	++	+	-1,7	++	3,5	+	1,7	++	-1,1
Hs.40368	adaptor-related protein complex 1, sigma 2 subunit	AP1S2	707	++	+	1,0	++	-2,8	++	-2,5	++	4,9
Hs.355832	Cell division cycle 42 (GTP binding protein, 25kDa)	CDC42	436	++	++	1,7	++	-1,1	++	1,0	++	2,5
Hs.380749	clathrin, light polypeptide (Lcb)	CLTB	315	++	++	-1,1	++	3,2	+	1,6	+	1,1
Hs.14376	actin, gamma 1	ACTG1	8753	++	+	1,1	+	1,5	++	-1,5	++	2,3
Hs.119000	actinin, alpha 1	ACTN1	1826	++	+	1,2	+	2,1	+	1,7	++	1,0
Hs.150101	lysosomal-associated membrane protein 1	LAMP1	2845	++	++	1,3	++	2,0	+	1,7	++	-1,1
Hs.85226	lipase A, lysosomal acid, cholesterol esterase (Wolman disease)	LIPA	5657	++	+	1,5	++	1,3	++	-1,2	++	2,3
Hs.121575	cathepsin D	CTSD	270	++	+	1,4	++	1,7	++	2,0	+	-1,1
Hs.11590	cathepsin F	CTSF	59	+	++	-2,1	++	3,0	+	1,1	+	-1,4
Hs.181301	cathepsin S	CTSS	1885	++	+	1,0	++	-2,1	+	1,3	++	2,3
Hs.255230	glucuronidase, beta	GUSB	261	++	++	1,5	++	1,9	++	2,1	++	-1,1
Hs.522169	Iduronate 2-sulfatase (Hunter syndrome)	IDS	547	++	++	-1,1	+	2,0	++	2,1	+	-1,1
0	AP-2 pathway											
Hs.19121	adaptor-related protein complex 2, alpha 2 subunit	AP2A2	441	++	++	-1,6	++	2,6	+	1,0	++	1,0
Hs.119591	adaptor-related protein complex 2, sigma 1 subunit	AP2S1	605	++	+	-1,3	++	2,1	++	1,1	+	1,4
Hs.184482	LDL receptor adaptor protein	ARH	219	++	+	-1,9	++	2,8	++	1,2	++	-1,2
0	AP-3 pathway											
Hs.446648	adaptor-related protein complex 3, beta 1 subunit	AP3B1	522	++	++	-1,1	+	-1,1	+	-1,1	++	2,6
Hs.19720	adaptor-related protein complex 3, sigma 2 subunit	AP3S2	323	++	+	-2,0	++	2,8	+	-1,1	++	1,2
Hs.20021	vesicle-associated membrane protein 1 (synaptobrevin 1)	VAMP1	118	+	++	-2,1	++	2,6	+	-1,4	+	1,0
Hs.371366	adaptor protein with pleckstrin homology and src homology 2 domains	APS	343	++	++	-2,0	++	2,3	++	-1,2	+	1,0
Hs.479	RAB5C, member RAS oncogene family	RAB5C	505	++	++	-2,5	+	1,7	++	-2,8	++	2,1
Hs.151536	RAB13, member RAS oncogene family	RAB13	946	++	+	-1,4	+	2,5	+	1,4	++	-1,4
Hs.5807	RAB14, member RAS oncogene family	RAB14	611	++	++	1,3	+	-2,0	+	1,1	++	2,8
Hs.6906	v-ral simian leukemia viral oncogene homolog A (ras related)	RALA	177	++	++	1,3	++	-1,1	++	2,5	++	-2,1
0	AP-4 pathway											
Hs.355832	cell division cycle 42 (GTP binding protein, 25kDa)	CDC42	436	++	+	1,7	+	-1,1	+	1,0	++	2,5
Hs.179735	ras homolog gene family, member C	RHOC	350	++	++	-1,1	+	1,6	+	-1,4	++	2,1
Hs.6838	ras homolog gene family, member E	ARHE	62	+	++	2,3	++	-1,7	+	1,2	+	1,7
Hs.301175	ras-related C3 botulinum toxin substrate 2 (rho family)	RAC2	3863	++	+	1,0	++	1,7	+	-1,9	+	2,0

6.3.3. REGULATION OF GENES IN THE VESICULAR TRANSPORT PATHWAY IN MACROPHAGES

A pool of 53 non redundant genes has been associated with cellular vesicular trafficking, n=24 (45.3%) of them were significantly regulated. Those genes were clustered in t-SNAREs and v-SNAREs. During E-LDL load, a downregulation could be observed in n=10 (18.9%) genes, E-LDL deload led to upregulation of n=6 (11.3%) (Table14). The Ox-LDL load and successive deload did not show such an amount of regulation.

Table 14: Genes related to the SNARE complex pathway that are regulated by E-LDL and Ox-LDL loading and successive HDL₃-mediated deloading.

Unigene	Gene name	Short	Mono	E-LDL		Ox-LDL						
				Load	Del.	Load	Del.					
0	Vesicular / vesicle-related proteins											
Hs.173878	Nipsnap homolog 1 (C. elegans)	NIPSNAP1	86	+	++	-2,5	++	2,6	++	-1,6	++	-1,2
Hs.431279	N-ethylmaleimide-sensitive factor	NSF	471	++	++	-1,2	+	2,1	++	2,0	++	1,1
Hs.75932	N-ethylmaleimide-sensitive factor attachment protein, alpha	NAPA	195	++	++	-2,0	++	1,3	++	-1,4	++	1,6
Hs.202308	Synaptosomal-associated protein, 23kDa	SNAP23	211	++	++	-1,3	+	-1,1	+	-1,3	++	3,0
Hs.82240	Syntaxin 3A	STX3A	50	+	-	2,3	-	1,6	+	4,0	++	2,5
Hs.421457	Syntaxin 5A	STX5A	116	++	++	-2,8	++	3,5	++	1,0	++	-1,1
Hs.434916	Syntaxin 7	STX7	116	++	++	-1,1	++	1,0	++	1,1	++	2,0
Hs.43812	Syntaxin 10	STX10	195	++	++	-2,1	++	2,3	++	-1,1	++	1,1
Hs.325862	Syntaxin binding protein 1	STXBP1	239	++	++	-2,3	++	2,6	++	1,4	+	-1,1
Hs.379204	Syntaxin binding protein 2	STXBP2	305	++	++	-2,0	++	2,1	++	1,0	++	1,1
Hs.20021	Vesicle-associated membrane protein 1 (synaptobrevin 1)	VAMP1	118	+	++	-2,1	++	2,6	++	-1,4	+	1,0
Hs.25348	Vesicle-associated membrane protein 2 (synaptobrevin 2)	VAMP2	99	++	++	-2,8	+	1,5	+	-1,5	+	1,1
Hs.66708	Vesicle-associated membrane protein 3 (cellubrevin)	VAMP3	1204	++	++	1,1	-	-1,4	-	-1,4	++	4,6
Hs.6651	Vesicle-associated membrane protein 4	VAMP4	193	++	++	-2,0	++	1,5	++	1,1	++	1,0
Hs.534425	Vesicle-associated membrane protein 5 (myobrevin)	VAMP5	18	-	-	-4,6	++	4,9	++	-2,6	+	-3,5
Hs.165195	VAMP-associated protein A, 33kDa	VAPA	2178	++	++	1,3	+	1,4	+	2,0	++	1,0
Hs.24167	Synaptobrevin-like 1	SYBL1	649	++	++	1,1	++	-1,7	+	1,1	++	2,8
Hs.414343	Synaptogyrin 1	SYNGR1	52	+	++	-1,7	+	5,3	++	1,5	+	1,1
Hs.401730	Synaptojanin 1	SYNJ1	183	++	+	1,1	++	-1,3	+	-1,5	++	2,3
Hs.434494	Synaptojanin 2	SYNJ2	66	+	++	-1,4	-	-2,6	++	2,8	+	-1,1
Hs.443661	Synaptojanin 2 binding protein	SYNJ2BP	58	++	++	-1,1	++	-2,5	-	-1,4	++	1,7
Hs.154679	Synaptotagmin I	SYT1	134	++	++	-2,0	++	1,9	++	-1,1	+	1,3

6.3.4. REGULATION OF GENES IN THE COP MACHINERY IN MACROPHAGES

The COP-I machinery is involved in trafficking from GOLGI to ER compartment, COP-II controls trafficking from ER to GOLGI. The genes involved in this pathway significantly regulated by E-LDL and Ox-LDL loading and HDL₃ deloading are listed in table 15. From n=62 genes, only 19 were significantly regulated, mostly during deload of E-LDL and ox-LDL loaded macrophages (Table 15). Nevertheless, the different loading status seems to affect completely different proteins in the COP-I / COP-II machinery, indicating different uptake and transport processes involved in E-LDL and Ox-LDL loading (Table 15).

ARL7 seems to play a key role in Ox-LDL shuttling and deloading, due to its involvement in vesicular trafficking via coated pit proteins, a fact which again underlines the fact that Ox-LDL is transported by coated pits more that E-LDL is.

Table 15: Genes related to the budding and fusion pathway that are regulated by E-LDL and Ox-LDL loading and successive HDL₃-mediated deloading.

Unigene	Gene name	Short	Mono	E-LDL		Ox-LDL	
				Load	Del.	Load	Del.
0	COP-machinery						
Hs.25277	ARF-GAP, RHO-GAP, ankyrin repeat and plekstrin homology	ARAP3	314	++	++	-2,0	+ 2,3 + -1,3 + 1,2
Hs.25584	ADP-ribosylation factor GTPase activating protein 1	ARFGAP1	216	++	++	-2,0	+ 2,6 ++ 1,0 + -1,1
Hs.310323	ADP-ribosylation factor guanine nucleotide-exchange factor 2	ARFGEF2	502	++	++	1,5 ++	-2,0 ++ 1,2 ++ 1,7
Hs.6838	Ras homolog gene family, member E	ARHE	62	+	+	2,3 ++	-1,7 ++ 1,2 ++ 1,7
Hs.127602	Rho GTPase activating protein 10	ARHGAP10	188	+	+	-1,6 +	3,7 + 1,2 + 1,0
Hs.435063	Rho GTPase activating protein 22	ARHGAP22	35	+	+	-1,4 ++	2,3 + 1,1 + -1,2
Hs.444036	Rho GTPase activating protein 4	ARHGAP4	70	++	+	-2,0 ++	2,6 ++ -1,6 ++ 1,1
Hs.6066	Rho guanine nucleotide exchange factor (GEF) 4	ARHGEF4	39	+	+	-2,0 +	1,5 ++ 1,1 + -1,3
Hs.355832	Cell division cycle 42 (GTP binding protein, 25kDa)	CDC42	436	++	++	1,7 ++	-1,1 ++ 1,0 ++ 2,5
Hs.510533	CDC42 binding protein kinase beta (DMPK-like)	CDC42BPB	68	++	++	-2,8 ++	2,5 ++ -1,1 + -1,1
Hs.372800	Rac/Cdc42 guanine nucleotide exchange factor (GEF) 6	ARHGEF6	206	++	++	-2,0 ++	2,6 ++ -1,4 ++ 1,1
Hs.162121	Coatomer protein complex, subunit alpha	COPA	767	++	++	-1,2 ++	-1,3 ++ -1,2 ++ 2,0
Hs.10326	Coatomer protein complex, subunit epsilon	COPE	433	++	+	-1,6 +	1,3 + -1,1 + 2,0
Hs.6671	COP9 constitutive photomorphogenic homolog subunit 4 (Arabidopsis)	COPS4	467	++	++	1,1 ++	1,3 ++ 2,0 ++ 1,2
Hs.15591	COP9 constitutive photomorphogenic homolog subunit 6 (Arabidopsis)	COPS6	336	++	++	-1,3 ++	2,8 ++ 2,0 ++ 1,2
Hs.286221	ADP-ribosylation factor 1	ARF1	557	++	++	1,1 +	-2,3 ++ -1,1 ++ 2,8
Hs.119177	ADP-ribosylation factor 3	ARF3	689	++	++	-1,5 ++	2,6 ++ 1,0 ++ 1,1
Hs.89474	ADP-ribosylation factor 6	ARF6	215	++	+	1,0 +	-4,0 + -1,1 ++ 3,2
Hs.372616	ADP-ribosylation factor-like 1	ARL1	328	++	++	1,2 ++	-1,1 ++ 1,2 ++ 2,0
Hs.182215	ADP-ribosylation factor-like 3	ARL3	191	++	++	-1,1 ++	2,0 ++ 1,4 ++ 1,1
Hs.245540	ADP-ribosylation factor-like 4	ARL4	110	+	+	1,5 +	-1,1 + 2,3 ++ 1,4
Hs.111554	ADP-ribosylation factor-like 7	ARL7	30	+	++	-1,3 ++	1,0 ++ 2,0 ++ -2,8
Hs.277255	ADP-ribosylation factor-like 10C	ARL10C	1417	++	++	1,3 ++	1,0 ++ 2,0 ++ 1,1
Hs.9552	ADP-ribosylation factor-like 2 binding protein	ARL2BP	426	++	++	-1,2 +	1,1 ++ -1,2 + 2,1
Hs.405689	ARF binding protein 1, golgi associated, gamma adaptin ear containing	GGA1	1742	++	++	-1,6 ++	2,6 ++ 1,5 ++ -1,3
Hs.133340	ARF binding protein 2, golgi associated, gamma adaptin ear containing	GGA2	138	++	++	1,0 ++	1,1 ++ 1,1 ++ 2,6
Hs.87726	ARF binding protein 3, golgi associated, gamma adaptin ear containing	GGA3	226	++	++	-2,0 ++	1,1 ++ -1,1 + 1,1
Hs.107614	Sec 6 (S. cerevisiae) homolog	SEC6	99	+	++	-1,7 ++	4,3 ++ 1,7 ++ -2,3
Hs.272927	Sec23 homolog A (S. cerevisiae)	SEC23A	180	++	++	1,3 ++	1,1 ++ 2,0 ++ 1,2
Hs.173497	Sec23 homolog B (S. cerevisiae)	SEC23B	413	++	++	-1,3 ++	1,2 ++ -1,4 ++ 2,6
Hs.300208	Sec23 interacting protein	SEC23IP	273	++	+	1,5 -	-1,6 + 1,6 ++ 2,8
Hs.365863	Sec10-like 1 (S. cerevisiae)	SEC10L1	215	++	-	3,5 -	-5,7 - -1,1 + 18,4
Hs.75232	Sec14-like 1 (S. cerevisiae)	SEC14L1	109	++	++	-1,4 +	-1,7 + -2,1 ++ 2,3
Hs.430576	Sec14-like 2 (S. cerevisiae)	SEC14L2	32	+	+	-1,1 +	3,0 + 1,4 + -1,9
Hs.330767	Sec63-like (S. cerevisiae)	SEC63	201	++	++	-1,3 +	-1,4 + -2,1 ++ 2,0

6.3.5. REGULATION OF GENES IN THE CALCIUM SIGNALLING PATHWAY IN MACROPHAGES

In apoE3/E3 macrophages, microarray analysis revealed the expression of n=100 genes which, based on their biological context, could stringently be assigned to the calcium transport pathway. Among these, n=44 (44%) genes were regulated by cholesterol flux and n=17 (17%) genes displayed a significant downregulation response to E-LDL load and even n=21 (21%) genes were upregulated during deload of E-LDL loaded macrophages.

As for Ox-LDL, only n=6 (6%) were downregulated upon loading and three were coordinately regulated, those are S100 calcium binding proteins (A8, A9, A12). Moreover, the calcium binding protein A8 (calgranulin A) was the strongest regulated gene in this pathway, with a 45.3- and 90.5- fold downregulation upon E-LDL and Ox-LDL load, respectively (Table 16).

Table 16: Genes related to the calcium signalling and metabolism pathway that are regulated by E-LDL and Ox-LDL loading and successive HDL₃-mediated deloading.

Unigene	Gene name	Short	Mono	E-LDL		Ox-LDL						
				Load	Del.	Load	Del.					
0	Ca⁺⁺											
Hs.75527	adenylosuccinate lyase	ADSL	486	++	++	-1,1	++	2,0	++	2,0	++	1,0
Hs.65425	calbindin 1, 28kDa	CALB1	24	+	+	-4,6	+	6,5	-	-1,3	+	-1,1
Hs.406234	calcium binding protein P22	CHP	473	++	++	-1,4	++	2,1	++	1,5	++	-1,1
Hs.425808	calmodulin 2 (phosphorylase kinase, delta)	CALM2	6032	++	++	1,2	++	1,5	++	-1,1	++	2,0
Hs.334330	calmodulin 3 (phosphorylase kinase, delta)	CALM3	288	++	++	-1,1	++	2,5	++	-1,3	++	1,6
Hs.155560	calnexin	CANX	2740	++	++	1,1	++	1,3	++	1,6	++	1,3
Hs.388469	calpain, small subunit 1 /// calpain, small subunit 1	CAPNS1	828	++	++	-1,1	++	1,0	++	-1,2	++	2,0
Hs.350899	calpain 2, (m/II) large subunit	CAPN2	2478	++	++	2,0	++	-1,1	++	2,8	++	1,6
Hs.433673	calreticulin	CALR	859	++	++	-4,6	++	9,2	++	1,1	++	-1,5
Hs.355832	Cell division cycle 42 (GTP binding protein, 25kDa)	CDC42	436	++	++	1,7	++	-1,1	++	1,0	++	2,5
Hs.172674	nuclear factor of activated T-cells, cytoplasmic, calcineurin-dependent 3	NFATC3	240	++	++	-1,1	++	-1,5	++	1,2	++	2,3
Hs.85701	phosphoinositide-3-kinase, catalytic, alpha polypeptide	PIK3CA	122	++	++	-1,1	++	-1,7	++	-1,2	++	2,6
Hs.239818	phosphoinositide-3-kinase, catalytic, beta polypeptide	PIK3CB	233	++	++	-1,1	++	2,0	++	2,0	++	-1,5
Hs.355888	phospholipase C, beta 2	PLCB2	75	+	+	-1,6	+	2,8	+	-1,2	+	1,5
Hs.437137	phospholipase C, beta 3 (phosphatidylinositol-specific)	PLCB3	107	+	+	-2,0	+	3,7	+	1,0	+	1,1
Hs.349611	protein kinase C, alpha	PRKCA	349	++	++	1,0	++	1,5	++	-1,6	++	2,0
Hs.155342	protein kinase C, delta	PRKCD	661	++	++	-1,2	++	-1,1	++	-2,0	++	2,6
Hs.315366	protein kinase C, eta	PRKCH	239	++	++	-1,4	++	1,3	++	2,0	++	-1,1
Hs.280604	protein phosphatase 3 (calcineurin B, type I)	PPP3R1	121	++	++	-2,0	++	2,6	++	1,2	++	1,0
Hs.81256	S100 calcium binding protein A4 (calvasculin, metastasin)	S100A4	2209	++	++	-1,1	++	2,8	++	1,5	++	-1,1
Hs.416073	S100 calcium binding protein A8 (calgranulin A)	S100A8	4289	++	++	-45,3	++	6,5	++	-90,5	++	6,5
Hs.112405	S100 calcium binding protein A9 (calgranulin B)	S100A9	861	++	++	-4,3	++	4,0	++	-16,0	++	6,1
Hs.19413	S100 calcium binding protein A12 (calgranulin C)	S100A12	145	++	++	-2,3	++	1,6	+	-2,1	+	1,2
Hs.446592	S100 calcium binding protein A13	S100A13	315	++	++	-2,3	+	2,5	++	-1,1	++	-1,3
Hs.288998	S100 calcium binding protein A14	S100A14	88	++	+	-2,3	+	1,6	+	-1,4	+	1,5
Hs.2962	S100 calcium binding protein P	S100P	58	++	++	-7,5	++	10,6	+	2,8	+	-1,6
Hs.83760	troponin I, skeletal, fast	TNNI2	5	-	-	1,5	++	3,2	++	2,6	+	1,1
Hs.436186	type 1 tumor necrosis factor receptor shedding aminopeptidase regulator	ARTS-1	143	++	++	1,0	++	2,8	++	2,1	++	1,0
0	Channels											
Hs.149900	inositol 1,4,5-triphosphate receptor, type 1	ITPR1	165	++	++	1,2	++	1,0	++	2,6	++	-1,2
Hs.427717	ryanodine receptor 3	RYR3	66	++	++	-2,1	++	1,7	++	-1,1	++	1,3
Hs.406751	inositol 1,4,5-triphosphate receptor, type 2	ITPR2	57	++	++	-1,6	++	1,7	++	-2,1	++	1,4
Hs.154210	endothelial differentiation, sphingolipid G-protein-coupled receptor, 1	EDG1	31	+	+	-3,5	++	4,0	++	-1,5	+	-1,1
Hs.125116	Calcium channel, voltage-dependent, alpha 1I subunit	CACNA1I	90	+	+	-2,5	++	3,0	+	-1,1	+	1,1
Hs.400460	Calcium channel, voltage-dependent, P/Q type, alpha 1A subunit	CACNA1A	63	++	++	-2,0	+	2,1	++	-1,4	++	1,4
Hs.371458	Chloride channel 6	CLCN6	160	+	+	-2,3	+	1,6	+	-2,0	+	2,0
Hs.408883	Sodium channel, voltage-gated, type I, beta	SCN1B	51	+	+	-1,6	+	2,3	+	-1,5	+	1,4
Hs.186877	Sodium channel, voltage-gated, type XI, alpha	SCN11A	48	++	++	-2,1	++	2,3	++	1,3	++	-1,2
Hs.121495	Potassium voltage-gated channel, Isk-related family, member 1	KCNE1	63	+	+	-2,3	++	2,3	+	-1,1	+	1,0
Hs.354740	Potassium large conductance calcium-activated channel, subfamily M, alpha member 1	KCNMA1	53	-	-	-1,7	++	4,3	++	1,1	++	1,0
Hs.463	Potassium inwardly-rectifying channel, subfamily J, member 1	KCNJ1	8	-	-	-4,0	-	4,9	-	-8,0	-	1,4
Hs.1547	Potassium inwardly-rectifying channel, subfamily J, member 2	KCNJ2	367	++	++	-1,1	++	1,4	++	-2,5	++	2,1
Hs.10082	Potassium intermediate/calcium-activated channel, subfamily N, member 4	KCNN4	1001	++	++	-1,1	++	2,0	++	-1,7	++	2,0

S100 calcium binding proteins are members of a multigenic family that comprises 19 members and are differentially expressed in a large number of cell types. Members of this protein family have been implicated in the Ca²⁺-dependent regulation of a variety of intracellular activities such as protein phosphorylation, enzyme activities, cell proliferation and differentiation, the dynamics of cytoskeleton constituents, the structural organization of membranes, intracellular Ca²⁺-homeostasis, inflammation, and in protection from oxidative cell damage. S100 proteins probably are an example of calcium-modulated, regulatory proteins that intervene in the fine tuning of a relatively large number of specific intracellular and extracellular activities.

6.3.6. REGULATION OF ABCA1-RELATED GENES IN THE EXOCYTOSIS PATHWAY IN MACROPHAGES

This category contains ABCA1-related genes, their interaction partners and genes involved in lipid metabolism in addition to genes which are, at least on the transcriptional level, similarly regulated as ABCA1. It is noticeable that from n=196 genes, n=36 (18.4%) are being downregulated upon E-LDL load, whereas n=34 (17.3%) are being upregulated by further deloading with HDL₃ (Table 17).

Table 17: Genes related to the exocytosis pathway and regulated by E-LDL and Ox-LDL loading and further HDL₃-mediated deloading.

Unigene	Gene name	Short	Mono	E-LDL				Ox-LDL				
				Load	Del.	Load	Del.					
0	Exocytosis											
Hs.147259	ATP-binding cassette, sub-family A (ABC1), member 1	ABCA1	130	++	++	2.0	++	-1.4	++	2.0	++	-1.2
Hs.21330	ATP-binding cassette, sub-family B (MDR/TAP), member 1	ABCB1	95	++	++	-3.2	+	3.0	+	-1.1	+	-1.1
Hs.496383	Acyl-Coenzyme A: cholesterol acyltransferase 1	SOAT1	188	++	++	2.0	++	-1.7	++	2.1	++	1.5
Hs.25584	ADP-ribosylation factor GTPase activating protein 1	ARFGAP1	216	++	++	-1.9	+	2.6	++	1.0	+	-1.1
Hs.436683	AFG3 ATPase family gene 3-like 2 (yeast)	AFG3L2	263	++	++	-1.1	++	2.1	++	2.3	++	-1.4
Hs.355832	Cell division cycle 42 (GTP binding protein, 25kDa)	CDC42	436	++	++	1.7	++	-1.1	++	1.0	++	2.5
Hs.162121	Coatomer protein complex, subunit alpha	COPA	767	++	++	-1.2	++	-1.3	++	-1.2	++	2.0
Hs.9641	Complement component 1, q subcomponent, alpha polypeptide	C1QA	35	+	+	-3.7	++	4.6	++	-4.6	++	1.1
Hs.272813	Dual oxidase 1	DUOX1	38	++	++	-2.8	+	1.5	+	1.0	+	1.0
Hs.82002	Endothelin receptor type B	EDNRB	55	++	+	-2.1	++	2.1	+	-1.2	+	1.1
Hs.77432	Epidermal growth factor receptor	EGFR	46	++	++	-2.3	++	2.5	++	-1.1	++	1.2
Hs.179986	Flotillin 1	FLOT1	564	++	++	-2.0	++	1.7	++	1.0	++	1.0
Hs.18799	Flotillin 2	FLOT2	528	++	++	-2.0	++	2.1	++	-1.2	++	1.4
Hs.446309	Glutathione S-transferase A1	GSTA1	107	++	++	-2.5	++	2.1	++	-1.1	++	1.1
Hs.279837	Glutathione S-transferase M2 (muscle)	GSTM2	132	++	++	-3.2	+	6.1	+	-1.5	++	1.6
Hs.2006	Glutathione S-transferase M3 (brain)	GSTM3	107	++	++	-3.2	++	3.0	++	1.2	++	1.2
Hs.405689	Golgi associated, gamma adaptin ear containing, ARF binding protein 1	GGA1	1742	++	++	-1.6	++	2.6	++	1.5	++	-1.3
Hs.406751	Inositol 1,4,5-triphosphate receptor, type 2	ITPR2	57	++	++	-1.6	++	1.7	++	-2.1	++	1.4
Hs.212296	Integrin, alpha 6	ITGA6	68	++	++	1.7	+	1.0	++	2.1	++	1.1
Hs.76038	Isopentenyl-diphosphate delta isomerase	ID1	1063	++	++	-4.0	++	3.7	++	-2.0	++	1.7
Hs.213289	Low density lipoprotein receptor (familial hypercholesterolemia)	LDLR	990	++	++	-8.6	++	3.2	++	-4.0	++	1.4
Hs.433391	Metallothionein 1G	MT1G	523	++	++	-4.0	++	3.7	++	4.9	++	-4.3
Hs.438462	Metallothionein 1H	MT1H	493	++	++	-5.3	++	5.3	+	4.6	++	-4.3
Hs.101474	Microtubule associated serine/threonine kinase 2	MAST2	149	++	++	-1.3	++	2.6	++	1.4	++	-1.2
Hs.196914	Minor histocompatibility antigen HA-1	HA-1	239	++	++	-2.0	++	3.7	++	1.1	+	-1.7
Hs.173878	Nipsnap homolog 1 (C. elegans)	NIPSNAP1	86	+	+	-2.5	++	2.6	++	-1.6	++	-1.2
Hs.439312	Phospholipid transfer protein	PLTP	4	-	+	-1.4	++	1.1	++	-3.0	++	1.5
Hs.24557	RAB11 family interacting protein 5 (class I)	RAB11FIP5	115	++	++	-2.5	++	2.5	++	-1.1	++	-1.1
Hs.190284	sterol regulatory element binding transcription factor 1	SREBF1	77	+	+	-3.2	++	1.7	+	1.1	+	-1.6
Hs.372800	Rac/Cdc42 guanine nucleotide exchange factor (GEF) 6	ARHGEF6	206	++	++	-2.0	++	2.6	++	-1.4	++	1.1
Hs.349656	Scavenger receptor class B, member 2	SCARB2	512	++	++	2.0	++	-2.8	++	-2.3	++	6.1
Hs.437096	SREBP CLEAVAGE-ACTIVATING PROTEIN	SCAP	182	++	++	-1.9	++	2.6	++	1.4	+	-1.3
Hs.439776	Stomatin	STOM	660	++	++	-2.0	++	2.5	++	-1.2	++	-1.1
Hs.414343	Synaptogyrin 1	SYNGR1	52	+	-	-1.7	+	5.3	++	1.5	+	1.1
Hs.434494	Synaptojanin 2	SYNJ2	66	+	+	-1.4	-	-2.6	+	2.8	+	-1.1
Hs.443661	Synaptojanin 2 binding protein	SYNJ2BP	58	++	++	-1.1	++	-2.5	++	-1.4	++	1.7
Hs.1501	Syndecan 2 (heparan sulfate proteoglycan 1)	SDC2	4756	++	++	1.4	++	-1.1	++	2.1	++	-1.1
Hs.397729	3-hydroxy-3-methylglutaryl-Coenzyme A synthase 1 (soluble)	HMGCS1	291	++	++	-2.1	++	3.0	++	-2.1	++	1.9

Among those genes was the sterol regulatory element binding transcription factor (SREBF1) which was downregulated by E-LDL load, 3-hydroxy-3-methylglutaryl-Coenzyme A reductase which was only Ox-LDL sensitive and was downregulated by load and upregulated by deload. In addition, genes involved in proteasomal degradation like (HSPA8; HSPD1; PSMA1; PSMC2; PSMD1; SLC's; Ubiquitination proteins) and genes functional in phagosomal maturation and degradation (RAB; RAS) were regulated, raising

the assumption that the proteasome might be involved in degradation of apolipoprotein components.

The ATPase, H⁺ transporting, lysosomal 34 kDa, V1 subunit D was identically regulated as ABCA1, as was acetyl-Coenzyme A acetyl-transferase 1 (SOAT1), implicating the theory that ATP-synthases may be involved in cholesterol uptake or depletion. In order to further strengthen this hypothesis, all significantly ATP-synthases were listed to see their expression at loading and further deloading. From n=18 ATP-synthase encoding genes, n=8 (44%) were upregulated by E-LDL deload but did not respond to Ox-LDL deloading (Table 18).

This indicates a more close relationship of the E-LDL uptake route, which enters the cell outside coated pits, with the membrane ATP-synthase complex than Ox-LDL which enters the cell via coated-pit dependent receptors.

Table 18: ATP-synthases and their regulation by E-LDL and Ox-LDL loading and successive HDL₃-mediated deloading.

Unigene	Gene name	Short	Mono	E-LDL		Ox-LDL	
				Load	Del.	Load	Del.
0	ATP synthases						
Hs.80986	ATP synthase, H+ transporting, mitochondrial F0 complex, subunit c (subunit 9), isoform 1	ATP5G1	329	++ ++	-1,1 ++	2,8 ++	1,7 + 1,2
Hs.85539	ATP synthase, H+ transporting, mitochondrial F0 complex, subunit e	ATP5I	683	++ +	1,0 ++	3,5 ++	1,7 ++ -1,5
Hs.235557	ATP synthase, H+ transporting, mitochondrial F0 complex, subunit f, isoform 2	ATP5J2	1456	++ +	-1,2 ++	2,5 +	1,4 + 1,2
Hs.107476	ATP synthase, H+ transporting, mitochondrial F0 complex, subunit g	ATP5L	2553	++ -	-1,5 ++	2,6 +	1,2 + 1,1
Hs.298280	ATP synthase, H+ transporting, mitochondrial F1 complex, alpha subunit, isoform 1	ATP5A1	2223	++ +	1,1 +	2,3 ++	1,6 - 1,2
Hs.406510	ATP synthase, H+ transporting, mitochondrial F1 complex, beta polypeptide	ATP5B	2246	++ ++	1,0 ++	2,0 ++	1,6 ++ 1,4
Hs.501304	ATP synthase, H+ transporting, mitochondrial F1 complex, delta subunit	ATP5D	339	++ ++	-1,7 ++	2,8 -	-1,1 - 1,0
Hs.177530	ATP synthase, H+ transporting, mitochondrial F1 complex, epsilon subunit	ATP5E	2085	++ ++	1,1 ++	2,1 ++	1,6 ++ -1,4
Hs.409140	ATP synthase, H+ transporting, mitochondrial F1 complex, O subunit	ATP5O	1444	++ ++	-1,1 +	2,3 +	1,5 + 1,1
Hs.386678	solute carrier family 16 (monocarboxylic acid transporters), member 3	SLC16A3	1216	++ ++	-2,0 ++	2,6 ++	-1,6 ++ 1,1
Hs.79172	solute carrier family 25 (mitochondrial carrier; adenine nucleotide translocator), member 5	SLC25A5	2961	++ ++	-1,2 ++	2,0 ++	1,4 ++ 1,1
Hs.350927	solute carrier family 25 (mitochondrial carrier; adenine nucleotide translocator), member 6	SLC25A6	1768	++ ++	-2,1 ++	3,5 ++	1,4 ++ -1,2
Hs.32951	solute carrier family 29 (nucleoside transporters), member 2	SLC29A2	36	+ +	-11,3 +	12,1 +	-1,4 + 1,1
Hs.407135	adenosine deaminase	ADA	59	+ ++	-2,5 ++	2,0 ++	-1,5 + -1,1
Hs.148822	adenosine deaminase, RNA-specific, B1 (RED1 homolog rat)	ADARB1	109	+ +	-1,9 +	2,5 +	-1,1 + 1,1
Hs.82927	adenosine monophosphate deaminase 2 (isoform L)	AMPD2	558	++ ++	-3,7 ++	4,9 ++	-1,3 ++ -1,4
Hs.205353	ectonucleoside triphosphate diphosphohydrolase 1	ENTPD1	241	++ ++	-1,4 ++	4,9 ++	-2,0 ++ 1,7

VI. DISCUSSION

ABC transporters have various functions in the human body and several ABC proteins (MDRs, MRPs, ABCG2) are responsible for drug export in treated tumor cells, providing cellular mechanisms for the development of multi drug resistance. Also, ABC transporters have greatly gained attention because mutations in these proteins are the cause of human inherited diseases. Among these are familial HDL deficiency also referred to as Tangier disease caused by mutations in ABCA1^{21,24,159} cystic fibrosis caused by mutations in the ABCC7/CFTR gene⁴¹, and sulfonylurea receptor ABCC8/SUR mutations associated with familial persistent hyperinsulinemic hypoglycemia of infancy (PHHI) which is characterized by dysregulated insulin secretion from pancreatic beta cells.

Since the identification of ABCA1 as a major component of the reverse cholesterol and phospholipid transport pathway, it is important to elucidate its functions and to identify its interaction partners. In addition, ABCA1 expressed in the liver, is the major player in the determination of plasma HDL-cholesterol and also exerts HDL-independent anti-atherogenic properties by reducing monocyte filopodia formation and subsequent subendothelial migration.

Several factors control the expression and activity of ABCA1. Lipid uptake by macrophage cells has been shown to be a potent inducer of ABCA1 expression¹¹⁵. Several transcriptional control elements acting via alternative promoters have been characterized. The ABCA1 upstream region contains a macrophage specific promoter preceding exon 1. This sequence binds the repressors ZNF202 and USF1/2, as well as the activating factors Sp1/Sp3 and the oxysterol-induced RXR/LXR heterodimer¹⁶⁶. The LXR/RXR responsive elements in promoter 1 triggers retinoic acid and oxysterol dependent activation of the ABCA1 promoter and thereby confer the observed induction of ABCA1 during lipid loading of macrophages.

The identification and molecular understanding of ABCA1-associated proteins will provide important insights into ABCA1 function. ApoA-I, as a primary acceptor of phospholipids, associates with ABCA1¹⁹⁵ as does Cdc42⁵².

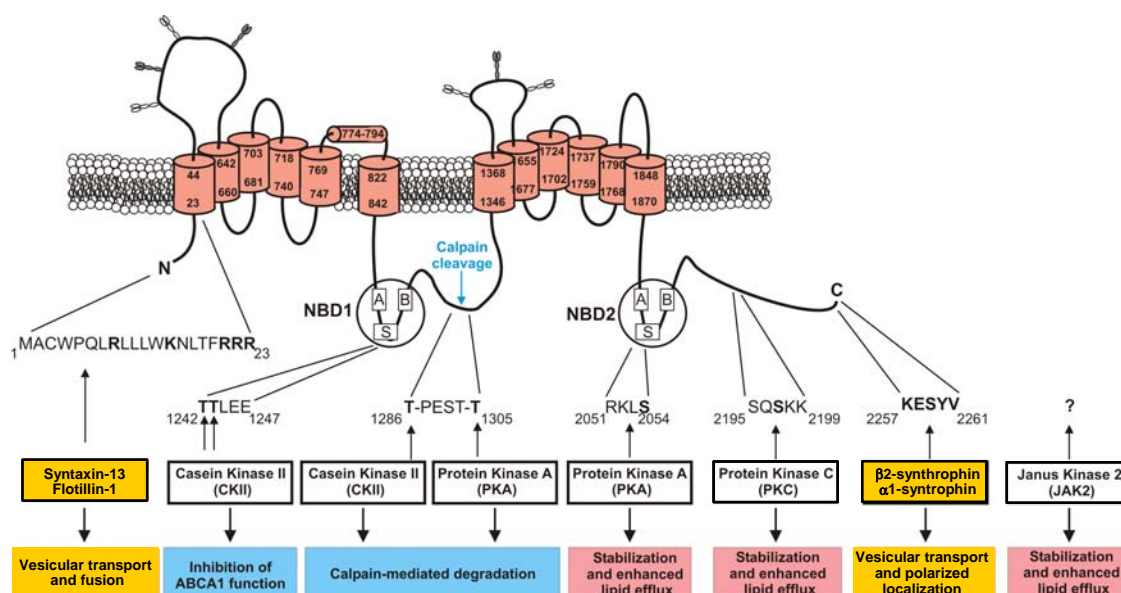


Figure 42: The domains of ABCA1 and interacting partners.

In this thesis we were able to show that ABCA1 interacts with several other proteins, namely: FADD, β 2-syntrophin, syntaxin 13 and flotillin-1, figure 42 shows the domains of ABCA1 and the interacting partners.

Fas-associated death domain protein (FADD) is an adaptor molecule that bridges the interactions between membrane death receptors (FAS) and initiator caspases, namely caspase-8 and caspase-10, in the cytoplasmic death-inducing signaling complex (DISC). Recent evidence indicates that FADD primarily resides in the nucleus and appears to shuttle between nucleus and cytoplasm. FADD plays a well-established role in transduction of apoptotic signals and other cellular processes.

We provided evidence that FADD directly interacts with ABCA1 in the hepatoma cell line HepG2, in the megakaryoblastic leukemia cell line Meg-01, and in primary human fibroblasts indicating that the association of ABCA1 with FADD is not cell-type specific. The FADD-ABCA1 interaction is a surprising finding that links HDL metabolism and reverse lipid efflux with a protein mainly described in the context of death receptor-induced apoptosis. Recombinant expression of the ABCA1 C-terminus and FADD-DN significantly reduced cellular efflux of choline phospholipid to apoA-I. This underlines the importance of proteins associated with the C-terminus of ABCA1 for ABCA1 function and

indicates that full-length FADD is one of these accessory proteins. The death effector domain of FADD is known to interact with the death effector domain of caspase 8⁸⁷. However, caspase 8 was not found in ABCA1/FADD complexes, and activation of caspases was not necessary for apoA-I-dependent phospholipid efflux. The expression of FADD was found to be reduced in primary fibroblasts from five TD patients compared with fibroblast from four controls. FADD expression was not altered in cholesterol-loaded or serum-starved cells nor influenced by stimulating reverse lipid efflux, and therefore the reduced expression of FADD in TD fibroblasts is not a secondary response to disturbed cholesterol homeostasis. FADD expression was reduced in fibroblasts from patients with mutated ABCA1 but was not down-regulated in HepG2 cells stably expressing ABCA1 C terminus or FADD-DN with reduced apolipoprotein A-I-dependent phospholipid efflux. Therefore the reduced expression of FADD may be a consequence of absent or defective ABCA1 protein. ABCA1 was suggested to be a phosphatidylserine translocase that facilitates phosphatidylserine exofacial flipping. The transient local exposure of anionic phospholipids in the outer membrane leaflet enhances the engulfment of apoptotic cells⁷⁵, endocytosis²⁰⁷, and binding of apoA-I. The association of ABCA1 with FADD shown here and the high expression of ABCA1 on platelets may reflect an ABCA1-related phosphatidylserine translocase effect. Alternatively the FADD/ABCA1 interaction may indicate an anti-apoptotic ABCA1 function independent from phosphatidylserine translocase activity.

Members of the ABC transporter superfamily are highly homologous. The alignment of the C-terminal region of ABCA1 and ABCR, the knowledge of causal mutations or polymorphisms, in addition to the recent finding that ABCA1 is not an active pump but may rather function as a regulator similar to ABCC7 (CFTR) or ABCC8 (SUR1) may be a useful approach to identify amino acids or peptides with important functions in these proteins. Besides the high conservation within the ABCA proteins, the C-terminal peptide sequence of ABCA1 is unique within this protein family representing a PDZ site. CFTR

was already shown to associate with PDZ domains¹⁴. The syntrophins α , $\beta 1$, $\beta 2$, $\gamma 1$, $\gamma 2$ are intracellular membrane proteins with multiple protein interaction domains. These include two functional pleckstrin homology domains (PH), a PDZ domain, and a C-terminal syntrophin-unique (SU) region. PH domains bind to proteins or phosphatidylinositol lipids and may mediate signal dependent membrane association. PDZ domains are molecular adaptors and position their targets in the appropriate position or cell compartments. PDZ domains either bind to carboxyterminal peptides or interact with a second PDZ domain. The second PH domain and the highly conserved SU domain of syntrophins are required for interaction with dystrophin/utrophin, and $\beta 2$ -syntrophin was found to be mainly associated with utrophin in skeletal muscle. In utrophin and dystrophin a central helical coiled-coil domain separates the actin binding N-terminal domain from the cysteine-rich C-terminal region. The WW domain in the cysteine-rich C-terminal region interacts with β -dystroglycan whereas the final C-terminal region of utrophin may associate with dystrobrevins and syntrophin. $\beta 2$ -Syntrophin was shown here to be expressed in monocytes, macrophages, fibroblasts, and megakaryocytic cells and therefore may be a general adaptor of membrane proteins to the actin cytoskeleton via utrophin, a protein highly homologous to dystrophin, which is abundant in various cells and tissues.

In this work we also identified $\beta 2$ -syntrophin as an ABCA1-interacting protein and further confirmed that utrophin also contributes to this complex. The function of this complex may be analogous to the ICA512 (islet cell autoantigen)- $\beta 2$ -syntrophin/utrophin complex in pancreatic β -cells where the exocytosis of secretory granules is hindered by the association of ICA512 enriched in the membrane of secretory vesicles with $\beta 2$ -syntrophin/utrophin/actin complexes. Stimulation of insulin secretion results in the dephosphorylation of $\beta 2$ -syntrophin by an ocadaic acid-sensitive phosphatase that promotes the dissociation of ICA512 from $\beta 2$ -syntrophin and the subsequent release of these vesicles.

ABCA1 was found to reside on intracellular vesicles and the trafficking of these vesicles may be hindered by an association of ABCA1 to the cytoskeleton via β 2-syntrophin/utrophin. ABCA1 protein is induced during foam cell formation whereas similar amounts of ABCA1 were found to be associated with β 2-syntrophin/ utrophin in E-LDL-loaded macrophages and controls. This indicates that in cholesterol loaded macrophage induction of ABCA1 synthesis enlarges the pool of ABCA1 not linked to the cytoskeleton further supporting an inhibitory role of its β 2-syntrophin association. The C-terminal sequence (KESYV) of ABCA1 has already been described as a binding target for the PDZ domains syntrophin⁶⁵. ABC-transporters have different functions and can be classified according to their ATPase activity and Mg⁺⁺-dependent ATP binding capacity, either as active transporters (transport pumps) revealing a high intrinsic ATPase activity like MDR1, or as transport regulators, having only a low ATPase activity like SUR1 and CFTR. The C-terminus of CFTR has been shown to bind PSD95-Discs large-ZO1 (PDZ) domain proteins. Whereas, CFTR N-terminus interacts with syntaxin 1A and SNAP-23⁴⁴ known to form the N-ethylmaleimide-sensitive factor attachment protein receptor (SNARE) complex with synaptosomal-associated protein 25 (SNAP-25) and vesicle-associated membrane protein (VAMP). The SNARE protein syntaxin 1A is well described to directly bind to CFTR and to modulate its activity. Homologies in mechanism and structure between ABCA1 and CFTR led us to the assumption that ABCA1 may interact with syntaxins which we aimed to identify. The regulation of syntaxins 2, 3, 4, 6, 7, 8 and 13 was investigated in macrophages loaded with E-LDL and syntaxins 3, 6 and 13 were found induced in lipid-loaded cells. Since ABCA1 is similarly regulated by atherogenic lipoproteins the direct interaction of ABCA1 with syntaxin 3, 6 and 13 was analyzed. Syntaxin 13 turned out to directly associate with ABCA1 whereas syntaxin 3 and 6 failed to bind to ABCA1.

To gain further insights into the functionality, we silenced syntaxin 13 in PMA differentiated HL-60 using specific siRNA probes. This led to a decrease of both syntaxin 13 and ABCA1 protein expression and reduced apoA-I mediated choline-phospholipid

efflux, indicating that syntaxin 13 stabilizes ABCA1 expression and thereby regulates ABCA1 mediated lipid release. ABCA1 co-purifies with Lubrol WX rafts and apoA-I preferentially depletes lipids from these microdomains⁵⁴. Both flotillin-1, recently described to copurify with Triton X-114 rafts, and syntaxin 13 were demonstrated in this thesis to be also associated with Lubrol WX rafts. Although flotillin-1 expression is not regulated during macrophage differentiation or incubation with atherogenic lipoproteins, flotillin-1 was found to directly interact with ABCA1 and therefore, ABCA1 forms a complex with either syntaxin 13, or flotillin-1 or both. Besides being localized at the plasma membrane, detergent insoluble microdomains have been detected in phagosomes and endosomes and may control internalization pathways. ABCA1 was detected in endosomes¹³⁸ and may also associate with phagosomes. The phagosome proteome was recently described and flotillin-1 is highly abundant in this cellular compartment⁶⁴. Purification of phagosomal proteins using the method described by Desjardin et al.⁵⁰ and subsequent immunoblot analysis confirmed this finding and, in addition, identified ABCA1 as a phagosomal protein. Syntaxin 13 was also co-purified and co-immunoprecipitation revealed a direct association of phagosomal ABCA1 and syntaxin 13.

Endocytosis is increased in Tangier fibroblasts as a consequence of enhanced membrane inward bending related to the phosphatidylserine translocase function of ABCA1²⁰⁷. Type II phagocytosis occurs through sinking of the particles into the cell and inward bending of the membrane and therefore is also enhanced in cells with ABCA1 deficiency as was shown in this work. Recombinant expression of ABCA1 in Tangier fibroblasts normalized the uptake of phagobeads by Tangier cells providing additional evidence that ABCA1 is involved in phagocytosis. Furthermore the effect of type II phagocytosis includes the reorganization of the cytoskeleton and Rho A, and Rho A was found accumulated in Tangier fibroblasts. These findings are not contradictory to the observation that ABCA1 promotes the engulfment of apoptotic cells, a phagocytic process involving Fc γ -receptors and pseudopodia extension initiated by outward bending of the membrane (type I

phagocytosis). Syntaxin 13 is a soluble NEM-sensitive factor-attachment protein receptor (SNARE) protein, a family of proteins which mediates the coordinated fusion of membranes through the formation of four-helical bundle structure protein complexes¹⁸⁸. Overexpression of syntaxin 13 blocks CFTR trafficking through the non-conventional pathway from the ER to the Golgi indicating a role of syntaxin 13 in CFTR maturation²⁰⁴. Furthermore, syntaxin 13 functions in membrane fusion events during the recycling of plasma membrane proteins as well as in lysosome and endosome fusion with the phagosome⁴². These findings raise the possibility that syntaxin 13 plays a role in phago-lysosomal release of lipids in macrophages.

HDL is mainly internalized by a receptor-mediated pathway not associated with clathrin-coated pits¹⁶² and apoA-I was identified in phagosomes isolated with latex beads, further supporting an internalization pathway different from classical coated pit endocytosis. The identification of ABCA1 as a regulator of phagocytosis may indicate a crosstalk of phagocytic and endocytic pathways involved in ABCA1-mediated efflux with cholesterol deposited in late endosomes and lysosomes as the preferred source. The enhanced uptake of apoA-I by endocytic and phagocytic ingestion may also explain the increased catabolism of apoA-I in Tangier patients.

In conclusion, our results indicate that ABCA1 forms a heteromeric complex with syntaxin 13 and flotillin-1. This complex is already formed in differentiated monocyte-derived macrophages and does not require induction by E-LDL loading. Syntaxin 13 deficiency causes ABCA1 protein degradation and therefore syntaxin 13 may be important in ABCA1 maturation and vesicular transport. These findings indicate that besides retroendocytosis of apoA-I and HDL, the phagosomal and lysosomal compartment may be involved in ABCA1 dependent choline-phospholipid efflux.

The latter findings related to vesicular transport and fusion prompted us to search for the link between syntaxin 13 and intracellular lipid trafficking. This link was the syntaxin 13 interacting protein (pallidin). Huang et al⁸⁶ showed that mutations in pallidin in mice lead

to „pallid“ and „gunmetal“ phenotypes. The latter mutants are defective in a more downstream event of vesicle-trafficking: namely, vesicle-docking and fusion. These mice suffer from hypo pigmentation, lung fibrosis, kidney lysosomal enzyme elevation and prolonged bleeding. Other described mutations in mice like the „mocha“ and „pearl“ mice have platelet storage pool deficiency (SPD), these mutants have defects in the Ap-3 complex^{86,199}. In drosophila, mutations in the adapter related protein complex 3 (AP-3) as well as mutations in ABCG5 and ABCG8 (both half-size ABC transporters which interact to form the functional full-size) lead to changes in the eye color, due to trafficking disturbances in lysosomes and related organelles⁸⁸.

In humans these phenotypes refer to diseases called Hermansky-Pudlak syndrome (HPS) and Chediak-Higachi syndrome (CHS), autosomal recessive disorders which lead to storage defects resulting, among others, from defects in secretory lysosomes. This leads to pulmonary fibrosis and prolonged bleeding.

Biochemical and genetic evidence indicates that the HPS-associated genes encode components of at least 3 distinct protein complexes: the adapter complex AP-3; the HPS1/HPS4 complex; and BLOC-1 (biogenesis of lysosome-related organelles complex-1), consisting of the proteins encoded at 2 mouse HPS loci, pallid and muted, and at least 3 other unidentified proteins.

The AP-3 pathway has many constituents as shown in literature: ARL7⁵⁷, Syntaxin 13 and ABCA1¹⁰, Syntaxin 13-interacting protein (pallidin), Cdc42^{83,163} ABCG1/G2/G4 (which leads to mutations: white, brown and scarlet), HPS1-7:Hermansky-Pudlak-Syndrome complex, P2-Purinergic receptors and GIRKs (G-protein coupled inward rectifying K-channels).

ABCA1 interacts with syntaxin 13 which in turn is linked to pallidin the syntaxin 13 interacting protein, the latter is linked to bleeding disorders in mice. This suggested pattern would create a direct link between ABCA1 and congenital bleeding disorders.

Recent publications show evidence that HDL-deficiency in Tangier patients is related to impaired platelet activation, which in turn results from genetic defects in the AP-3 gene¹⁴¹. Lipoprotein analysis of sera from pallidin knock-out and pallidin wild type mice performed at our institute indicated that pallidin knock-out mice had less free cholesterol and less triglyceride compared to wild type mice. In addition, the composition of HDL revealed that pallidin knock-out mice had less sphingomyelin (SPM) and less phosphatidylcholine (PC). In the cellular membrane, phosphatidylserine (PS) and phosphatidylethanolamine (PE) are mainly located in the inner monolayer whereas the outer layer consists dominantly of the choline-containing phospholipids, phosphatidylcholine (PC) and sphingomyelin (SPM)

170

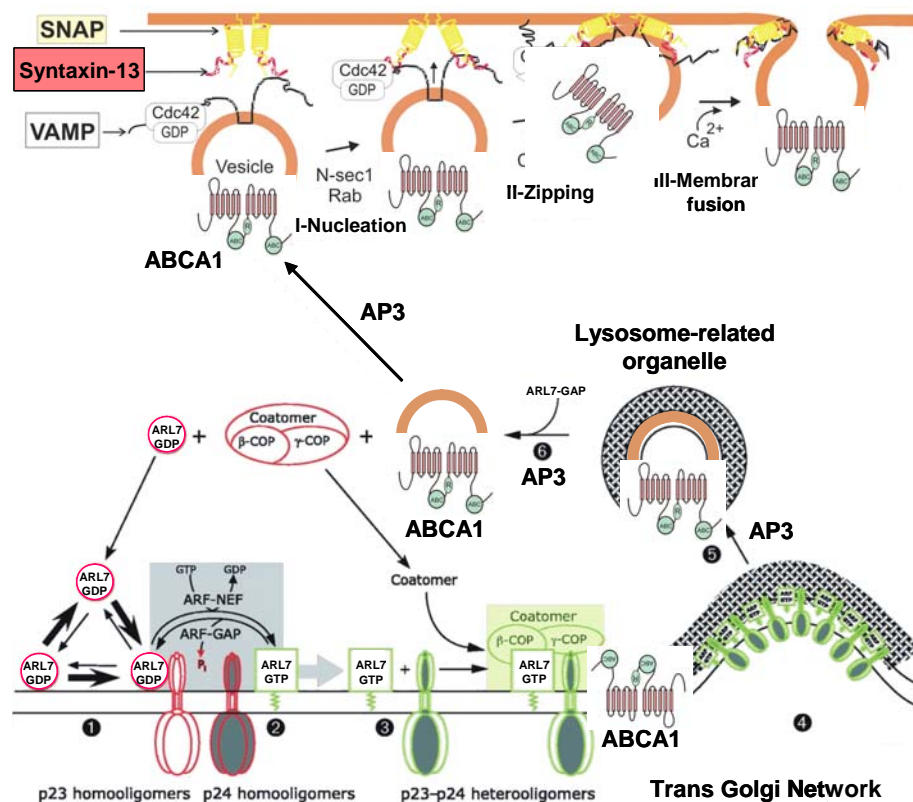


Figure 43: The relation between syntaxins and the lysosomal pathway. The AP-3 pathway has many constituents as shown in literature: ARL7⁵⁷, Syntaxin 13 and ABCA1¹⁰, Syntaxin 13-interacting protein (pallidin), Cdc42^{83,163} ABCG1/G2/G4 (which leads to mutations: white, brown and scarlet), HPS1-7:Hermansky-Pudlak-Syndrome complex, P2-Purinergic receptors and GIRKs (G-protein coupled inward rectifying K-channels).

An initial process in coagulation is the loss of membrane asymmetry and the redistribution of PS from the inner to the outer leaflet of the platelet plasma membrane ¹¹³. At least in monocytic cells, ABCA1 facilitates PS exofacial flipping ⁷⁴ and the high abundance of ABCA1 in platelets would suggest a similar action in thrombocytes.

Besides residing at the plasma membrane, ABCA1 is located in phagosomes and additional lysosome-related cellular compartments. A defect in lysosome-related compartments may impair the transport of ABCA1 to the cell membrane leading to loss of ABCA1-dependent PS flipping. This could eventually lead to impaired coagulation and prolonged bleeding in the pallidin mouse. Furthermore, cholesterol may be trapped in lysosomes due to defects in BLOC-1 and AP-3 pathway. This might explain reduced free cholesterol in the HDL fraction.

The gene expression profiling data presented in this study reveal that in human macrophages cholesterol influx and efflux is associated with the regulation of three major functional pathways of the cell: the nuclear compartment, the ribosomal complex and the ubiquitin proteasome pathway. Importantly, our results demonstrate differential regulation during E-LDL and Ox-LDL loading and further HDL₃ dependent unloading of these pathways in cells carrying the Apo E3/E3 genotype.

In Apo E3/E3 macrophages cholesterol efflux following E-LDL loading resulted in the synchronous upregulation of significant numbers of nuclear and ribosomal genes, while in HDL₃-dependent unloading of Ox-LDL loaded macrophages the genes were not regulated. These findings provide evidence for differential regulation of nuclear and ribosomal genes in macrophage cholesterol export according to the type of modified LDL used to mimic atherogenic cholesterol loading.

Nuclear and transcriptional genes were induced in HDL treated E-LDL foam cells but only minor regulatory response was detected in Ox-LDL loaded cells incubated with HDL₃.

Thus our data indicate that the export of E-LDL and Ox-LDL derived cholesterol involves clusters of inversely regulated nuclear, ribosomal and proteasomal networks suggesting

the involvement of distinct regulatory complexes in the cellular processing of either modified lipoprotein class. This is in agreement with our recent observation that E-LDL and Ox-LDL have a different impact on the cellular cholesterol and sphingolipid metabolism in macrophages (Paper accepted in Cytometry).

Cholesterol uptake by macrophages mediated by E-LDL and Ox-LDL resulted in the suppression of components of the nuclear, ribosomal and proteasomal networks. This effect occurred largely independent of whether E-LDL or Ox-LDL was used as a cholesterol source; this is in contrast to the inverse responses found during cholesterol export.

Together, our results (i) identify the nuclear compartment, the ribosome and the ubiquitin proteasome system as transcriptional regulatory complexes involved in the control of cholesterol trafficking in the cell and (ii) demonstrate a differential regulation of gene clusters by two different modified LDL types.

Among the nuclear genes that showed significant implication in cholesterol flux are the cyclins D1, D2, D3, E1, F and multiple components of the RNA polymerase II complex including the RNA polymerase II peptides A, E, F, H, I, and L, respectively. To date, little is known about the role of cholesterol within the nucleus. A recent report demonstrated that inhibition of cholesterol esterification in vascular smooth muscle cells, which induces their arrest in G1, is accompanied by down-regulation of cyclin D1 mRNA thus establishing a link between cholesterol metabolism and the control of cell cycle G1/S transition¹¹. Our finding that cholesterol export induces the concerted upregulation of the mRNAs of multiple cyclins strongly supports the existence of an interlink between the cell cycle and cholesterol trafficking. Recently, the presence of cholesterol has been demonstrated in chromatin and two fractions were identified, one soluble and another which is only extractable after SMase or proteinase K digestion³. Although initial data point to a role of intranuclear cholesterol in the control of DNA synthesis, no information is currently available whether there is a link between cholesterol and the RNA polymerase II

complex. The coordinate upregulation of the RNA polymerase II constituents A, E, F, H, I, and L in response to sustained cholesterol export establish for the first time such a functional interlink. It will be challenging to elucidate the molecular mechanisms that are implicated in this novel regulatory network.

The second intriguing finding of our study comes from the realization that cholesterol export influences the gene expression of a substantial portion of structural elements of the large and small ribosomal subunits. Coordinated expression of the ribosomal protein (RP) genes at the transcriptional level is a prerequisite for ensuring a roughly equimolar accumulation of ribosomal proteins. Transcriptional studies in rapidly proliferating cells indicated equivalent expression of RNA polymerases on three unlinked murine RP genes, consistent with the equal abundance of the corresponding mRNAs¹³⁰ suggesting that similar promoter strength and mRNA processing efficiency might provide a basis for the coordinated expression of RP genes. However, whether this concept applies to all RP genes or to distinctive subsets of genes is presently unclear. We found that a fraction of 65 out of the 85 known eukaryotic ribosomal proteins¹⁵⁰ were upregulated under conditions of cholesterol efflux. The regulation of the majority of the RPS and RPL genes (70%) during cholesterol flux provides initial evidence for the synchronization of the assembly of the ribosome complex on the gene regulatory level. It supports the assumption that the maintenance of the ribosome complex requires coordinate regulation of its structural components. Moreover, our data demonstrate a large scale regulatory impact on RP mRNA levels suggesting that cholesterol flux affects the availability of functional ribosomal complexes. Based on such a mechanism, cholesterol may thus indirectly control the cellular translation machinery.

The processing of lipids in macrophages occurs within the lysosome, and subsequent storage in cytoplasmic lipid droplets. Ox-LDL induces less cytoplasmic cholesteryl ester accumulation than E-LDL, a result of the chemical alterations during oxidation, leading to (i) conversion of a large proportion of cholesterol to oxysterols, and (ii) oxidation of the

fatty acyl group of LDL cholesteryl esters, rendering them resistant to lysosomal hydrolysis and trapping them within these organelles⁹⁴. But this is only the fact if mildly oxidized LDL is used and most of the lipoprotein cholesterol is intact, nevertheless, E-LDL yields higher amounts of cholesterol than does Ox-LDL this is due to cholesterol esterase treatment of E-LDL leading to higher amount of free cholesterol entering the cell when loaded with E-LDL, which is subsequently esterified by ACAT after leaving the lysosome.

Human scavenger receptor class B type II (SCARB2), which is a splice variant of SR-BI, is a lysosomal integral membrane glycoprotein which promotes cholesterol efflux¹³⁴, was found inversely regulated by E- and Ox-LDL. E-LDL load led to an increase but Ox-LDL load led to a decrease of expression, further deloading had inverse effects. This could indicate that SCARB2 may play a role in depletion of Ox-LDL but not E-LDL from the cell. In fact, further processing of Ox-LDL is different from processing of E-LDL and Ox-LDL is trapped in the lysosome, an assumption which may rely on the different regulation of the COP-I and COP-II machinery during loading of macrophages with different lipids.

E-LDL seemed to address fewer COP-I (responsible for trafficking from GOLGI to ER) and COP-II (responsible for ER to GOLGI trafficking) machinery genes, whereas Ox-LDL mainly regulated COP-II machinery genes.

On the other hand, ATP synthases were mainly upregulated during E-LDL but not Ox-LDL deload, this could be due to the increased amount of cholesterol in E-LDL loaded macrophages compared to Ox-LDL loaded macrophages, since HDL3 functions as a cholesterol acceptor resulting in ATP-dependent cholesterol efflux through ABCA1.

Taken together, the previously presented data suggest that the endocytic and exocytic pathway seems to be closely controlled by the concert of the following genes: ABCA1, ApoA1, ATP-synthase and SR-BI. ApoA1 interacts with and regulates the hydrolysis activity of α - β chains of the ATP-synthase which is a receptor for ApoE-rich HDL. Thus, the ATP-synthase either promotes the conversion of ADP to ATP or contrariwise. The presence of ATP either increases the influx by raising the pace of phagocytosis which is ATP-

dependent, or increases the activity of ABCA1 leading to increases efflux. The internal regulator of cholesterol homeostasis is NPC1 which controls the cholesterol transport intracellularly.

In conclusion, all the data raised by gene array technology hold a great scientific potential. Gene arrays can provide a broad overview on gene expression; also the transcriptional profiling can reveal patterns of gene expression which can be used to predict functional changes of the cell. Nevertheless, this data can not be adapted without verification since the technology still bears an amount of uncertainty derived from several factors including cross-interactions, inaccurate oligonucleotide sequences or SNPs, which can lead to an improper annealing and a false result. The chip-technology is, however, a very powerful tool in predicting regulations of pathways and establishing links between various cellular pathways and foreseeing tendencies in the expression of genes, which can help to relate gene expression to certain diseases.

VII. REFERENCES

- (1) Acton S, Rigotti A, Landschulz KT et al. Identification of scavenger receptor SR-BI as a high density lipoprotein receptor. *Science*. 1996;271:518-520.
- (2) Aden DP, Fogel A, Plotkin S, Damjanov I, Knowles BB. Controlled synthesis of HBsAg in a differentiated human liver carcinoma-derived cell line. *Nature*. 1979;282:615-616.
- (3) Albi E, Magni MV. The presence and the role of chromatin cholesterol in rat liver regeneration. *J Hepatol*. 2002;36:395-400.
- (4) Albrecht C, McVey JH, Elliott JI et al. A novel missense mutation in ABCA1 results in altered protein trafficking and reduced phosphatidylserine translocation in a patient with Scott syndrome. *Blood*. 2005.
- (5) Allikmets R. Simple and complex ABCR: genetic predisposition to retinal disease. *Am J Hum Genet*. 2000;67:793-799.
- (6) Anderson RG, Goldstein JL, Brown MS. A mutation that impairs the ability of lipoprotein receptors to localise in coated pits on the cell surface of human fibroblasts. *Nature*. 1977;270:695-699.
- (7) Asztalos BF, Brousseau ME, McNamara JR et al. Subpopulations of high density lipoproteins in homozygous and heterozygous Tangier disease. *Atherosclerosis*. 2001;156:217-225.
- (8) Aviram M, Bierman EL, Oram JF. High density lipoprotein stimulates sterol translocation between intracellular and plasma membrane pools in human monocyte-derived macrophages. *J Lipid Res*. 1989;30:65-76.
- (9) Band AM, Ali H, Vartiainen MK et al. Endogenous plasma membrane t-SNARE syntaxin 4 is present in rab11 positive endosomal membranes and associates with cortical actin cytoskeleton. *FEBS Lett*. 2002;531:513-519.
- (10) Bared SM, Buechler C, Boettcher A et al. Association of ABCA1 with Syntaxin 13 and Flotillin-1 and Enhanced Phagocytosis in Tangier Cells. *Mol Biol Cell*. 2004.

- (11) Batetta B, Mulas MF, Sanna F et al. Role of cholesterol ester pathway in the control of cell cycle in human aortic smooth muscle cells. *FASEB J.* 2003;17:746-748.
- (12) Beentjes JA, van Tol A, Sluiter WJ, Dullaart RP. Low plasma lecithin:cholesterol acyltransferase and lipid transfer protein activities in growth hormone deficient and acromegalic men: role in altered high density lipoproteins. *Atherosclerosis.* 2000;153:491-498.
- (13) Beisiegel U, Weber W, Havinga JR et al. Apolipoprotein E-binding proteins isolated from dog and human liver. *Arteriosclerosis.* 1988;8:288-297.
- (14) Bezprozvanny I, Maximov A. PDZ domains: More than just a glue. *Proc Natl Acad Sci U S A.* 2001;98:787-789.
- (15) Bhakdi S. [An alternative hypothesis of the pathogenesis of atherosclerosis]. *Herz.* 1998;23:163-167.
- (16) Bhakdi S, Dorweiler B, Kirchmann R et al. On the pathogenesis of atherosclerosis: enzymatic transformation of human low density lipoprotein to an atherogenic moiety. *J Exp Med.* 1995;182:1959-1971.
- (17) Bhattacharya M, Babwah AV, Ferguson SS. Small GTP-binding protein-coupled receptors. *Biochem Soc Trans.* 2004;32:1040-1044.
- (18) Blanchette-Mackie EJ, Dwyer NK, Amende LM et al. Type-C Niemann-Pick disease: low density lipoprotein uptake is associated with premature cholesterol accumulation in the Golgi complex and excessive cholesterol storage in lysosomes. *Proc Natl Acad Sci U S A.* 1988;85:8022-8026.
- (19) Blanchette-Mackie EJ, Scow RO. Movement of lipolytic products to mitochondria in brown adipose tissue of young rats: an electron microscope study. *J Lipid Res.* 1983;24:229-244.
- (20) BLIGH EG, DYER WJ. A rapid method of total lipid extraction and purification. *Can J Biochem Physiol.* 1959;37:911-917.
- (21) Bodzioch M, Orso E, Klucken J et al. The gene encoding ATP-binding cassette transporter 1 is mutated in Tangier disease. *Nat Genet.* 1999;22:347-351.

- (22) Borst P, Zelcer N, van Helvoort A. ABC transporters in lipid transport. *Biochim Biophys Acta*. 2000;1486:128-144.
- (23) Brady RO, Filling-Katz MR, Barton NW, Pentchev PG. Niemann-Pick disease types C and D. *Neurol Clin*. 1989;7:75-88.
- (24) Brooks-Wilson A, Marcil M, Clee SM et al. Mutations in ABC1 in Tangier disease and familial high-density lipoprotein deficiency. *Nat Genet*. 1999;22:336-345.
- (25) Brown MS, Goldstein JL. A receptor-mediated pathway for cholesterol homeostasis. *Science*. 1986;232:34-47.
- (26) Brunet S, Thibault P, Gagnon E et al. Organelle proteomics: looking at less to see more. *Trends Cell Biol*. 2003;13:629-638.
- (27) Buechler C, Boettcher A, Bared SM, Probst MC, Schmitz G. The carboxyterminus of the ATP-binding cassette transporter A1 interacts with a beta2-syntrophin/utrophin complex. *Biochem Biophys Res Commun*. 2002;293:759-765.
- (28) Cardoso LE, Mourao PA. Glycosaminoglycan fractions from human arteries presenting diverse susceptibilities to atherosclerosis have different binding affinities to plasma LDL. *Arterioscler Thromb*. 1994;14:115-124.
- (29) Carstea ED, Morris JA, Coleman KG et al. Niemann-Pick C1 disease gene: homology to mediators of cholesterol homeostasis. *Science*. 1997;277:228-231.
- (30) Carstea ED, Polymeropoulos MH, Parker CC et al. Linkage of Niemann-Pick disease type C to human chromosome 18. *Proc Natl Acad Sci U S A*. 1993;90:2002-2004.
- (31) Castellano F, Chavrier P, Caron E. Actin dynamics during phagocytosis. *Semin Immunol*. 2001;13:347-355.
- (32) Cerione RA. Cdc42: new roads to travel. *Trends Cell Biol*. 2004;14:127-132.
- (33) Chambenoit O, Hamon Y, Marguet D et al. Specific docking of apolipoprotein A-I at the cell surface requires a functional ABCA1 transporter. *J Biol Chem*. 2001;276:9955-9960.

- (34) Chapman ER, An S, Barton N, Jahn R. SNAP-25, a t-SNARE which binds to both syntaxin and synaptobrevin via domains that may form coiled coils. *J Biol Chem.* 1994;269:27427-27432.
- (35) Chen W, Sun Y, Welch C et al. Preferential ATP-binding cassette transporter A1-mediated cholesterol efflux from late endosomes/lysosomes. *J Biol Chem.* 2001;276:43564-43569.
- (36) Chen W, Wang N, Tall AR. A PEST deletion mutant of ABCA1 shows impaired internalization and defective cholesterol efflux from late endosomes. *J Biol Chem.* 2005.
- (37) Choi HY, Karten B, Chan T et al. Impaired ABCA1-dependent lipid efflux and hypoalphalipoproteinemia in human Niemann-Pick type C disease. *J Biol Chem.* 2003;278:32569-32577.
- (38) Chou SF, Chen HL, Lu SC. Up-regulation of human deoxyribonuclease II gene expression during myelomonocytic differentiation of HL-60 and THP-1 cells. *Biochem Biophys Res Commun.* 2002;296:48-53.
- (39) Christoforidis S, McBride HM, Burgoyne RD, Zerial M. The Rab5 effector EEA1 is a core component of endosome docking. *Nature.* 1999;397:621-625.
- (40) Cibulsky SM, Fei H, Levitan IB. Syntaxin-1A binds to and modulates the Slo calcium-activated potassium channel via an interaction that excludes syntaxin binding to calcium channels. *J Neurophysiol.* 2004.
- (41) Cohn JA, Friedman KJ, Noone PG et al. Relation between mutations of the cystic fibrosis gene and idiopathic pancreatitis. *N Engl J Med.* 1998;339:653-658.
- (42) Collins RF, Schreiber AD, Grinstein S, Trimble WS. Syntaxins 13 and 7 function at distinct steps during phagocytosis. *J Immunol.* 2002;169:3250-3256.
- (43) Collins SJ, Gallo RC, Gallagher RE. Continuous growth and differentiation of human myeloid leukaemic cells in suspension culture. *Nature.* 1977;270:347-349.
- (44) Cormet-Boyaka E, Di A, Chang SY et al. CFTR chloride channels are regulated by a SNAP-23/syntaxin 1A complex. *Proc Natl Acad Sci U S A.* 2002;99:12477-12482.

- (45) Cushing SD, Berliner JA, Valente AJ et al. Minimally modified low density lipoprotein induces monocyte chemotactic protein 1 in human endothelial cells and smooth muscle cells. *Proc Natl Acad Sci U S A*. 1990;87:5134-5138.
- (46) Davies JP, Chen FW, Ioannou YA. Transmembrane molecular pump activity of Niemann-Pick C1 protein. *Science*. 2000;290:2295-2298.
- (47) de Villiers WJ, Smart EJ. Macrophage scavenger receptors and foam cell formation. *J Leukoc Biol*. 1999;66:740-746.
- (48) De Vree JM, Jacquemin E, Sturm E et al. Mutations in the MDR3 gene cause progressive familial intrahepatic cholestasis. *Proc Natl Acad Sci U S A*. 1998;95:282-287.
- (49) Dermine JF, Duclos S, Garin J et al. Flotillin-1-enriched lipid raft domains accumulate on maturing phagosomes. *J Biol Chem*. 2001;276:18507-18512.
- (50) Desjardins M, Huber LA, Parton RG, Griffiths G. Biogenesis of phagolysosomes proceeds through a sequential series of interactions with the endocytic apparatus. *J Cell Biol*. 1994;124:677-688.
- (51) Deuticke B. [Passive transport mechanisms in the erythrocyte membrane]. *Arzneimittelforschung*. 1972;22:2043-2049.
- (52) Diederich W, Orso E, Drobnik W, Schmitz G. Apolipoprotein AI and HDL(3) inhibit spreading of primary human monocytes through a mechanism that involves cholesterol depletion and regulation of CDC42. *Atherosclerosis*. 2001;159:313-324.
- (53) Doige CA, Ames GF. ATP-dependent transport systems in bacteria and humans: relevance to cystic fibrosis and multidrug resistance. *Annu Rev Microbiol*. 1993;47:291-319.
- (54) Drobnik W, Borsukova H, Bottcher A et al. Apo AI/ABCA1-dependent and HDL3-mediated lipid efflux from compositionally distinct cholesterol-based microdomains. *Traffic*. 2002;3:268-278.
- (55) Duff GW, Atkins E. The detection of endotoxin by in vitro production of endogenous pyrogen: comparison with limulus amebocyte lysate gelation. *J Immunol Methods*. 1982;52:323-331.

- (56) Edfeldt K, Swedenborg J, Hansson GK, Yan ZQ. Expression of toll-like receptors in human atherosclerotic lesions: a possible pathway for plaque activation. *Circulation*. 2002;105:1158-1161.
- (57) Engel T, Lueken A, Bode G et al. ADP-ribosylation factor (ARF)-like 7 (ARL7) is induced by cholesterol loading and participates in apolipoprotein AI-dependent cholesterol export. *FEBS Lett*. 2004;566:241-246.
- (58) Falcone DJ, Hajjar DP, Minick CR. Lipoprotein and albumin accumulation in reendothelialized and deendothelialized aorta. *Am J Pathol*. 1984;114:112-120.
- (59) Fielding CJ, Fielding PE. Intracellular cholesterol transport. *J Lipid Res*. 1997;38:1503-1521.
- (60) Fields S, Sternglanz R. The two-hybrid system: an assay for protein-protein interactions. *Trends Genet*. 1994;10:286-292.
- (61) Fitzgerald ML, Morris AL, Rhee JS et al. Naturally occurring mutations in the largest extracellular loops of ABCA1 can disrupt its direct interaction with apolipoprotein A-I. *J Biol Chem*. 2002;277:33178-33187.
- (62) Galle J, Heinloth A, Wanner C, Heermeier K. Dual effect of oxidized LDL on cell cycle in human endothelial cells through oxidative stress. *Kidney Int Suppl*. 2001;78:S120-S123.
- (63) Garcia A, Barbaras R, Collet X et al. High-density lipoprotein 3 receptor-dependent endocytosis pathway in a human hepatoma cell line (HepG2). *Biochemistry*. 1996;35:13064-13071.
- (64) Garin J, Diez R, Kieffer S et al. The phagosome proteome: insight into phagosome functions. *J Cell Biol*. 2001;152:165-180.
- (65) Gee SH, Quenneville S, Lombardo CR, Chabot J. Single-amino acid substitutions alter the specificity and affinity of PDZ domains for their ligands. *Biochemistry*. 2000;39:14638-14646.
- (66) Glass C, Pittman RC, Weinstein DB, Steinberg D. Dissociation of tissue uptake of cholesterol ester from that of apoprotein A-I of rat plasma high density lipoprotein:

selective delivery of cholesterol ester to liver, adrenal, and gonad. *Proc Natl Acad Sci U S A.* 1983;80:5435-5439.

(67) Goldstein JL, Anderson RG, Brown MS. Coated pits, coated vesicles, and receptor-mediated endocytosis. *Nature.* 1979;279:679-685.

(68) Goldstein JL, Ho YK, Basu SK, Brown MS. Binding site on macrophages that mediates uptake and degradation of acetylated low density lipoprotein, producing massive cholesterol deposition. *Proc Natl Acad Sci U S A.* 1979;76:333-337.

(69) Gotto AM, Jr., Pownall HJ, Havel RJ. Introduction to the plasma lipoproteins. *Methods Enzymol.* 1986;128:3-41.

(70) Greene DJ, Skeggs JW, Morton RE. Elevated triglyceride content diminishes the capacity of high density lipoprotein to deliver cholesteryl esters via the scavenger receptor class B type I (SR-BI). *J Biol Chem.* 2001;276:4804-4811.

(71) Greenspan P, St Clair RW. Retroendocytosis of low density lipoprotein. Effect of lysosomal inhibitors on the release of undegraded ¹²⁵I-low density lipoprotein of altered composition from skin fibroblasts in culture. *J Biol Chem.* 1984;259:1703-1713.

(72) Guendouzi K, Collet X, Perret B, Chap H, Barbaras R. Remnant high density lipoprotein₂ particles produced by hepatic lipase display high-affinity binding and increased endocytosis into a human hepatoma cell line (HEPG2). *Biochemistry.* 1998;37:14974-14980.

(73) Hackam DJ, Rotstein OD, Bennett MK et al. Characterization and subcellular localization of target membrane soluble NSF attachment protein receptors (t-SNAREs) in macrophages. Syntaxins 2, 3, and 4 are present on phagosomal membranes. *J Immunol.* 1996;156:4377-4383.

(74) Hamon Y, Broccardo C, Chambenoit O et al. ABC1 promotes engulfment of apoptotic cells and transbilayer redistribution of phosphatidylserine. *Nat Cell Biol.* 2000;2:399-406.

(75) Hamon Y, Chambenoit O, Chimini G. ABCA1 and the engulfment of apoptotic cells. *Biochim Biophys Acta.* 2002;1585:64-71.

- (76) Han J, Hajjar DP, Febbraio M, Nicholson AC. Native and modified low density lipoproteins increase the functional expression of the macrophage class B scavenger receptor, CD36. *J Biol Chem.* 1997;272:21654-21659.
- (77) Han SR, Momeni A, Strach K et al. Enzymatically modified LDL induces cathepsin H in human monocytes: potential relevance in early atherogenesis. *Arterioscler Thromb Vasc Biol.* 2003;23:661-667.
- (78) Harder T, Kellner R, Parton RG, Gruenberg J. Specific release of membrane-bound annexin II and cortical cytoskeletal elements by sequestration of membrane cholesterol. *Mol Biol Cell.* 1997;8:533-545.
- (79) Haynes MP, Phillips MC, Rothblat GH. Efflux of cholesterol from different cellular pools. *Biochemistry.* 2000;39:4508-4517.
- (80) Heeren J, Grewal T, Laatsch A et al. Recycling of apoprotein E is associated with cholesterol efflux and high density lipoprotein internalization. *J Biol Chem.* 2003;278:14370-14378.
- (81) Henriksen T, Mahoney EM, Steinberg D. Enhanced macrophage degradation of low density lipoprotein previously incubated with cultured endothelial cells: recognition by receptors for acetylated low density lipoproteins. *Proc Natl Acad Sci U S A.* 1981;78:6499-6503.
- (82) Herz J, Hamann U, Rogne S et al. Surface location and high affinity for calcium of a 500-kd liver membrane protein closely related to the LDL-receptor suggest a physiological role as lipoprotein receptor. *EMBO J.* 1988;7:4119-4127.
- (83) Hirano K, Matsuura F, Tsukamoto K et al. Decreased expression of a member of the Rho GTPase family, Cdc42Hs, in cells from Tangier disease - the small G protein may play a role in cholesterol efflux. *FEBS Lett.* 2000;484:275-279.
- (84) Holtta-Vuori M, Tanhuanpaa K, Mobius W, Somerharju P, Ikonen E. Modulation of cellular cholesterol transport and homeostasis by Rab11. *Mol Biol Cell.* 2002;13:3107-3122.
- (85) Hsu SC, TerBush D, Abraham M, Guo W. The exocyst complex in polarized exocytosis. *Int Rev Cytol.* 2004;233:243-265.

- (86) Huang L, Kuo YM, Gitschier J. The pallid gene encodes a novel, syntaxin 13-interacting protein involved in platelet storage pool deficiency. *Nat Genet.* 1999;23:329-332.
- (87) Hueber AO, Zornig M, Bernard AM, Chautan M, Evan G. A dominant negative Fas-associated death domain protein mutant inhibits proliferation and leads to impaired calcium mobilization in both T-cells and fibroblasts. *J Biol Chem.* 2000;275:10453-10462.
- (88) Huizing M, Gahl WA. Disorders of vesicles of lysosomal lineage: the Hermansky-Pudlak syndromes. *Curr Mol Med.* 2002;2:451-467.
- (89) Hurt-Camejo E, Camejo G, Rosengren B et al. Effect of arterial proteoglycans and glycosaminoglycans on low density lipoprotein oxidation and its uptake by human macrophages and arterial smooth muscle cells. *Arterioscler Thromb.* 1992;12:569-583.
- (90) Hurt-Camejo E, Olsson U, Wiklund O, Bondjers G, Camejo G. Cellular consequences of the association of apoB lipoproteins with proteoglycans. Potential contribution to atherogenesis. *Arterioscler Thromb Vasc Biol.* 1997;17:1011-1017.
- (91) Hussain MM, Strickland DK, Bakillah A. The mammalian low-density lipoprotein receptor family. *Annu Rev Nutr.* 1999;19:141-172.
- (92) Ioannou YA. The structure and function of the Niemann-Pick C1 protein. *Mol Genet Metab.* 2000;71:175-181.
- (93) Ishibashi S, Goldstein JL, Brown MS, Herz J, Burns DK. Massive xanthomatosis and atherosclerosis in cholesterol-fed low density lipoprotein receptor-negative mice. *J Clin Invest.* 1994;93:1885-1893.
- (94) Jessup W, Wilson P, Gaus K, Kritharides L. Oxidized lipoproteins and macrophages. *Vascul Pharmacol.* 2002;38:239-248.
- (95) Jian B, Llera-Moya M, Ji Y et al. Scavenger receptor class B type I as a mediator of cellular cholesterol efflux to lipoproteins and phospholipid acceptors. *J Biol Chem.* 1998;273:5599-5606.

- (96) Kaminski WE, Orso E, Diederich W et al. Identification of a novel human sterol-sensitive ATP-binding cassette transporter (ABCA7). *Biochem Biophys Res Commun.* 2000;273:532-538.
- (97) Kaminski WE, Piehler A, Pullmann K et al. Complete coding sequence, promoter region, and genomic structure of the human ABCA2 gene and evidence for sterol-dependent regulation in macrophages. *Biochem Biophys Res Commun.* 2001;281:249-258.
- (98) Kaminski WE, Piehler A, Schmitz G. Genomic organization of the human cholesterol-responsive ABC transporter ABCA7: tandem linkage with the minor histocompatibility antigen HA-1 gene. *Biochem Biophys Res Commun.* 2000;278:782-789.
- (99) Kaminski WE, Wenzel JJ, Piehler A, Langmann T, Schmitz G. ABCA6, a novel subclass ABC transporter. *Biochem Biophys Res Commun.* 2001;285:1295-1301.
- (100) Kapinsky M, Torzewski M, Buchler C et al. Enzymatically degraded LDL preferentially binds to CD14(high) CD16(+) monocytes and induces foam cell formation mediated only in part by the class B scavenger-receptor CD36. *Arterioscler Thromb Vasc Biol.* 2001;21:1004-1010.
- (101) Kiechl S, Wiedermann CJ, Willeit J. Toll-like receptor 4 and atherogenesis. *Ann Med.* 2003;35:164-171.
- (102) Kierszenbaum AL. Fusion of membranes during the acrosome reaction: a tale of two SNAREs. *Mol Reprod Dev.* 2000;57:309-310.
- (103) Kirchhoff C, Osterhoff C, Young L. Molecular cloning and characterization of HE1, a major secretory protein of the human epididymis. *Biol Reprod.* 1996;54:847-856.
- (104) Klucken J, Buchler C, Orso E et al. ABCG1 (ABC8), The human homolog of the *Drosophila* white gene, is a regulator of macrophage cholesterol and phospholipid transport. *Proc Natl Acad Sci U S A.* 2000;97:817-822.
- (105) König J, Nies AT, Cui Y, Leier I, Keppler D. Conjugate export pumps of the multidrug resistance protein (MRP) family: localization, substrate specificity, and MRP2-mediated drug resistance. *Biochim Biophys Acta.* 1999;1461:377-394.

- (106) Kramer W, Girbig F, Corsiero D et al. Aminopeptidase N (CD13) is a molecular target of the cholesterol absorption inhibitor ezetimibe in the enterocyte brush border membrane. *J Biol Chem.* 2005;280:1306-1320.
- (107) Krieger M, Kozarsky K. Influence of the HDL receptor SR-BI on atherosclerosis. *Curr Opin Lipidol.* 1999;10:491-497.
- (108) Kritharides L, Christian A, Stoudt G, Morel D, Rothblat GH. Cholesterol metabolism and efflux in human THP-1 macrophages. *Arterioscler Thromb Vasc Biol.* 1998;18:1589-1599.
- (109) Kruth HS. Lipoprotein cholesterol and atherosclerosis. *Curr Mol Med.* 2001;1:633-653.
- (110) Kruth HS. Sequestration of aggregated low-density lipoproteins by macrophages. *Curr Opin Lipidol.* 2002;13:483-488.
- (111) Kruth HS, Skarlatos SI, Gaynor PM, Gamble W. Production of cholesterol-enriched nascent high density lipoproteins by human monocyte-derived macrophages is a mechanism that contributes to macrophage cholesterol efflux. *J Biol Chem.* 1994;269:24511-24518.
- (112) Kruth HS, Zhang WY, Skarlatos SI, Chao FF. Apolipoprotein B stimulates formation of monocyte-macrophage surface-connected compartments and mediates uptake of low density lipoprotein-derived liposomes into these compartments. *J Biol Chem.* 1999;274:7495-7500.
- (113) Kunzelmann-Marche C, Freyssinet JM, Martinez MC. Regulation of phosphatidylserine transbilayer redistribution by store-operated Ca²⁺ entry: role of actin cytoskeleton. *J Biol Chem.* 2001;276:5134-5139.
- (114) Kurzchalia TV, Parton RG. Membrane microdomains and caveolae. *Curr Opin Cell Biol.* 1999;11:424-431.
- (115) Langmann T, Klucken J, Reil M et al. Molecular cloning of the human ATP-binding cassette transporter 1 (hABC1): evidence for sterol-dependent regulation in macrophages. *Biochem Biophys Res Commun.* 1999;257:29-33.

- (116) Lee MH, Lu K, Patel SB. Genetic basis of sitosterolemia. *Curr Opin Lipidol.* 2001;12:141-149.
- (117) Lefevre C, Audebert S, Jobard F et al. Mutations in the transporter ABCA12 are associated with lamellar ichthyosis type 2. *Hum Mol Genet.* 2003;12:2369-2378.
- (118) Liebisch G, Lieser B, Rathenberg J, Drobnik W, Schmitz G. High-throughput quantification of phosphatidylcholine and sphingomyelin by electrospray ionization tandem mass spectrometry coupled with isotope correction algorithm. *Biochim Biophys Acta.* 2004;1686:108-117.
- (119) Lindgren V, Luskey KL, Russell DW, Francke U. Human genes involved in cholesterol metabolism: chromosomal mapping of the loci for the low density lipoprotein receptor and 3-hydroxy-3-methylglutaryl-coenzyme A reductase with cDNA probes. *Proc Natl Acad Sci U S A.* 1985;82:8567-8571.
- (120) Lindstedt L, Lee M, Oorni K, Bromme D, Kovanen PT. Cathepsins F and S block HDL3-induced cholesterol efflux from macrophage foam cells. *Biochem Biophys Res Commun.* 2003;312:1019-1024.
- (121) Liscum L, Faust JR. Low density lipoprotein (LDL)-mediated suppression of cholesterol synthesis and LDL uptake is defective in Niemann-Pick type C fibroblasts. *J Biol Chem.* 1987;262:17002-17008.
- (122) Liscum L, Klansek JJ. Niemann-Pick disease type C. *Curr Opin Lipidol.* 1998;9:131-135.
- (123) Liu J, Shapiro JI. Endocytosis and signal transduction: basic science update. *Biol Res Nurs.* 2003;5:117-128.
- (124) LOWRY OH, ROSEBROUGH NJ, FARR AL, RANDALL RJ. Protein measurement with the Folin phenol reagent. *J Biol Chem.* 1951;193:265-275.
- (125) Martina JA, Moriyama K, Bonifacino JS. BLOC-3, a protein complex containing the Hermansky-Pudlak syndrome gene products HPS1 and HPS4. *J Biol Chem.* 2003;278:29376-29384.

- (126) Martinez LO, Agerholm-Larsen B, Wang N, Chen W, Tall AR. Phosphorylation of a pest sequence in ABCA1 promotes calpain degradation and is reversed by ApoA-I. *J Biol Chem.* 2003;278:37368-37374.
- (127) Martinez LO, Jacquet S, Esteve JP et al. Ectopic beta-chain of ATP synthase is an apolipoprotein A-I receptor in hepatic HDL endocytosis. *Nature.* 2003;421:75-79.
- (128) Martinez LO, Jacquet S, Terce F et al. New insight on the molecular mechanisms of high-density lipoprotein cellular interactions. *Cell Mol Life Sci.* 2004;61:2343-2360.
- (129) McBride HM, Rybin V, Murphy C et al. Oligomeric complexes link Rab5 effectors with NSF and drive membrane fusion via interactions between EEA1 and syntaxin 13. *Cell.* 1999;98:377-386.
- (130) Meyuhas O, Perry RP. Construction and identification of cDNA clones for mouse ribosomal proteins: application for the study of r-protein gene expression. *Gene.* 1980;10:113-129.
- (131) Mora S, Pessin JE. An adipocentric view of signaling and intracellular trafficking. *Diabetes Metab Res Rev.* 2002;18:345-356.
- (132) Morel DW, Hessler JR, Chisolm GM. Low density lipoprotein cytotoxicity induced by free radical peroxidation of lipid. *J Lipid Res.* 1983;24:1070-1076.
- (133) Mosser J, Lutz Y, Stoeckel ME et al. The gene responsible for adrenoleukodystrophy encodes a peroxisomal membrane protein. *Hum Mol Genet.* 1994;3:265-271.
- (134) Mulcahy JV, Riddell DR, Owen JS. Human scavenger receptor class B type II (SR-BII) and cellular cholesterol efflux. *Biochem J.* 2004;377:741-747.
- (135) Nakatsu F, Ohno H. Adaptor protein complexes as the key regulators of protein sorting in the post-Golgi network. *Cell Struct Funct.* 2003;28:419-429.
- (136) Napoli C, D'Armiento FP, Mancini FP et al. Fatty streak formation occurs in human fetal aortas and is greatly enhanced by maternal hypercholesterolemia. Intimal accumulation of low density lipoprotein and its oxidation precede monocyte recruitment into early atherosclerotic lesions. *J Clin Invest.* 1997;100:2680-2690.

- (137) Naureckiene S, Sleat DE, Lackland H et al. Identification of HE1 as the second gene of Niemann-Pick C disease. *Science*. 2000;290:2298-2301.
- (138) Neufeld EB, Remaley AT, Demosky SJ et al. Cellular localization and trafficking of the human ABCA1 transporter. *J Biol Chem*. 2001;276:27584-27590.
- (139) Nickel W, Brugger B, Wieland FT. Protein and lipid sorting between the endoplasmic reticulum and the Golgi complex. *Semin Cell Dev Biol*. 1998;9:493-501.
- (140) Nielsen LB, Nordestgaard BG, Stender S, Kjeldsen K. Aortic permeability to LDL as a predictor of aortic cholesterol accumulation in cholesterol-fed rabbits. *Arterioscler Thromb*. 1992;12:1402-1409.
- (141) Nofer JR, Herminghaus G, Brodde M et al. Impaired platelet activation in familial high density lipoprotein deficiency (Tangier disease). *J Biol Chem*. 2004;279:34032-34037.
- (142) Norkin LC. Simian virus 40 infection via MHC class I molecules and caveolae. *Immunol Rev*. 1999;168:13-22.
- (143) Ogura M, Morishima Y, Ohno R et al. Establishment of a novel human megakaryoblastic leukemia cell line, MEG-01, with positive Philadelphia chromosome. *Blood*. 1985;66:1384-1392.
- (144) Okamura N, Kiuchi S, Tamba M et al. A porcine homolog of the major secretory protein of human epididymis, HE1, specifically binds cholesterol. *Biochim Biophys Acta*. 1999;1438:377-387.
- (145) Oram JF, Johnson CJ, Brown TA. Interaction of high density lipoprotein with its receptor on cultured fibroblasts and macrophages. Evidence for reversible binding at the cell surface without internalization. *J Biol Chem*. 1987;262:2405-2410.
- (146) Oram JF, Lawn RM, Garvin MR, Wade DP. ABCA1 is the cAMP-inducible apolipoprotein receptor that mediates cholesterol secretion from macrophages. *J Biol Chem*. 2000;275:34508-34511.
- (147) Peng Y, Akmentin W, Connelly MA et al. Scavenger receptor BI (SR-BI) clustered on microvillar extensions suggests that this plasma membrane domain is a

way station for cholesterol trafficking between cells and high-density lipoprotein. *Mol Biol Cell*. 2004;15:384-396.

(148) Pentchev PG, Blanchette-Mackie EJ, Liscum L. Biological implications of the Niemann-Pick C mutation. *Subcell Biochem*. 1997;28:437-451.

(149) Pentchev PG, Kruth HS, Comly ME et al. Type C Niemann-Pick disease. A parallel loss of regulatory responses in both the uptake and esterification of low density lipoprotein-derived cholesterol in cultured fibroblasts. *J Biol Chem*. 1986;261:16775-16780.

(150) Perry RP. The architecture of mammalian ribosomal protein promoters. *BMC Evol Biol*. 2005;5:15.

(151) Peters MF, Adams ME, Froehner SC. Differential association of syntrophin pairs with the dystrophin complex. *J Cell Biol*. 1997;138:81-93.

(152) Rapoport I, Miyazaki M, Boll W et al. Regulatory interactions in the recognition of endocytic sorting signals by AP-2 complexes. *EMBO J*. 1997;16:2240-2250.

(153) Riento K, Galli T, Jansson S et al. Interaction of Munc-18-2 with syntaxin 3 controls the association of apical SNAREs in epithelial cells. *J Cell Sci*. 1998;111 (Pt 17):2681-2688.

(154) Ritter M, Buechler C, Kapinsky M, Schmitz G. Interaction of CD163 with the regulatory subunit of casein kinase II (CKII) and dependence of CD163 signaling on CKII and protein kinase C. *Eur J Immunol*. 2001;31:999-1009.

(155) Ross R. Atherosclerosis is an inflammatory disease. *Am Heart J*. 1999;138:S419-S420.

(156) Ross R. Atherosclerosis--an inflammatory disease. *N Engl J Med*. 1999;340:115-126.

(157) Rothblat GH, Llera-Moya M, Atger V et al. Cell cholesterol efflux: integration of old and new observations provides new insights. *J Lipid Res*. 1999;40:781-796.

(158) Rothman JE, Wieland FT. Protein sorting by transport vesicles. *Science*. 1996;272:227-234.

- (159) Rust S, Rosier M, Funke H et al. Tangier disease is caused by mutations in the gene encoding ATP-binding cassette transporter 1. *Nat Genet.* 1999;22:352-355.
- (160) Schmidt A, Hannah MJ, Huttner WB. Synaptic-like microvesicles of neuroendocrine cells originate from a novel compartment that is continuous with the plasma membrane and devoid of transferrin receptor. *J Cell Biol.* 1997;137:445-458.
- (161) Schmidt A, Wolde M, Thiele C et al. Endophilin I mediates synaptic vesicle formation by transfer of arachidonate to lysophosphatidic acid. *Nature.* 1999;401:133-141.
- (162) Schmitz G, Assmann G, Robenek H, Brennhausen B. Tangier disease: a disorder of intracellular membrane traffic. *Proc Natl Acad Sci U S A.* 1985;82:6305-6309.
- (163) Schmitz G, Buechler C. ABCA1: regulation, trafficking and association with heteromeric proteins. *Ann Med.* 2002;34:334-347.
- (164) Schmitz G, Kaminski WE. ABC transporters and cholesterol metabolism. *Front Biosci.* 2001;6:D505-D514.
- (165) Schmitz G, Kaminski WE, Porsch-Ozcurumez M et al. ATP-binding cassette transporter A1 (ABCA1) in macrophages: a dual function in inflammation and lipid metabolism? *Pathobiology.* 1999;67:236-240.
- (166) Schmitz G, Langmann T. Structure, function and regulation of the ABC1 gene product. *Curr Opin Lipidol.* 2001;12:129-140.
- (167) Schmitz G, Niemann R, Brennhausen B, Krause R, Assmann G. Regulation of high density lipoprotein receptors in cultured macrophages: role of acyl-CoA:cholesterol acyltransferase. *EMBO J.* 1985;4:2773-2779.
- (168) Schnitzer JE, Liu J, Oh P. Endothelial caveolae have the molecular transport machinery for vesicle budding, docking, and fusion including VAMP, NSF, SNAP, annexins, and GTPases. *J Biol Chem.* 1995;270:14399-14404.
- (169) Schroder NW, Opitz B, Lamping N et al. Involvement of lipopolysaccharide binding protein, CD14, and Toll-like receptors in the initiation of innate immune responses by *Treponema* glycolipids. *J Immunol.* 2000;165:2683-2693.

- (170) Schroit AJ, Zwaal RF. Transbilayer movement of phospholipids in red cell and platelet membranes. *Biochim Biophys Acta*. 1991;1071:313-329.
- (171) Schwenke DC, Carew TE. Initiation of atherosclerotic lesions in cholesterol-fed rabbits. I. Focal increases in arterial LDL concentration precede development of fatty streak lesions. *Arteriosclerosis*. 1989;9:895-907.
- (172) Schwenke DC, Carew TE. Initiation of atherosclerotic lesions in cholesterol-fed rabbits. II. Selective retention of LDL vs. selective increases in LDL permeability in susceptible sites of arteries. *Arteriosclerosis*. 1989;9:908-918.
- (173) Schwenke DC, St Clair RW. Influx, efflux, and accumulation of LDL in normal arterial areas and atherosclerotic lesions of white Carneau pigeons with naturally occurring and cholesterol-aggravated aortic atherosclerosis. *Arterioscler Thromb*. 1993;13:1368-1381.
- (174) Scow RO, Blanchette-Mackie EJ. Transport of fatty acids and monoacylglycerols in white and brown adipose tissues. *Brain Res Bull*. 1991;27:487-491.
- (175) Shaw G. The pleckstrin homology domain: an intriguing multifunctional protein module. *Bioessays*. 1996;18:35-46.
- (176) Shulenin S, Noguee LM, Annilo T et al. ABCA3 gene mutations in newborns with fatal surfactant deficiency. *N Engl J Med*. 2004;350:1296-1303.
- (177) Silver DL, Wang N, Xiao X, Tall AR. High density lipoprotein (HDL) particle uptake mediated by scavenger receptor class B type 1 results in selective sorting of HDL cholesterol from protein and polarized cholesterol secretion. *J Biol Chem*. 2001;276:25287-25293.
- (178) Smith EB. Transport, interactions and retention of plasma proteins in the intima: the barrier function of the internal elastic lamina. *Eur Heart J*. 1990;11 Suppl E:72-81.
- (179) Stangl H, Cao G, Wyne KL, Hobbs HH. Scavenger receptor, class B, type I-dependent stimulation of cholesterol esterification by high density lipoproteins, low density lipoproteins, and nonlipoprotein cholesterol. *J Biol Chem*. 1998;273:31002-31008.

- (180) Steinberg D, Witztum JL. Is the oxidative modification hypothesis relevant to human atherosclerosis? Do the antioxidant trials conducted to date refute the hypothesis? *Circulation*. 2002;105:2107-2111.
- (181) Stohr J, Schindler G, Rothe G, Schmitz G. Enhanced upregulation of the Fc gamma receptor IIIa (CD16a) during in vitro differentiation of ApoE4/4 monocytes. *Arterioscler Thromb Vasc Biol*. 1998;18:1424-1432.
- (182) Sudhof TC, Goldstein JL, Brown MS, Russell DW. The LDL receptor gene: a mosaic of exons shared with different proteins. *Science*. 1985;228:815-822.
- (183) Sugiyama T, Wright SD. Soluble CD14 mediates efflux of phospholipids from cells. *J Immunol*. 2001;166:826-831.
- (184) Suzuki H, Kurihara Y, Takeya M et al. A role for macrophage scavenger receptors in atherosclerosis and susceptibility to infection. *Nature*. 1997;386:292-296.
- (185) Swanson JA, Watts C. Macropinocytosis. *Trends Cell Biol*. 1995;5:424-428.
- (186) Tabas I, Li Y, Brocia RW et al. Lipoprotein lipase and sphingomyelinase synergistically enhance the association of atherogenic lipoproteins with smooth muscle cells and extracellular matrix. A possible mechanism for low density lipoprotein and lipoprotein(a) retention and macrophage foam cell formation. *J Biol Chem*. 1993;268:20419-20432.
- (187) Takei K, Haucke V. Clathrin-mediated endocytosis: membrane factors pull the trigger. *Trends Cell Biol*. 2001;11:385-391.
- (188) Teng FY, Wang Y, Tang BL. The syntaxins. *Genome Biol*. 2001;2:REVIEWS3012.
- (189) Thieblemont N, Wright SD. Transport of bacterial lipopolysaccharide to the golgi apparatus. *J Exp Med*. 1999;190:523-534.
- (190) Thuahnai ST, Lund-Katz S, Dhanasekaran P et al. Scavenger receptor class B type I-mediated cholesteryl ester-selective uptake and efflux of unesterified cholesterol. Influence of high density lipoprotein size and structure. *J Biol Chem*. 2004;279:12448-12455.

- (191) Torii S, Takeuchi T, Nagamatsu S, Izumi T. Rab27 effector granuphilin promotes the plasma membrane targeting of insulin granules via interaction with syntaxin 1a. *J Biol Chem*. 2004;279:22532-22538.
- (192) Tsuchiya S, Yamabe M, Yamaguchi Y et al. Establishment and characterization of a human acute monocytic leukemia cell line (THP-1). *Int J Cancer*. 1980;26:171-176.
- (193) Uitto J, Pulkkinen L, Ringpfeil F. Molecular genetics of pseudoxanthoma elasticum: a metabolic disorder at the environment-genome interface? *Trends Mol Med*. 2001;7:13-17.
- (194) Van Eck M, Pennings M, Hoekstra M, Out R, Van Berkel TJ. Scavenger receptor BI and ATP-binding cassette transporter A1 in reverse cholesterol transport and atherosclerosis. *Curr Opin Lipidol*. 2005;16:307-315.
- (195) Wang N, Silver DL, Costet P, Tall AR. Specific binding of ApoA-I, enhanced cholesterol efflux, and altered plasma membrane morphology in cells expressing ABC1. *J Biol Chem*. 2000;275:33053-33058.
- (196) Wang N, Tall AR. Regulation and mechanisms of ATP-binding cassette transporter A1-mediated cellular cholesterol efflux. *Arterioscler Thromb Vasc Biol*. 2003;23:1178-1184.
- (197) Wang X, Reape TJ, Li X et al. Induced expression of adipophilin mRNA in human macrophages stimulated with oxidized low-density lipoprotein and in atherosclerotic lesions. *FEBS Lett*. 1999;462:145-150.
- (198) Watari H, Blanchette-Mackie EJ, Dwyer NK et al. Niemann-Pick C1 protein: obligatory roles for N-terminal domains and lysosomal targeting in cholesterol mobilization. *Proc Natl Acad Sci U S A*. 1999;96:805-810.
- (199) White RA, Peters LL, Adkison LR et al. The murine pallid mutation is a platelet storage pool disease associated with the protein 4.2 (pallidin) gene. *Nat Genet*. 1992;2:80-83.
- (200) Williams DL, Llera-Moya M, Thuahnai ST et al. Binding and cross-linking studies show that scavenger receptor BI interacts with multiple sites in apolipoprotein

- A-I and identify the class A amphipathic alpha-helix as a recognition motif. *J Biol Chem.* 2000;275:18897-18904.
- (201) Witztum JL, Steinberg D. The oxidative modification hypothesis of atherosclerosis: does it hold for humans? *Trends Cardiovasc Med.* 2001;11:93-102.
- (202) Yla-Herttuala S, Salonen JT. [Role of lipid oxidation in the development of atherosclerosis]. *Duodecim.* 1994;110:1643-1652.
- (203) Yla-Herttuala S, Solakivi T, Hirvonen J et al. Glycosaminoglycans and apolipoproteins B and A-I in human aortas. Chemical and immunological analysis of lesion-free aortas from children and adults. *Arteriosclerosis.* 1987;7:333-340.
- (204) Yoo JS, Moyer BD, Bannykh S et al. Non-conventional trafficking of the cystic fibrosis transmembrane conductance regulator through the early secretory pathway. *J Biol Chem.* 2002;277:11401-11409.
- (205) Yuhanna IS, Zhu Y, Cox BE et al. High-density lipoprotein binding to scavenger receptor-BI activates endothelial nitric oxide synthase. *Nat Med.* 2001;7:853-857.
- (206) Zerial M, McBride H. Rab proteins as membrane organizers. *Nat Rev Mol Cell Biol.* 2001;2:107-117.
- (207) Zha X, Genest J, Jr., McPherson R. Endocytosis is enhanced in Tangier fibroblasts: possible role of ATP-binding cassette protein A1 in endosomal vesicular transport. *J Biol Chem.* 2001;276:39476-39483.
- (208) Zhang HF, Basra HJ, Steinbrecher UP. Effects of oxidatively modified LDL on cholesterol esterification in cultured macrophages. *J Lipid Res.* 1990;31:1361-1369.
- (209) Zhang M, Dwyer NK, Neufeld EB et al. Sterol-modulated glycolipid sorting occurs in niemann-pick C1 late endosomes. *J Biol Chem.* 2001;276:3417-3425.
- (210) Grandl M, Bared SM, Liebisch G, Werner T, Barlage S, Schmitz G. E-LDL and Ox-LDL Differentially regulate ceramide and cholesterol raft microdomains in human macrophages. *Cytometry.* Accepted

VIII. SUMMARY

The ATP-binding cassette transporter 1 (ABCA1) has recently been identified as a major regulator of systemic HDL. The main focus of this work was to identify and further characterize ABCA1-interactive proteins. A Yeast-Two-Hybrid screening with the last 144 amino acids of the ABCA1 C-terminus as bait was performed. Our results indicate that ABCA1 forms a heteromeric complex with each of: Fas-associated death domain (FADD), β 2-syntrophin, syntaxin 13 and flotillin-1, indicating a role for ABCA1 beyond mere reverse cholesterol transport. The interactions of the identified putative ABCA1-associated proteins were confirmed by independent approaches. In addition, functional studies were performed to elucidate the physiological consequences of these protein complexes.

The finding that FADD directly interacts with ABCA1 is surprising and links cellular HDL metabolism with a protein mainly described in the context of death receptor-induced apoptosis, since FADD plays a well-established role in transduction of apoptotic signals and other cellular processes. The FADD/ABCA1 interaction may indicate an anti-apoptotic ABCA1 function independent from a suggested phosphatidylserine translocase activity.

The C-terminal sequence of ABCA1 has been described previously as a binding motif for the PDZ domains of syntrophin. We showed that ABCA1 binds β 2-syntrophin, a PDZ protein that acts as a general adaptor of membrane proteins to the actin cytoskeleton via utrophin, a protein highly homologous to dystrophin.

The cystic fibrosis transmembrane conductance regulator (CFTR), a member of the ABC transporter family, has been reported to interact with syntaxin 1A. Thereupon, we investigated the interaction of ABCA1 with syntaxins and identified syntaxin 13 as a direct ABCA1-interactor in this family. Syntaxin 13, through its interacting protein pallidin (syntaxin 13 interacting protein), is linked to Hermansky-Pudlak syndrome (HPS) and Chediak-Higachi syndrome (CHS). These lysosomal storage diseases are associated with pulmonary fibrosis and prolonged bleeding caused by defects in the Adapter protein-3 complex (AP-3). Recent publications show that ABCA1 mutations in Tangier patients are related to impaired platelet activation due to the presence of ABCA1, syntaxin 13 and syntaxin 13-interacting protein in the AP-3 pathway.

Moreover, ABCA1 deficiency leads to enhanced phagocytosis in Tangier macrophages and fibroblasts, related to disturbances of the AP-3 pathway. The enhanced uptake of apoA-I by endocytic and phagocytic ingestion may also explain the increased catabolism of apoA-I in Tangier patients. Syntaxin 13 deficiency causes ABCA1 protein degradation and therefore syntaxin 13 may be important in ABCA1 maturation and vesicular transport. This finding links ABCA1 to a potential regulator of phagocytosis indicating that both the phagosomal and lysosomal compartment may be involved in ABCA1-dependent choline-phospholipid efflux.

The integral membrane protein flotillin-1 was also found to interact with ABCA1. Overexpression of flotillin-1 enhances filipodia formation, linking ABCA1 to migration and cytoskeletal changes.

In the second part of the work human monocyte-derived macrophages were loaded with differently modified atherogenic LDLs, namely enzymatically degraded LDL (E-LDL) and oxidized LDL (Ox-LDL), and subsequently deloaded by HDL₃ in order to ascertain differential gene regulation within lipid-related pathways. This characterization was performed by Affymetrix U133a gene chips. The processing of lipids in macrophages occurs within the lysosome combined with subsequent storage in cytoplasmic lipid droplets. Our results indicate that Ox-LDL induces less cytoplasmic cholesteryl ester accumulation than E-LDL, a result of the chemical alterations during oxidation. We further showed that cholesterol efflux influences the gene expression of a substantial portion of structural elements of the large and small ribosomal subunits. Deloading of E-LDL, but not Ox-LDL, loaded macrophages led to a distinguished upregulation of genes in the polymerase-II complex, indicating a close relationship between E-LDL, taken up outside clathrin coated pits by phagocytosis, and the control mechanisms at the transcriptional level. This E-LDL specific effect continues more downstream in the translation machinery represented by the 40S and 60S ribosomal genes as well as in the proteasomal degradation machinery where unneeded proteins are promptly degraded.

In addition, ATP synthases were also upregulated during HDL₃-induced deloading of E-LDL, but not Ox-LDL, loaded macrophages, possibly due to the increased amount of cholesterol in E-LDL compared to Ox-LDL-loaded macrophages, since HDL₃ functions as a cholesterol acceptor resulting in ATP-dependent cholesterol efflux through ABCA1. In addition, LDL-receptor mediated cholesterol uptake downregulates intracellular cholesterol synthesis by inhibition of HMGCoA reductase and inhibition of LDL-receptor by feedback mechanism. This cholesterol sensitive regulatory system leads to subsequent deloading of E-LDL whereas Ox-LDL is trapped inside the cell. Thus, certain modification types of lipoproteins may indirectly control cellular translation machinery.

PUBLICATION LIST

- **Bared SM**, Buechler C, Boettcher A, Dayoub R, Sigrüener A, Grandl M, Rudolph C, Dada A, Schmitz G. Association of ABCA1 with syntaxin 13 and flotillin-1 and enhanced phagocytosis in tangier cells. *Mol Biol Cell*. 2004 Dec;15(12):5399-407 (Impact: 8,81)
- Grandl M, **Bared SM**, Liebisch G, Werner T, Barlage S, Schmitz G. E-LDL and Ox-LDL Differentially regulate ceramide and cholesterol raft microdomains in human macrophages. *Cytometry*. Accepted (Impact: 2,48)
- Buechler C, Bodzioch M, **Bared SM**, Sigrüener A, Boettcher A, Lapicka-Bodzioch K, Aslanidis C, Duong CQ, Grandl M, Langmann T, Dembinska-Kiec A, Schmitz G. Expression pattern and raft association of NIPSNAP3 and NIPSNAP4, highly homologous proteins encoded by genes in close proximity to the ATP-binding cassette transporter A1. *Genomics*. 2004 Jun;83(6):1116-24 (Impact: 4,6)
- Duong CQ, **Bared SM**, Abu-Khader A, Buechler C, Schmitz A, Schmitz G. Expression of the lysophospholipid receptor family and investigation of lysophospholipid-mediated responses in human macrophages. *Biochim Biophys Acta*. 2004 Jun 1;1682(1-3):112-9. (Impact: 2,64)
- Buechler C, Ullrich H, Aslanidis C, **Bared SM**, Lingenhel A, Ritter M, Schmitz G. Lipoprotein (a) downregulates lysosomal acid lipase and induces interleukin-6 in human blood monocytes. *Biochim Biophys Acta*. 2003 Sep 23;1642(1-2):25-31. (Impact: 2,64)
- Buechler C, **Bared SM**, Aslanidis C, Ritter M, Drobnik W, Schmitz G. Molecular and functional interaction of the ATP-binding cassette transporter A1 with Fas-associated death domain protein. *J Biol Chem*. 2002 Nov 1;277(44):41307-10. (Impact: 6,56)
- Buechler C, Boettcher A, **Bared SM**, Probst MC, Schmitz G. The carboxyterminus of the ATP-binding cassette transporter A1 interacts with a beta2-syntrophin/utrophin complex. *Biochem Biophys Res Commun*. 2002 May 3;293(2):759-65. (Impact: 3,25)
- Ritter M, Buechler C, Boettcher A, Barlage S, Schmitz-Madry A, **Bared SM**, Orso E, Schmiedeknecht G, Baehr CH, Fricker G, Schmitz G. Cloning and characterization of a novel apolipoprotein A-I binding protein, AI-BP, secreted by cells of the kidney proximal tubules in response to HDL or ApoA-I. *Genomics*. 2002 May;79(5):693-702. (Impact: 4,6)
- Kaminski WE, Piehler A, Pullmann K, Porsch-Ozcurumez M, Duong C, **Bared SM**, Buchler C, Schmitz G. Complete coding sequence, promoter region, and genomic structure of the human ABCA2 gene and evidence for sterol-dependent regulation in macrophages. *Biochem Biophys Res Commun*. 2001 Feb 16;281(1):249-58. (Impact: 3,25)

Eidesstattliche Erklärung

Familienname: Maa Bared
Vorname: Salim
Geburtsdatum: 11.05.1972

Ich erkläre hiermit an Eides statt, daß ich die vorliegende Arbeit ohne unzulässige Hilfe Dritter und ohne Benutzung anderer als der angegebenen Hilfsmittel angefertigt habe; die aus anderen Quellen direkt oder indirekt übernommenen Daten und Konzepte sind unter Angabe des Literaturzitats gekennzeichnet (Siehe Kapitel „References“).

Bei der Auswahl und Auswertung folgenden Materials haben mir die nachstehend aufgeführten Personen in der jeweils beschriebenen Weise entgeltlich/unentgeltlich geholfen:

- 1-.....
- 2-.....
- 3-.....

Weitere Personen waren an der inhaltlich-materiellen Herstellung der vorliegenden Arbeit nicht beteiligt. Insbesondere habe ich hierfür nicht die entgeltliche Hilfe eines Promotionsberaters oder anderer Personen in Anspruch genommen. Niemand hat von mir weder unmittelbar noch mittelbar geldwerte Leistungen für Arbeiten erhalten, die im Zusammenhang mit dem Inhalt der vorliegenden Dissertation stehen.

Die Arbeit wurde bisher weder im In- noch im Ausland in gleicher oder ähnlicher Form einer anderen Prüfungsbehörde vorgelegt.

Ich versichere an Eides statt, daß ich nach bestem Wissen die reine Wahrheit gesagt und nichts verschwiegen habe.

Vor Aufnahme der obigen Versicherung an Eides statt wurde ich über die Bedeutung der eidesstattlichen Versicherung und die strafrechtlichen Folgen einer unrichtigen oder unvollständigen eidesstattlichen Versicherung belehrt.



Regensburg, 10.06.2005

Salim Maa Bared